



**babcock & wilcox nuclear operations group**

► p.o. box 785 ► lynchburg, va 24505-0785 usa ► phone 434.522.6000  
► www.babcock.com

January 29, 2009  
09-019

E. William Brach  
Director, Spent Fuel Project Office  
Office of Nuclear Material Safety and Safeguards  
U.S. Nuclear Regulatory Commission  
Washington, DC 20555-0001

**References:**

- 1) Docket No. 71-5086
- 2) Letter dated May 30, 2008, BWXT (Cole) to NRC (SFST), Request to Transfer Certificates of Compliances in Parallel with the Transfer of Control of Special Nuclear Materials License No. SNM-42 (TAC L32657)
- 3) Letter dated May 30, 2008, BWXT (Cole) to NRC (SFST), Supplement to BWX Technologies, Inc. Letter Dated May 30, 2008 (TAC L32657)
- 4) Letter dated October 28, 2008, NRC (Saverot) to BWXT (Cole), Request for Additional Information for the Review of the Model No. UNC-2600 Package (TAC L24272)
- 5) Telephone conversation dated November 17, 2008, BWXT (Stevens) to NRC (Saverot) Request to Provide Additional Information by January 31, 2009
- 6) Letter dated December 3, 2008, BWXT (Cole) to NRC (Brach) Response to Request for Additional Information for Review of the Model No. UNC-2600 Package (TAC L24272)

**Subject:** Response to Request for Additional Information for Review of the Model No. UNC-2600 Package and Renewal Application for Certificate of Compliance No. 5086 (TAC L24272)

**Dear Mr. Brach:**

By letter dated May 30, 2008 (References 2 and 3), BWX Technologies, Inc. (BWXT) submitted a request to the U.S. Nuclear Regulatory Commission (NRC) to transfer the Certificate of Compliance No. 5086 for the Model No. UNC-2600 package to Babcock & Wilcox Nuclear Operations Group, Inc. (B&W NOG). BWXT received a request for additional information (RAI) dated October 28, 2008 (Reference 4).

A member of our staff contacted Mr. Pierre Saverot by phone on November 12, 2008 and on November 17, 2008 and requested that BWXT provide the response to the RAI at the time of certificate renewal for this package. Effective January 11, 2009, Materials License SNM-42, Docket 70-27, was transferred from BWXT to B&W NOG.

The certificate renewal request for this package is provided as an enclosure to this letter and contains the full revised Safety Analysis Report for Packaging (SARP). The information requested by the RAI (Reference 4) is provided below:

### **RAI Question**

*Evaluate whether a 9-meter (30 foot) drop test at a shallow angle orientation could result in lid separation. If the analysis results in lid separation, examine the effect of such lid separation on the ability of the package to meet the requirements of 10 CFR 71.*

*The licensing basis for the drum-type package that was tested assumed that the lid would remain attached to the drum. Separation of the lid from these drum-type packages could adversely affect the criticality evaluation required to meet 10 CFR 71.55 (b) & (e), and affect the assessment of an array of damaged packages, as required by 10 CFR 71.59 (a)(2). Thus, the results of the shallow angle drop testing could invalidate the basis for approval of the transportation package.*

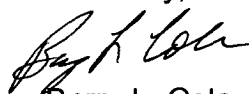
*This information is needed to determine compliance with 10 CFR 71.55 (b) & (e) and 71.59 (a)(2).*

### **B&W NOG's Response**

In lieu of performing the shallow angle drop test, which B&W NOG believes the container would not survive, the mass limit per container was reduced to 375 grams U235 and the Criticality Safety Index (CSI) was increased to 50 which limits the shipment to a maximum of two containers. This ensures a shipment shall contain less than the minimum critical mass of fuel. Consequently, even if the container is ruptured and the entire contents were ejected, a criticality is not possible. This information is provided throughout the enclosed revised SARP.

Should you have any questions in this regard, please contact me at (434) 522-5665.

Sincerely,



Barry L. Cole  
Manager, Licensing and Safety Analysis  
(Licensing Officer)

Enclosure

cc: NRC, Resident Inspector  
NRC, Region II  
NRC, Amy Snyder  
NRC, Pierre Saverot

**Enclosure**

# Summary of Changes:

Section 1.1 – Updated quantity and TI to CSI information

Section 1.2.3 (2) – Updated quantity allowed

Section 1.2.3 (3) – Deleted “with the U-235 weight constituting less than 7.4% of the total weight of fuel components being shipped ( $\leq 265$  lbs.)”

Section 6.1 – Added a “Revised Analysis”.

Table 6.1.1 – Added a “Revised Table” to update quantities

Section 6.2 – Added a “Revised Analysis”.

Sections 6.3, 6.4 and 6.5 – Added “Original Analysis” by the headings to clarify original information

Section 7.0 – Updated quantities

Sections 8.2.1 and 8.2.7.1 – Updated to allow for maintenance to be performed only when containers are in service. Due to the safety hazards of handling these containers, they remain out of service when not needed.

**UNC 2600**

**Safety Analysis Report for Packaging**

**Application for License**

**USA/5086/B(U)F**

**Babcock & Wilcox  
Nuclear Operations Group, Inc.  
Lynchburg, Va.**

**January 2009**

## Table of Contents

Page 1 of 3

	<u>Page</u>
1. General Information	
1.1. Introduction	1
1.2. Package Description	1
1.2.1. Packaging	1
1.2.2. Operational Features	2
1.2.3. Contents of Packages	2
2. Structural Evaluation	
2.1. Structural Evaluations	3
2.1.1. Discussion	3
2.2. Weights and Center of Gravity	4
2.3. Mechanical Properties of Materials	4
2.4. General Standards for all Packages	4
2.4.1. Minimum Package Size	4
2.4.2. Tamperproof Features	4
2.4.3. Positive Closure	4
2.4.4. Chemical and Galvanic Reactions	4
2.5. Lifting and Tiedown Standards for All Pkgs	5
2.5.1. Lifting Devices	5
2.5.2. Tiedown Devices	5
2.6. Normal Conditions of Transport	5
2.6.1. Heat	5
2.6.2. Cold	5
2.6.3. & 2.6.4 Pressure	5
2.6.5. Vibration	5
2.6.6. Water Spray	6
2.6.7. Free Drop	6
2.6.8. Corner Drop	6
2.6.9. Penetration	6
2.6.10. Compression	6
2.7. Hypothetical Accident Conditions	6
2.7.1. Free Drop	6
2.7.2. Puncture Test	6
2.7.3. Thermal Test	8
2.7.4. Water Immersion	8
2.7.5. Summary of Damage	9
2.8. Special Form	10
2.9. Fuel Rods	10
2.10. Appendix	10

## Table of Contents (cont'd)

Page 2 of 3

		<u>Page</u>
	2.10.1. Drop Test Photographs and FEA Depiction	10
	2.10.2. Engineering Evaluation of End and Side Drop	10
3.	Thermal Evaluation	11
4.	Containment	
	4.1. Containment Boundary	11
	4.2. Requirements for Normal Conditions of Transport	11
	4.2.1. Release of Radioactive Materials	11
	4.2.2. Pressurization of Containment Vessel	11
	4.2.3. Coolant Containment	11
	4.2.4. Coolant Loss	11
	4.3. Containment Requirements for Hypothetical Accident Condition	12
	4.3.1. Fission Gas Products	12
	4.3.2. Release of Contents	12
5.	Shielding Evaluation	12
6.	Criticality Evaluation	
	6.1. Discussion and Results	12
	6.2. Package Fuel Loading	16
	6.3. Model Specification	18
	6.3.1. Description of Calculational Model	18
	6.3.2. Package Regional Densities	18
	6.4. Criticality Calculations	18
	6.4.1. Calculation or Experimental Model	18
	6.4.2. Fuel Loadings or Other Contents	18
	Loading Optimization	18
	6.4.3. Criticality Results	18
	6.5. Critical Benchmark Experiments	22
	6.5.1. Benchmark Experiments and Applicability	22
	6.5.2. Details of Benchmark Calculations	23
	6.5.3. Results of Benchmark Calculations	23
7.	Operating Procedure	
	7.1. Procedures for Loading Package Discussion and Results	24
	7.2. Procedures for Unloading Package	26
	7.3. Preparation of Empty Packages for Shipment	27



## Table of Contents (cont'd)

Page 3 of 3

	<u>Page</u>
8. Acceptance Tests and Maintenance Program	
8.1. Acceptance	
8.1.1. Visual Inspection	27
8.1.2. Structural and Pressure Tests	28
8.1.3. Leak Tests	28
8.1.4. Component Tests	28
8.1.5. Tests for Shielding Integrity	28
8.1.6. Thermal Acceptance Tests	28
8.2. Maintenance Program	
8.2.1. Structural and Pressure Tests	28
8.2.2. Leak Tests	29
8.2.3. Subsystem Maintenance	29
8.2.4. Valves, Rupture Discs, and Gaskets on Containment Vessel	29
8.2.5. Shielding	29
8.2.6. Thermal	29
8.2.7. Miscellaneous	29

## 1.0 General Information

This package consists of an outer steel drum and an inner steel cage assembly which centers and firmly locates an inner steel box. This box contains the fuel elements authorized for shipment. All aspects of design modification, fabrication, and use are controlled under the QA Plan approved under Docket 71-0088.

### 1.1 Introduction:

The UNC 2600 package is used to ship fuel elements with U-235 enrichments up to 100%. Each package is limited to a maximum of 375 grams. U-235, and is assigned a Criticality Safety Index (CSI) of 50 based on criticality control requirements.

### 1.2 Package Description:

#### 1.2.1 Packaging:

##### (1) Weights:

Nominal empty container	840 lbs
Max. weight of contents	265 lbs
Nominal gross weight	1105 lbs

##### (2) Materials of Construction:

The package is constructed of mild steel, using two high strength steel bolted closure flanges to retain the fuel box in an inner steel cage. The fuel box is also of mild steel construction. An oak wood block measuring at least 2-1/2" long is positioned at each end of the fuel box to prevent product damage and distribute the load in an end drop accident. Additionally, rubber bumpers are used at both ends, external to the cage, also to distribute the axial loads. The construction details are shown in Drawing B-2600-2, Sheets 1, 2, 3, 4, and 5, Rev. 1 which is provided in Appendix 2.10.1.

(3) Description: (All Dimensions are Nominal)

The fuel box (inner container) is an 11 gage steel box with inside dimensions of 2-5/8" x 7" x 96". It is supported in a 22-1/2" I. D. by 102-1/2" long 14 gage steel drum by a welded reinforced insert cage. This cage is 97" long, and is formed by nine 21-1/2" diameter by 3/8" thick steel plates (disks) spaced approximately 12" apart by 1-3/4" x 1/4" steel strips welded radially to each of the nine disks. The 12" sections at either end of the cage are further strengthened by eight 1" x 1" (1/8" angle) welded to the structure.

A channel to hold the fuel box is formed through the center of the cage by 1-1/2" x 1-1/2" x 1/8" angle irons which are also welded to each disk. Four additional 1" x 1" x 1/8" angles are used to further strengthen this fuel box slot. The fuel box is retained within the cage channel by two 1/2" thick" diameter high strength 4130 steel closure flanges which are secured to each end of the cage with eight 7/8" SAE Grade 5 steel bolts.

The outer container closure is a 14 gage drum lid which is secured to the drum with a 12 gage bolt locking ring with drop forged lugs, one of which is threaded, having a 5/8" diameter bolt.

(4) Pressure Relief:

Pressure buildup is precluded because the drum lid has no gasket, facilitating pressure equalization.

**1.2.2 Operational Features**

Use of the package is simple, with minimal operational features. Proper use of the package is described in Section 7.

**1.2.3 Contents of Package**

(1) Type and Form of Material

The UNC-2600 package is used to ship unirradiated fuel elements. The contained uranium may be enriched up to 100% in the U-235 isotope. Each element may be wrapped in protective plastic.

(2) Maximum Quantity of Material Per Package:

375 gram U-235 as clad fuel elements

(3) Fuel Geometry Constraints:

The inner 11 gage steel box confines the uranium materials to a 2-5/8" x 7" cross section.

## 2.0 Structural Evaluations

### 2.1 Structural Evaluations:

#### 2.1.1 Discussion:

Section 1.2 identifies the principal construction details of the package design. Drawing B-2600-1 details the original design which had been drop tested, and is provided in Appendix 2.10.2. The current design, specified in Drawing B-2600-2 has been analytically evaluated using Finite Element Analysis (FEA).

The current design improves the mechanical retention of the fuel box within the cage, using a 12" O.D. x 1/2" thick 4130 AMS 6370 heat treated steel closure flange secured with eight 7/8" SAE Grade 5 steel bolts to each end of the cage. The use of these closure flanges adds less than 40 lbs. to the empty weight of the original package, and this is offset by a reduction in the product loading from 308 lbs. to 265 lbs. Additionally, the current design specifies that the bumper disks at each end of the cage be fabricated of a 60 durometer,  $\geq 2500$  psi rubber with a Bell Brittle Point temperature of at least -70F.

A prototype package (Drawing B-2600-1), representative of the original design has been previously tested as described in Section 2.7. The current design (Drawing B-2600-2) has been additionally evaluated for the drop test conditions using FEA. This evaluation is also described in Section 2.7.

**2.2 Weights and Center of Gravity:**

The center of gravity is essentially the center of the package in both the loaded and empty conditions.

**2.3 Mechanical Properties of Materials:**

The package is primarily fabricated of mild steel, and the 12" diameter closure flanges are 4130 AMS 6370 heat treated (Rockwell C = 28-33) steel. The properties of these steels, the SAE Grade 5 steel bolts, and the Rubber disks at each end of the cage are provided in Appendix 2.10.4.

**2.4 General Standards For All Packages:****2.4.1 Minimum Package Size:**

The package dimensions shown in drawing B-2600-2 exceed the minimum package size specifications of 10 CFR 71.

**2.4.2 Tamperproof Features:**

A tamperproof seal is inserted in the end of the bolt which secures the cover ring seal closure at the front of the package.

**2.4.3 Positive Closure:**

The inner box which contains the fuel is held closed with steel banding. The banded box is constrained by the angle iron channel within the welded cage assembly. This cage assembly is retained within the outer container, as demonstrated by the accident test sequence and the analysis discussed in Section 2.7. The outer container lid is held closed by the ring seal which is bolted closed.

**2.4.4 Chemical and Galvanic Reactions:**

The steel package construction is not vulnerable to degradation from such reactions during shipment, or as a result of accident conditions.

**2.5 Lifting and Tiedown Standards For All Packages:****2.5.1 Lifting Devices:**

Packages are lifted to and from the transport vehicle using appropriate slings, and other normal techniques. These are engaged with fork lifts or other standard mechanisms.

**2.5.2 Tie Down Devices:**

No tie down devices are incorporated as part of the package design.

**2.6 Normal Conditions of Transport:****2.6.1 Heat and      2.6.2 Cold**

The low carbon steel construction of the package drums and internals, and the design and construction of the fuel elements retain ductility through a temperature range of -40 to +130 degrees, F. The rubber bumpers have a Bell Brittle Point at or below -70 F, and are serviceable at the specified -40 F. The package design imposes minimal stresses, and fracture of the steel construction or the non-brittle zirconium fuel cladding will not occur.

**2.6.3 and 2.6.4 Pressure:**

The package is closed with an ungasketed lid, and will not retain pressure differentials. If a gasketed lid were incorrectly applied, the outer drum may dimple, but the containment of the uranium contents will remain unimpaired.

**2.6.5 Vibration:**

Vibration will not effect this welded package construction.

**2.6.6      Water Spray:**

Criticality analysis assumes optimum water moderation. Because the drum lid has no gasket, water will drain from the package as fast as it leaks in, and the test will have no effect on the subsequent drop test. Therefore this test has no effect.

**2.6.7      Free Drop    and    2.6.8 Corner Drop:**

Please refer to the description of the 30 foot and 40" penetration tests provided in Section 2.7.

**2.6.9      Penetration:**

This package is constructed of 14 gage steel, and will pass the penetrations test to which the lighter gage (6L Sect. 49CFR178.103) package was subjected.

**2.6.10     Compression:**

The steel ribbed construction of the package will easily support a linear loading of 60 lbs/inch. (five times the package loading).

**2.7      Hypothetical Accident Conditions****2.7.1      Free Drop and 2.7.2 Puncture Test:**

- (a) Analysis - The original package design shown in Drawing B-2600-1 was physically tested and shown to retain the fuel within its design containment. This testing is described in 2.7.1 (b). The current package design incorporates improved retention features for holding the box within the cage, and is constructed as specified in Drawing B-2600-2. The testing described in Section 2.7.1 (b) is supplemented for this design with an FEA evaluation described in Section 2.7.2 ( c ), and included as Appendix 2.10.4.

(b) Prototype Testing: Drawing B-2600-1

- 1) Date of the Test: - October 27, 1966
- 2) Location: - UNC Fuel Division - New Haven, Ct.
- 3) Weights:

Drum (Tare)	804 lbs.
Load (Net)	308 lbs.
Total (Gross)	1112 lbs.

4) Description of the Tests:

The ability of the UNC 2600 package to withstand the hypothetical accident conditions specified in Section 10 CFR 71.73 has been evaluated by performing the drop test, and evaluating the other conditions as described in this section. The as tested package was constructed to the specifications of Drawing B-2600-1.

A solid inconel bar was placed into the inner box to simulate the weight of the SNM bearing materials. The inner box was closed as specified, and placed and secured in the cage, which in turn was secured into the outer container, all as specified.

This assembled package was then dropped onto a concrete driveway in such a manner to cause maximum deformation. The package initially impacted on the edge of the lid with the remainder of the package continuing in a downward direction causing top, bottom, and side deformation.

The puncture test was performed to cause the package to impact on the drum weld, considered its most vulnerable position. This sequence did not dislodge the inner box from the cage, or the cage from the container. The tests did cause some deformation of the container, in effect snugging the drum to the cage. It also deformed the ring seal which secures the drum lid. Appendix 2.10.3 contains a series of photographs showing the drop tests and the resulting damage.



Had the puncture test been performed on the end of the package, it would not have dislodged the cage from the drum, or the box from the cage. The 6" diameter pin would have partially flattened the inner box end handle from an original height of 1-3/4" to approximately a 1" height. It may have come in contact with the end disk which transmits its load inward through a series of radially placed and welded angle irons and bars, and welded angle irons forming the box channel. This construction gives the cage assembly at least as much stiffness as the box.

Accordingly, a penetration test on the end would not affect the ability of the package to retain the inner fuel box.

(c) Analytical Analysis of the Current Design: Drawing 2600-2

The current design shown in Drawing B-2600-2 improves the fuel box retention by specifying a 12" diameter 1/2" thick steel closure flange secured with eight (8) 7/8" bolts to each end of the cage. This arrangement strengthens the previously demonstrated design of Drawing B-2600-1.

In addition to considering the tests described in Section 2.7.1 (b), computer execute Finite Element Analysis (FEA) were performed. These analyses assumed that the package was end, corner, and side dropped from an elevation of 30 ft., and demonstrates that attained stresses do not jeopardize the retention of the fuel box within the cage. A penetration test of 40" drop onto the closure flange was also simulated. The details of these analyses are provided as Appendix 2.10.4.

**2.7.3 Thermal Test and 2.7.4 Water Immersion**

The thermal test was not performed because, 1) the package is constructed of steel, and 2) the fuel will withstand the specified temperatures. The rubber bumpers and the wood spacers may char, and therefore the accident condition criticality analysis assumes no axial spacing beyond the ends of cage.

The immersion test was not performed because the criticality evaluation assumes full moderation in both the normal and accident condition. The immersion pressure test was not performed because the lid has no gasket, and water will enter the package, equalizing the pressure. Further, the ribbed 14 gage construction will assure the shape of the cage under all conditions.

### 2.7.5 Summary of Damage:

The test series performed on the original (Drawing B-2600-1) design demonstrated that the inner box was retained within the cage, and that the cage was retained within the drum. For the current design, (Drawing B-2600-2) these tests are supplemented with FEA evaluations of an end, corner (45 deg. and Center of Gravity over impact point) and side drop.

The end drop took no structural credit for the drum, but did allow it to retain the rubber during the compressive impact. The drum and lid were included in the corner drop model, and the lid was retained with a closure force calculated to be sufficient to retain an internal pressure of 15 psi (178.116-13, 1988 edition). Analysis shows the lid to separate from the drum on the 45 degree and center of gravity over impact point corner impacts. The FEA evaluations are detailed in Appendix 2.10.4, and clearly demonstrate that the fuel box is retained in the cage.

The side and corner drops deform the drum sufficiently to retain the cage. In the case of the perfect end drop, the outer bars and angle irons of the cage are shown to deform, trapping the cage in the drum.

The damage after the physical 30 ft. free fall test is best shown in Figure 5 of Appendix 2.10.3. A precise determination of side deformation was made using an FEA drop evaluation with impact on the package side. The 3/8" thick disks are deformed to the extent of a <1.352" loss from their radii, and the total loss of radius to the drum is <1.852", as depicted Figure 10 of Appendix 2.10.3. This results in a cross sectional area reduction of <15.7 sq. in. (Mark's Handbook, page 35, 1951 edition), corresponding to a >11.026" effective radius for the damaged package.

The puncture test dented the outer container but did not part the weld, as shown in Figure 8 of Appendix 2.10.3. Figure 9 shows the overall damage to the package.

The conditions used for the nuclear criticality safety evaluation of the damaged package are based on the 1.852 inch deformation from the side drop described above. The square pitch representation for this damaged package uses a 10.26" radius to accommodate its area in a triangular array pattern. The damaged package is evaluated with a total length of 97", assuming loss of the lid, and all axial spacing outside of the cage. Additionally, the analysis ignores the neutron poisoning presence of the steel in the outer drum and the cage.

**2.8 Special Form, and 2.9 Fuel Rods:**

Not applicable

**2.10 Appendix:**

**2.10.1 Drop Test Photographs and FEA Depiction**

The photographs and the FEA depiction referred to in Section 2.7.1 are included in Appendix 2.10.3 at the end of this document. These are listed below:

Figure

No. Description

1. Container and internal supports prior to assembly.
2. Container, inner cage, and inner container during assembly.
3. Container at free fall position.
4. Container showing damage after free fall.
5. Container with lid removed showing maximum damage after free fall.
6. Blank
7. Container after puncture test.
8. Container showing maximum damage after puncture test.
9. Inner container during disassembly after test sequence showing negligible damage.
10. Depiction of FEA side drop.

**2.10.2 Engineering Evaluation of End and Side Drop**

The Engineering evaluation of the upgraded design (Drawing B-2600-2) is provided as Appendix 2.10.4.

### **3.0 Thermal Evaluation**

The uranium materials are unirradiated, of low specific activity, and therefore require no thermal evaluation.

### **4.0 Containment**

#### **4.1 Containment Boundary:**

The design features of the fuel elements provide primary retention of the uranium. No piece has a dimension less than 0.5 mm, and each has at least one dimension greater than 5 mm. The test series and subsequent analysis demonstrated that the elements are retained within the inner box, and that the box is retained within the cage.

The thermal test conditions have no effect on the fuel elements which are not pyrophoric, and are constructed with metals having melting point exceeding the 1475 degree F temperatures specified for the thermal test. Accordingly, there will be no release of radioactive material from this package.

Drawing B-2600-2 provides a complete set of specifications for the package.

#### **4.2 Requirements For Normal Conditions of Transport:**

As stated in paragraph 2.6, the package withstands the accident conditions of transport, and therefore will withstand the less severe normal transportation test conditions.

##### **4.2.1 Release of Radioactive Materials**

The uranium is contained by the design of the fuel elements which are unaffected by the test series.

##### **4.2.2 Pressurization of Containment Vessel**

##### **4.2.3 Coolant Containment**

##### **4.2.4 Coolant Loss**

Items 4.2.2, 4.2.3, and 4.2.4 are not applicable to this package.

### **4.3 Containment Requirements For Hypothetical Accident Conditions**

Testing and evaluation of the package to the requirements of Appendix B of 10CFR71 was described in Paragraph 2.7, above.

#### **4.3.1 Fission Gas Products**

Not Applicable.

#### **4.3.2 Release of Contents**

The specified test conditions will not result in any release of radioactive materials from the fuel elements. The package withstood the drop test intact with the cage retaining the fuel box. All structural materials as well as the construction of the fuel elements remain unaffected by the specified thermal test.

## **5.0 Shielding Evaluation**

The low levels of radioactivity preclude the need for shielding evaluation.

## **6.0 Criticality Evaluation**

### **6.1 Discussion and Results**

#### **Original Analysis**

The design features of the current design of this package are provided in drawing B-2600-2, which shows that the fuel components are contained in an 11 gage steel box with inner dimensions of 2-5/8" x 7" x  $\leq 96$ ". This box has a 2-1/2" long oak wood block at each end, limiting the fuel length to 91" under normal conditions of transport. The box is centered within a 22-1/2" diameter x 102-1/2" long 14 gage steel drum.

KENO analysis demonstrates that 200 packages in a triangular array are subcritical under normal conditions of transport, and that 72 packages in triangular array are subcritical under accident conditions. Triangle and square array equivalence is discussed in Appendix 6.1.1.

An allowable Class II shipment therefore consists of 35 packages, with each assigned a 1.4 TI. Table 6.1.1 summarizes the criticality evaluation of this package.

**Revised Analysis**

During the recertification of the container, NRC requested that the container be evaluated for a shallow angle drop. If the container failed, the assumption would be that the contents were lost. Since the containers were not expected to survive the drop test and the ejection of two inner containers into water could result in a critical condition, the loading of the container was reduced to 375 grams U235 per container and limited to two containers.

**Table 6.1.1 (Original)**  
**Summary of Criticality Evaluation**  
**Fissile Class II**

Normal Conditions

Number of packages calculated to be subcritical with optimum water moderation and close water reflection.	200
Package size, cc (22-1/2" O. D. x 102-1/2" lg.)	6.68E+5
Package size in a triangular array, cc Effective radius for a square pattern model of a triangular array	7.37E+5 10.47"

Accident Conditions

Number of packages calculated to be subcritical with optimum interspersed water moderation and close water reflection.	72
Optimum interspersed moderation, gm water/cc	0.06
Package size after drop, 22-1/2" O.D. x 97" lg. drum with a <1.852" lateral dent.	
Effective package size (22.052" O. D. x 97" lg.) with dented drum	6.07E+5 cc
Dented drum package size in a triangular array.	6.69E+5 cc
Effective radius for a square pattern model With dented drum	10.26"
Transport Index	1.4 (35 Packages)

Please refer to Section 2.7.5 and Appendix 6.1.1 for a discussion of square and triangular arrays.

Table 6.1.1 (Revised)

## Summary of Criticality Evaluation

## Fissile

Accident Conditions (assuming ejection of the content)

Number of packages calculated to be subcritical with optimum interspersed water moderation and close water reflection.	2
Optimum interspersed moderation, gm water/cc	1.00
Package size after drop, inner container ejected.	
Effective package size (2-5/8" x 7" x ≤96" lg.)	
CSI	50 (2 Packages)



## 6.2 Package Fuel Loading

### **Original Analysis**

The package contains up to 8.9 kg. U-235, with 100% U-235 enrichment. The uranium is in the form of fuel elements, and constitutes no more than 7.4 weight percent of the uranium-zirconium solids in the box. Analysis assumes optimum moderation for both normal and accident conditions of transport, 100% U-235, and that the uranium is present in metal form. Table 6.2.2 provides the fuel parameters for the inner box, including the appropriate number densities for the 91" fuel length (normal conditions), and 96" fuel length (accident conditions).

### **Revised Analysis**

The package contains up to 375 grams U-235 with 100% enriched uranium. The uranium is in the form of clad fuel elements. The form of the uranium is assumed to be metal. The combination of two containers is 750 grams U-235. This is less than the minimum critical mass for uranium (LA-10860, Figure 10) mixed with water assuming the uranium is homogeneously and optimally mixed with water in a sphere and reflected by water. To achieve a spherical configuration, the fuel elements would have to be ground in to a very fine powder or chemically dissolved. Neither is credible from a dropped container.

**Table 6.2.2**

**Number Densities  
and Sig. P For  
UNC 2600 Package**

**Uranium Metal-Zirconium Metal  
91 Inch Fuel Length**

Gm. U-235	3000	4000	5000	6000	7000	8000
Length, In.	91	91	91	91	91	91
Width, In.	7.00	7.00	7.00	7.00	7.00	7.00
Thick, In.	2.625	2.625	2.625	2.625	2.625	2.625
Vol. cu in	1672.125	1672.125	1672.125	1672.125	1672.125	1672.125
Vol. cc	27406	27406	27406	27406	27406	27406
Gm U/cc	0.109	0.146	0.182	0.219	0.255	0.292
CC U	160.43	213.90	267.38	320.86	374.33	427.81
Gm Zr	37541	50054	62568	75081	87595	100108
CC Zr	5775	7701	9626	11551	13476	15401
CC H2O	21470	19492	17513	15534	13556	11577
Gm H2O/cc	0.783	0.711	0.639	0.567	0.495	0.422
N U-235	2.81E-04	3.74E-04	4.68E-04	5.61E-04	6.55E-04	7.48E-04
N H	5.23E-02	4.75E-02	4.28E-02	3.78E-02	3.30E-02	2.82E-02
N O	2.61E-02	2.37E-02	2.13E-02	1.89E-02	1.65E-02	1.41E-02
N Zr	9.04E-03	1.21E-02	1.51E-02	1.81E-02	2.11E-02	2.41E-02
Sig P U-235	4471	3112	2296	1753	1364	1073
H/U	186	127	91	67	50	38
I. D.	92510	92510	92509	92509	92508	92508

**96 Inch Fuel Length**

Gm. U-235	3000	4000	5000	6000	7000	8000
Length, In.	96	96	96	96	96	96
Width, In.	7.00	7.00	7.00	7.00	7.00	7.00
Thick, In.	2.625	2.625	2.625	2.625	2.625	2.625
Vol. cu in	1764	1764	1764	1764	1764	1764
Vol. cc	28912	28912	28912	28912	28912	28912
Gm U/cc	0.104	0.138	0.173	0.208	0.242	0.277
CC U	160.43	213.90	267.38	320.86	374.33	427.81
Gm Zr	37541	50054	62568	75081	87595	100108
CC Zr	5775	7701	9626	11551	13476	15401
CC H2O	22976	20997	19019	17040	15062	13083
Gm H2O/cc	0.795	0.726	0.658	0.589	0.521	0.453
N U-235	2.66E-04	3.55E-04	4.43E-04	5.32E-04	6.20E-04	7.09E-04
N H	5.30E-02	4.85E-02	4.39E-02	3.93E-02	3.48E-02	3.02E-02
N O	2.65E-02	2.42E-02	2.20E-02	1.97E-02	1.74E-02	1.51E-02
N Zr	8.57E-03	1.14E-02	1.43E-02	1.71E-02	2.00E-02	2.29E-02
Sig P U-235	4770	3336	2476	1902	1492	1185
H/U	199	137	99	74	56	43
I. D.	92510	92510	92509	92509	92508	92508

### **6.3 Model Specifications (Original Analysis)**

The package was evaluated using Keno 5a/PC, Version 1.2 (ORNL/NUREG-0200). This KENO release incorporates updated Hansen Roach cross sections.

#### **6.3.1 Description of Calculational Model**

Figure 6.3.2 shows the KENO modeling for both the normal and damaged 2600 package in triangular arrays. Square pattern equivalence of triangular arrays is demonstrated in Appendix 6.1.1.

#### **6.3.2 Package Regional Densities**

Table 6.2.2 provides the atomic number densities and appropriate Sig.p values associated with the optimal range of box loading.

### **6.4 Criticality Calculations (Original Analysis)**

This section describes the Calculational model used to determine the nuclear reactivity for the UNC-2600 packages.

#### **6.4.1 Calculation or Experimental Model**

Please refer to Section 6.3.

#### **6.4.2 Fuel Loadings or Other Contents Loading Optimization**

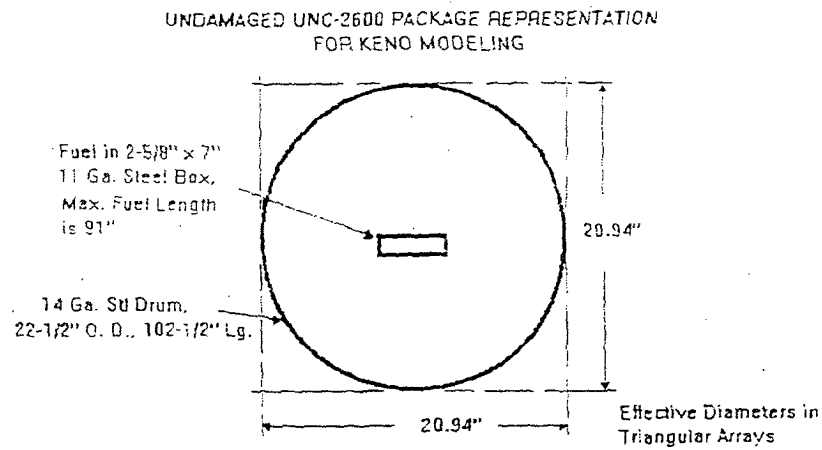
Criticality analysis covers a sufficiently broad range of fuel loadings to identify the optimum value. These analyses demonstrate that the proposed shipping limits satisfy the requirements of Section 10 CFR 71.59 for the array, and 10 CFR 71.55 for a single package.

#### **6.4.3 Criticality Results**

Table 6.4.3 provides the results of KENO analysis for the undamaged and damaged package arrays, as well as the analysis for a single package with full flooding. The KENO input data file for an analysis of an array of undamaged packages is shown in Figure 6.4.3.

Figure 6.3.2

Schematic Representation of KENO Models



Area of a 22-1/2" diameter in a Triangular array is 438.4 sq. inches  
Effective radius in sq. array is 10.47"

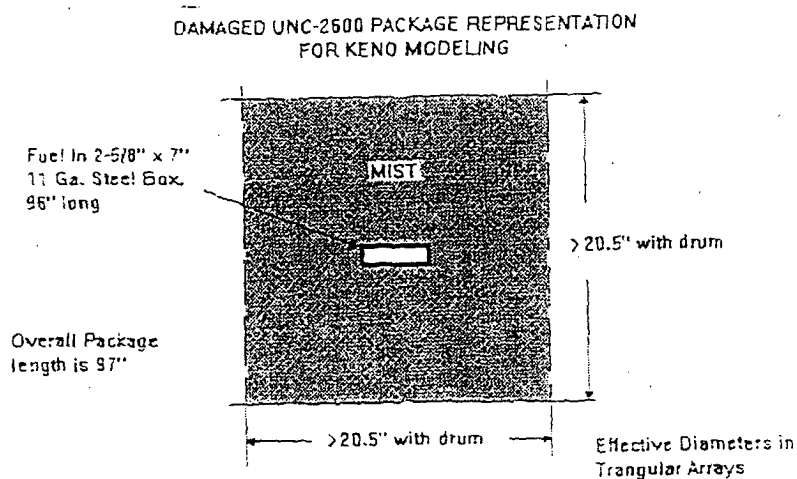


Table 6.4.3

**KENO Evaluation of Array of UNC-2600 Packages**

200 Undamaged Packages in 10 x 2 x 10 Array, 91" Fuel Length

Gm. U-235	
3000	$0.8269 \pm 0.005$
4000	$0.8404 \pm 0.005$
5000	$0.8312 \pm 0.006$
6000	$0.8067 \pm 0.005$

72 Damaged Packages in 9 x 1 x 8 Array, 96" Fuel Length

Gm. U-235	Mist Density			
	<u>0.02</u>	<u>0.04</u>	<u>0.06</u>	<u>0.08</u>
4000			$0.8722 \pm 0.004$	
5000		$0.8978 \pm 0.005$	$0.8987 \pm 0.004$	
6000	$0.8613 \pm 0.004$	$0.8984 \pm 0.005$	$0.8989 \pm 0.004$	$0.8720 \pm 0.005$
7000			$0.8972 \pm 0.005$	
8000			$0.8887 \pm 0.005$	

72 Damaged Packages in 6 x 2 x 6 Array, 96" Fuel Length

Gm. U-235	Mist Density			
	<u>0.02</u>	<u>0.04</u>	<u>0.06</u>	<u>0.08</u>
6000		$0.8983 \pm 0.005$	$0.9075 \pm 0.005$	$0.8824 \pm 0.005$

Single Undamaged Package	$0.6246 \pm 0.004$
Single Damaged Package	$0.6229 \pm 0.005$

Figure 6.4.3

## Sample KENO Data File For Undamaged Package Analysis

```

200 Undamaged 2600 Packages in Triangle Array,    4000 gm U  0.00 Mist
READ PARA
      TME=60.0    GEN=103    NPG=301    LIB=41
      FLX=NO      FDN=NO      AMX=NO      FAR=NO      RUN=YES      END PARA
      MIXT        SCT=1
      1          92510 3.74-4    1102 4.75-2    8100 2.37-2    40100 1.21-2
      2          502 0.00001    MIX=3 100 1.0    MIX=4 502 1.0
END MIXT
READ GEOM
UNIT 1
COM=' Undamaged Package '
CUBOID          1 1 2P8.89          2P115.57          2P3.334
CUBOID          4 1 2P8.89          2P121.92          2P3.334
CUBOID          3 1 2P9.193        2P122.22          2P3.638
YCYLINDER       2 1 26.4           2P130.0
YCYLINDER       3 1 26.59          2P130.2
CUBOID          2 1 2P26.59        2P130.2           2P26.59
END GEOM
READ BOUNDS ALL=WATER END BOUNDS
READ ARRAY  NUX=10  NUY=2  NUZ=10  END ARRAY
READ START  NST=5   NBX=1  END START  END DATA

```

On the basis of the studies reported in Y-1858, "Validation Checks of the ANISN and KENO codes By Correlation With Experimental Data", and Y-1948, "Validation of the KENO Code For Nuclear Criticality Safety Calculations of Moderated, Low-Enriched Uranium Systems"; any calculation yielding  $(k_e + 2\text{sig} + \text{bias}) = 0.95$  is taken as critical.

## 6.5 Critical Benchmark Experiments (Original Analysis)

This section provides justification for the validity of the Computational methods.

### 6.5.1 Benchmark Experiments and Applicability

Benchmark validation of the KENO analysis is documented as stated in Section 6.4.3; above, and shows no meaningful bias. In addition, the operation of the program installed on the PC was verified by running six test cases. The results for this verification are provided in Table 6.5.1, and demonstrate the proper operation of the program.

**Table 6.5.1**

#### **Operational Verification of KENO5A/PC**

<u>KENO Case (1)</u>	<u>Description</u>	<u>k<sub>e</sub></u>
k.01	2C8 Bare	$0.9997 \pm 0.004$
k.03	2C8 with 15.24 cm. Par Refl.	$1.0007 \pm 0.006$
k.04	2C8 with 15.24 cm. Auto. Refl	$0.9979 \pm 0.006$
k.05	2C8 with 12" Par. Albedo	$1.0191 \pm 0.004$
k.12	4 aq., 4 metal	$1.0067 \pm 0.006$
k.18	1F27	$1.0057 \pm 0.008$

- (1) "KENO5A-PC Monte Carlo Criticality Program with Supergrouping", RSIC Computer Code Collection, CCC-548, May, 1991

**6.5.2      Details of Benchmark Calculations**

The details of the benchmark calculations are provided in Y-1858 and Y-1948 cited in Section 6.4.3. The details of the operational checks are provided in CCC-548, and are cited in Table 6.5.1.

**6.5.3      Results of Benchmark Calculations**

Please refer to Section 6.5.2.



## **7.0 Operating Procedures**

The UNC-2600 Package is used to ship up to 375 g U-235 of fuel elements in non-decomposable form, and up to 100% enrichment in the U-235 isotope. The detailed loading and unloading procedures are given below and are in compliance with subpart G of 10CFR71. All operating procedures for the UNC-2600 shipping package are approved by NOG plant management. These procedures have been prepared to meet the intent of NUREG/CR-4775, "Guide for Preparing Operating Procedures for Shipping Packages".

### **7.1 Procedures For Loading Package Discussion and Results**

Each new container must first be inspected by Quality Control as specified in Section 8. Unacceptable shipping packages shall be marked accordingly, and appropriately repaired before use.

#### **PROCEDURE**

1. Assure that the package is to be loaded in accordance with the Certificate of Compliance as specified in written procedures and check lists. Compliance with these procedures and completion of the check list shall be recorded on appropriate shipping documentation.
2. Each UNC-2600 package shall be inspected prior to each use. The following requirements are to be checked;
  - That the maintenance inspections required by Section 8.2 have been conducted within the 12 months of use.
  - Compliance with the requirements of Section 8.2.7.1.
  - That the package is in unimpaired physical condition.
  - Inspect inner box for damage.
  - Inspect bolts for thread condition.
  - Inspect the top closure flange surfaces for damage. Inspect drum lid, ring seal, and locking bolts for damage, and replace as necessary.

3. Requirements for Loading Box:

- Verify that the shipment consists only of fuel elements. Each element may be wrapped in protective plastic.
- Elements shorter than 91" may be positioned with longer oak wood spacers at the ends of the box to prevent their movement during transport.
- Each box is limited to 265 lbs. consisting of elements, wrapping, and wood spacers.
- Each loaded box is to be strapped closed with three (3) 0.02" tk. x 1/2" wide x 24" lg. (approx.) steel banding straps.

4. Requirements for Loading Box into Package:

- Slide the sealed box into the channel, assuring the end is flush with the face of the disk.
- Locate the 12" diam. 1/2" thick steel closure flange to align the bolt into the bolt holes, and secure each bolt with a nut. These are to engage the bolts welded to the backside of the disk, and tightened to a snug closure.

5. Requirements For Sealing Package:

- Place the rubber disk into the package to fill the free space at the front end of the package.
- Close the front of the package with a 14 ga. drum lid which has no gasket.
- Secure this lid with a 12 ga. ring seal, and secure the seal by torquing (40-45 ft. lbs.) the locking bolt into the threaded end of the ring seal. Tighten jam nut against the locking bolt, and apply the tamper-safe seal to the locking bolt.

6. Survey Requirements:

- Removable surface contamination

$\leq 2200$  (beta and gamma) dpm per 100 sq. cm.

$\leq 220$  (alpha) dpm per 100 sq. cm.

- Radiation levels  $\leq 200$  mrem per hour on contact.
  - Radiation levels  $< 10$  mrem per hour at 1 meter.
7. Each shipment of the UNC 2600 package shall require the preparation of, and retention for three years, of those records specified in 10CFR71.91 as appropriate.
  8. Verify that each package has a proper metal identification plate welded to the outer drum.

## 7.2 Procedures For Unloading Package

The UNC-2600 package is designed to be unloaded with commonly available tools and equipment in accordance with the following procedures:

### PROCEDURE

1. Prior to unloading, verify that the following documentation is included with the shipment.
  - Radiological survey data
  - Packing list
2. Conduct a survey prior to unloading to assure that:
  - Removable surface contamination
    - $\leq 2200$  (beta and gamma) dpm per 100 sq. cm.
    - $\leq 220$  (alpha) dpm per 100 sq. cm.
  - Radiation levels  $\leq 200$  mrem per hour on contact
  - Radiation levels  $< 10$  mrem per hour at 1 meter
3. Remove the tamper-safe seal, drum lid, and the rubber disk to expose the bolted closure flange.
4. Loosen and remove the eight closure flange bolt nuts and remove the flange.

5. Remove the inner box from the package using a manual or mechanical means. Remove the three steel closure bands from the box, and remove the elements from the box in accordance with applicable criticality control limits.
6. Replace the empty box into the package, and resecure the closure flange with the eight bolt nuts finger tightened. Replace the drum lid with the ring seal, and secure.

### 7.3 Preparation of Empty Package for Shipment

Empty UNC-2600 packages will be prepared for shipment by verifying the absence of fuel, closing all closure bolts, and securing the lid with a ring seal. The locking bolt is to be tamper-sealed, and appropriate labels are to be affixed to the package exterior to signify that it is empty.

A survey shall be performed on the outer package surface to ascertain that the removable surface contamination is  $\leq 2200$  (beta and gamma) dpm per 100 sq. cm or  $\leq 220$  (alpha) dpm per 100 sq. cm.

## 8.0 Acceptance Tests and Maintenance Program

### 8.1 Acceptance Tests

These tests are to be performed before the package is initially entered into service.

#### 8.1.1 Visual Inspection

- Prior to the initial use of each UNC-2600 package a visual inspection shall be made to assure the following requirements are met:
- There are no tears to the outer package.
- That the closure flange bolts can be properly secured without interference.
- The lid lip and top drum curl fit properly and are not damaged to the extent that the closure ring will not fit the outer drum.

**8.1.2      Structural and Pressure Tests**

No structural or pressure tests are required. Vendor and/or receipt inspections and annual maintenance inspections for dimensions and weld integrity verify structural adequacy.

**8.1.3      Leak Tests**

There are no requirements for leak tests of the package.

**8.1.4      Component Tests**

The following tests, inspections, and verifications apply to the components of the shipping package:

- The closure flanges shall be identified to assure tracability to certification of composition and heat treatment. These flanges shall also be free of raised metal, burrs, or significant dents.
- The rubber disks shall be identified to assure tracability to certification of composition.

**8.1.5      Tests for Shielding Integrity**

Not applicable.

**8.1.6      Thermal Acceptance Tests**

Not applicable.

**8.2      Maintenance Program****8.2.1      Structural and Pressure Tests**

A general inspection of the shipping package shall be made annually while in service. See Section 8.2.7.1. Maintenance shall be performed prior to placing containers back into services once removed.

**8.2.2      Leak Tests**

Not applicable.

**8.2.3      Subsystem Maintenance**

Not applicable.

**8.2.4      Valves, Rupture Discs, and Gaskets on Containment Vessel**

Not applicable.

**8.2.5      Shielding**

Not applicable.

**8.2.6      Thermal**

Not applicable.

**8.2.7      Miscellaneous**

The following inspections are to be conducted;

**8.2.7.1      Within 12 Months Before Use, and Annually while in service.**

- The outer surface of the drum shall be visually inspected for rust and scratches. Such defects shall be sanded off and repainted. Any significant dents will be reworked.
- The inner cage will be removed from the outer drum and inspected for rust and broken welds. The former will be sanded and repainted, and the latter repaired.
- The bottom closure flange shall be inspected to assure that the bolt nuts are properly secured.

**8.2.7.2 Prior to Every Shipment**

- Inspect inner box for damage.
- Inspect bolts for thread condition.
- Inspect the top closure flange surfaces for damage.
- Inspect drum lid, ring seal, and locking bolts for damage, and replace as necessary.

**Appendix 2.10.1**

**Drawing B-2600-2, Sheets 1,2,3,4,5 and 6  
Current Package Design**



*Figure Withheld Under 10 CFR 2.390*

THOMAS GUTMAN CONSULTANT W. HARTFORD, CT.		
Drawn BY RH Date 10/21/93	UNC-2600	
Approved BY TG Date 10/21/93	UPGRADED PACKAGE	
Reviewed BY WK Date 10/21/93		
NOT TO SCALE	DWG. # B-2600-2	REV. 3
SHEET 1 OF 6		

Figure Withheld Under 10 CFR 2.390

THOMAS GUTMAN CONSULTANT W. HARTFORD, CT.		
Drawn BY RH Date 10/21/93	UNC-2600	
Approved BY IG Date 10/21/93	UPGRADED PACKAGE	
Reviewed BY WK Date 10/11/93	DWG.# B-2600-2	REV. 3
NOT TO SCALE		
SHEET 2 OF 6		

*Figure Withheld Under 10 CFR 2.390*

THOMAS GUTMAN CONSULTANT W. HARTFORD, CT.		
Drawn BY RH Date 10/21/93	UNC-2600	
Approved BY IG Date 10/21/93	UPGRADED PACKAGE	
Reviewed BY WK Date 10/21/93		
NOT TO SCALE	DWG. # B-2600-2	REV. 3
SHEET 3 OF 6		

### Scrap Assembly Box

Item #	# Reqd.	Name of Part	Stock Size	Material
1a	1	Bottom Plate	11 Ga. x 7" x 96"	LCCGS
1b	2	Side Plate	11 Ga. x 2-5/8" x 96"	LCCGS
1c	2	End Plate	11 Ga. x 2-5/8" x 7-1/4"	LCCGS
1d	1	Lid	11 Ga. x 96-1/4" x 7-9/16" (Approx.)	LCCGS
1e	1	Hinge	MS-35830-2D, (or Equiv.) 0.093" tk. x 96" lg.	Steel
1f	2	Side Angle	1" x 1" x 1/8" x 96-1/4" Angle	LCCGS
1g	2	End Angle	1" x 1" x 1/8" x 7-1/4" Angle	LCCGS
1h	2	Wood Positioner	2-3/8" x 2-1/2" x 6-3/4"	Oak wood
1i	1	Grip Wire Assy.	3/16" diam. wire x Approx. 16" lg including swaged ball shank.	Gal. or stainless steel
1i(a)	2	Tab	Ball retained by 1/4" tk. x 9/16" x 3/4" steel tabs welded to box. 5/16" hole in tabs to engage swaged ball.	
1i(b)	2	Tapered protector (optional)	1/4" tk. x 9/16" high x 2-1/2" lg. tapered at both ends to 1/4" land on top to help guide box into cage.	Steel
1j	3	Banding Straps	0.02" tk x 1/2" x 24" (approx) With 0.02" lockclips	Steel

- Box seam welds are continuous. Side angle welds 1/8" fillet, 3" lg. every 6" for the 96" lengthwise runs. Welds for packages procured on or before 10-9-92 are visually inspected. Welds for new construction are per AWS D-1.3.
- Matl. LCCGS is low carbon, commercial grade steel, also referred to as "mild steel"

### Barrel Assembly

Item #	# Reqd.	Name of Part	Stock Size	Material
2a	1	Bottom Drum	14 Ga. 22-1/2" O. D. x 52" lg. Drum	LCCGS
2b	1	Top Drum with no bottom	14 Ga. 22-1/2" O. D. x 52" lg Drum	LCCGS
2c	1	Lid with no gasket	14 Ga. for 55 gal. Drum	LCCGS
2d	1	Ring Seal with 5/8" Bolt Closure drilled for tamper seal.*	12 Ga. For 55 gal Drum Bolt is torqued to 40-45 ft. lbs.	LCCGS

\* Ring seal per 49CFR 178.103-5, 1988 edition.

- Welds are continuous. Welds for packages procured on or before 10-9-92 are visually inspected. Welds for new construction are per AWS D-1.3
- Matl. LCCGS is low carbon, commercial grade steel, also referred to as "mild steel"

<b>Revisions/Date</b> REV 1 8-27-93 1.) ADD SHEETS 4,5 2.) GRIP WIRE REV. TO 3/16" DIA. AIRCRAFT WIRE ATTACHED WITH PAD EYES, OR EQUIV. 3.) END VIEW REV. TO SHOW ANGLE 4.) BOLTS TO SAE GRADE 5 5.) IMPROVED ASSEMBLED VIEWS FOR CLARIFICATION	<b>Revisions/Date</b> REV 2 9-08-94 GRIP WIRE IS 3/16" DIAM. AIRCRAFT CONTROL WIRE. APP. 16" LG. USE OF WIRE ON BOTH ENDS OF BOX OPTIONAL WIRE CONNECTED USING 1/4" TK. 9/16" x 3/4" TK. STL TABS WELDED TO BOX. 1/4" FILLET WELDS SPACED TO ACCOMMODATE WIRE IN 5/16" HOLE. WIRE SECURED USING SWAGED BALL AND SINGLE SHANK. TABS MAY BE PROTECTED WITH TAPERED PROTECTOR TO EASE PLACEMENT INTO CAGE.	<b>Revisions/Date</b> REV 3 10-18-94 10/24/94 "GRIP WIRE ASSEMBLY" USED AS DEFINITION TO REPLACE PRIOR REFERENCES TO "AIRCRAFT GRIP WIRE" AND "AIRCRAFT CONTROL WIRE". ONE GRIP WIRE ASSEMBLY PER BOX.	<b>THOMAS GUTMAN CONSULTANT</b> <b>W. HARTFORD, CT.</b> Drawn BY RH Date 10/21/93 Approved BY TG Date 10/21/93 Reviewed BY WK Date 10/21/93 NOT TO SCALE DWG.# B-2600-2 REV. 3
SHEET 4 OF 6			

## Cage Assembly

<u>Item #</u>	<u># Reqd.</u>	<u>Name of Part</u>	<u>Stock Size</u>	<u>Material</u>
3a	9	Cage Disk	3/8" x 21-1/2" diam	LCCGS
3b	8	Rib	1/4" x 1-3/4" x 97" bar	LCCGS
3c	4	Support angle	1-1/2" x 1-1/2" x 1/8" angle, 97" lg	LCCGS
3d	16	Stiffener angle	1" x 1" x 1/8" angle, 11-45/64" lg.	LCCGS
3e	4	Support angle	1" x 1" x 1/8" angle, 97" lg.	LCCGS
3f	16	Bolts	7/8" diam x 1-3/4" lg, with lock washers and nuts to fit	SAE Grade 5
3g	2	Closure Flange	1/2" tk x 12" diam	4130 AMS 6370 stl, Ht trt to Rock. C =28 -33 60 Durometer, ≤ 2500 psi Rubber Bell Brittle point, -70 F.
3h	2	Rubber bumper	19" diam x 1-3/4" tk	

- Welds are 3/16" fillet. Welds for packages procured on or before 10-9-92 are visually inspected. Welds for new construction are per AWS D-1.1.
- Matl. LCCGS is low carbon, commercial grade steel, also referred to as "mild steel"
- Closure flange bolts with lock washers are snugged, but not torqued.
- Closure flange and rubber bumper to be physically marked to identify the steel or rubber, to show the steel hardness, and to identify the drawing number. Cognizant QC to mark.

## Name Plate

<u>Item #</u>	<u># Reqd.</u>	<u>Name of Part</u>	<u>Contents of Plate</u>	<u>Material</u>
4a	1	Name plate	1/16" tk, and sized to fit lettering	LCCGS or SST

Plate spot welded to drum, engraved with 1/2" high lettering to show at least:

- Model UNC-2600
- Gross weight of package: 1105 lbs.
- Cert. of Compl. number 5086
- 1/8" lettering to show  
Year of manufacture  
Serial #

## Weights

Package Gross Weight: 1105 lbs  
Maximum Weight of Contents: 265 lbs.

## Inspection and Acceptance Criteria

- All parts to be free of raised metal, burrs, or significant dents and rust.
- Verify the identification on the Closure Flanges and the Rubber disks. These shall be traceable to the material identification, and the heat treat processing.
- Verify weld inspections for new packages. These must be certified to AWS D-1.1 or D-1.3.
- For packages procured by B&W prior to 10-9-92, verify that all welds are visually acceptable.
- Verify the presence of a name plate showing the model number and maximum gross weight.

<u>Revisions/Date</u>	<u>Revisions/Date</u>	<u>Revisions/Date</u>	<b>THOMAS GUTMAN CONSULTANT W. HARTFORD, CT.</b>		
REV 1 8-27-93 1) ADD SHEETS 4.5 2) GRIP WIRE REV. TO 3/16" DIA. AIRCRAFT WIRE ATTACHED WITH PAD EYES, OR EQUIV. 3.) END VIEW REV. TO SHOW ANGLE. 4.) BOLTS TO SAE GRADE 5 5.) IMPROVED ASSEMBLED VIEWS FOR CLARIFICATION	REV 2 9-08-94 GRIP WIRE IS 3/16" DIAM. AIRCRAFT CONTROL WIRE. APP. 16" LG. USE OF WIRE ON BOTH ENDS OF BOX OPTIONAL WIRE CONNECTED USING 1/4" TK. 9/16" x 3/4" TK STL TABS WELDED TO BOX 1/4" FILLET WELDS SPACED TO ACCOMMODATE WIRE IN 3/16" HOLE. WIRE SECURED USING SWAGED BALL AND SINGLE SHANK. TABS MAY BE PROTECTED WITH TAPERED PROTECTOR TO EASE PLACEMENT INTO CAGE	REV 3 10-18-94 10/20/94 "GRIP WIRE ASSEMBLY" USED AS DEFINITION TO REPLACE PRIOR REFERENCES TO "AIRCRAFT GRIP WIRE" AND "AIRCRAFT CONTROL WIRE". ONE GRIP WIRE ASSEMBLY PER BOX.	Drawn By RH Date 10/21/93	UNC-2600	REV. 3
			Approved By TG Date 10/21/93	UPGRADED PACKAGE	
			Reviewed By WK Date 10/21/93	DWG.# B-2600-2	
			NOT TO SCALE		
SHEET 5 OF 6					

*Figure Withheld Under 10 CFR 2.390*

<b>THOMAS GUTMAN CONSULTANT W. HARTFORD, CT.</b>		
Drawn BY RH Date 10/21/93	UNC-2800	
Approved BY TG Date 10/21/93	UPGRADED PACKAGE	
Reviewed BY WK Date 10/21/93	DWG.# B-2800-2	REV. 3
NOT TO SCALE		
SHEET 0 OF 6		

**CERTIFICATE OF COMPLIANCE 5086;**

**Appendix 2.10.2**

**UNC-2600 PACKAGE**

**January, 2009**

Appendix 2.10.2

Drawing B-2600-1  
Original Package Design

Figure Withheld Under 10 CFR 2.390

THOMAS GUTMAN CONSULTANT W. HARTFORD, CT.		
Drawn by R.D.H. Date 11/1/92	UNC-2600 PACKAGE AS TESTED	
Approved by T.G. Date 11/1/92		
Scale: NOT TO SCALE	DWG# B-2600-1	Rev 0



**Appendix 2.10.3**

**Photographs and depiction of Package Drop**

Figure 3 - Container at free fall test position

Figure 4 - Container showing damage after free fall test

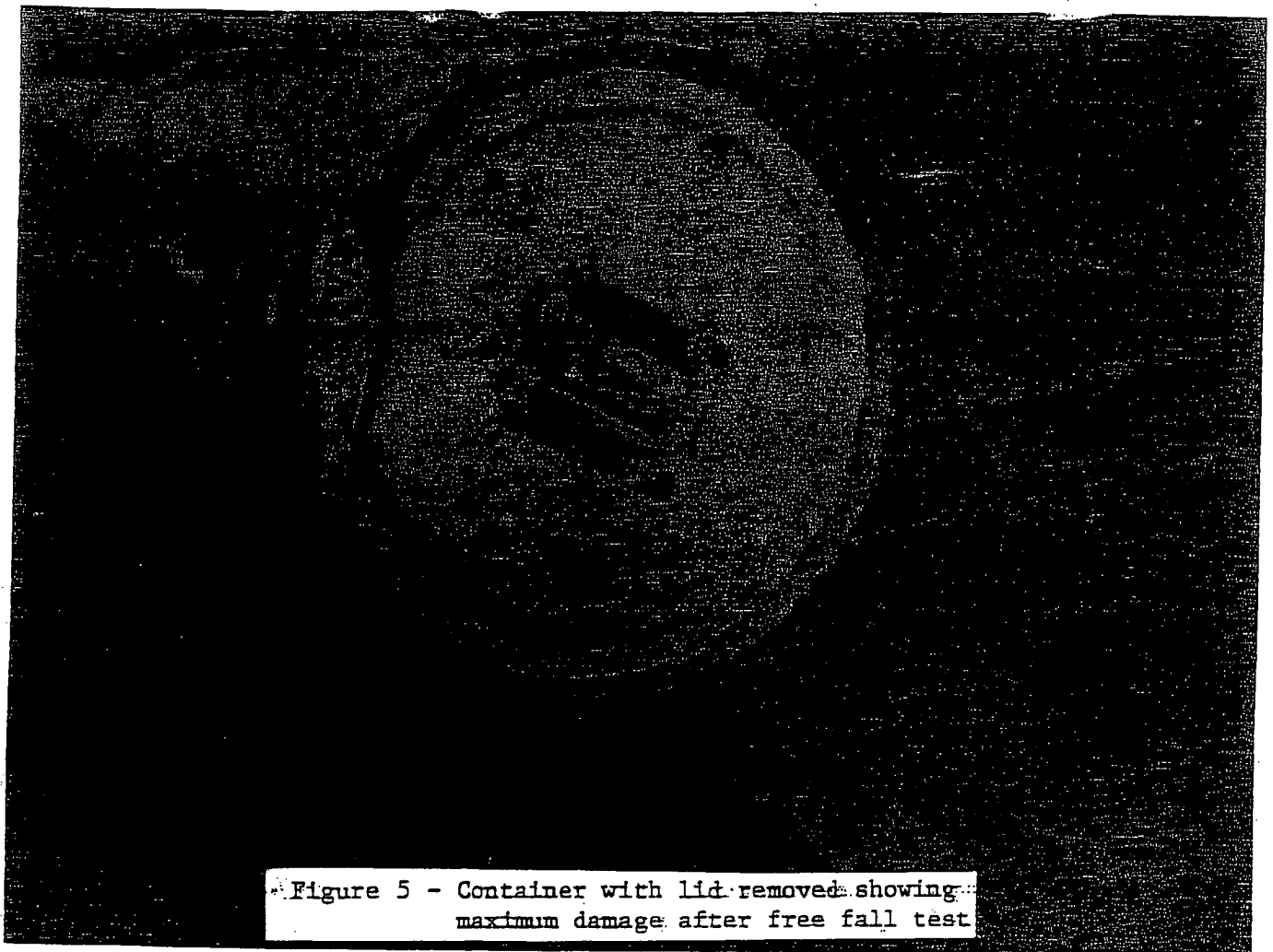
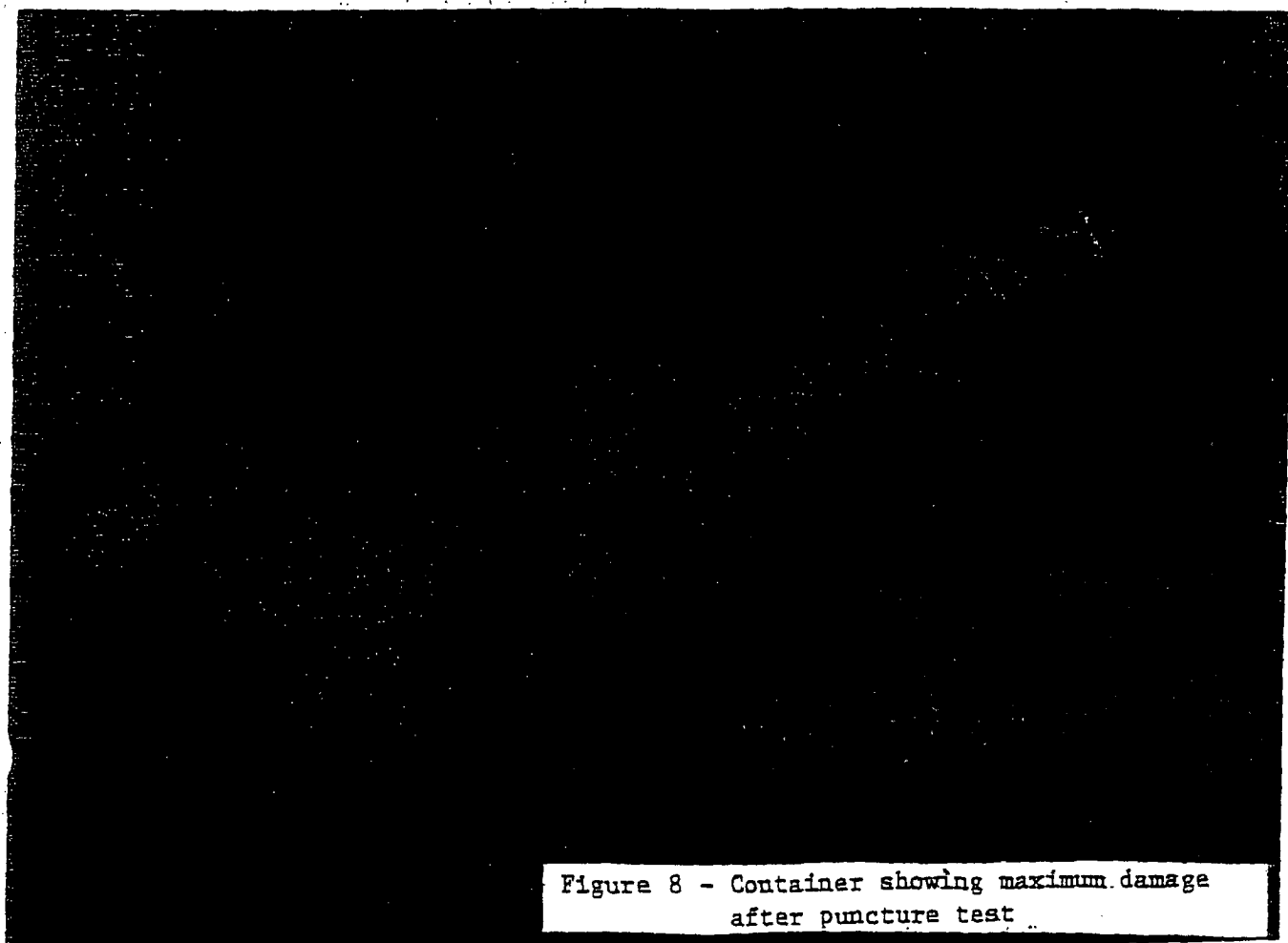
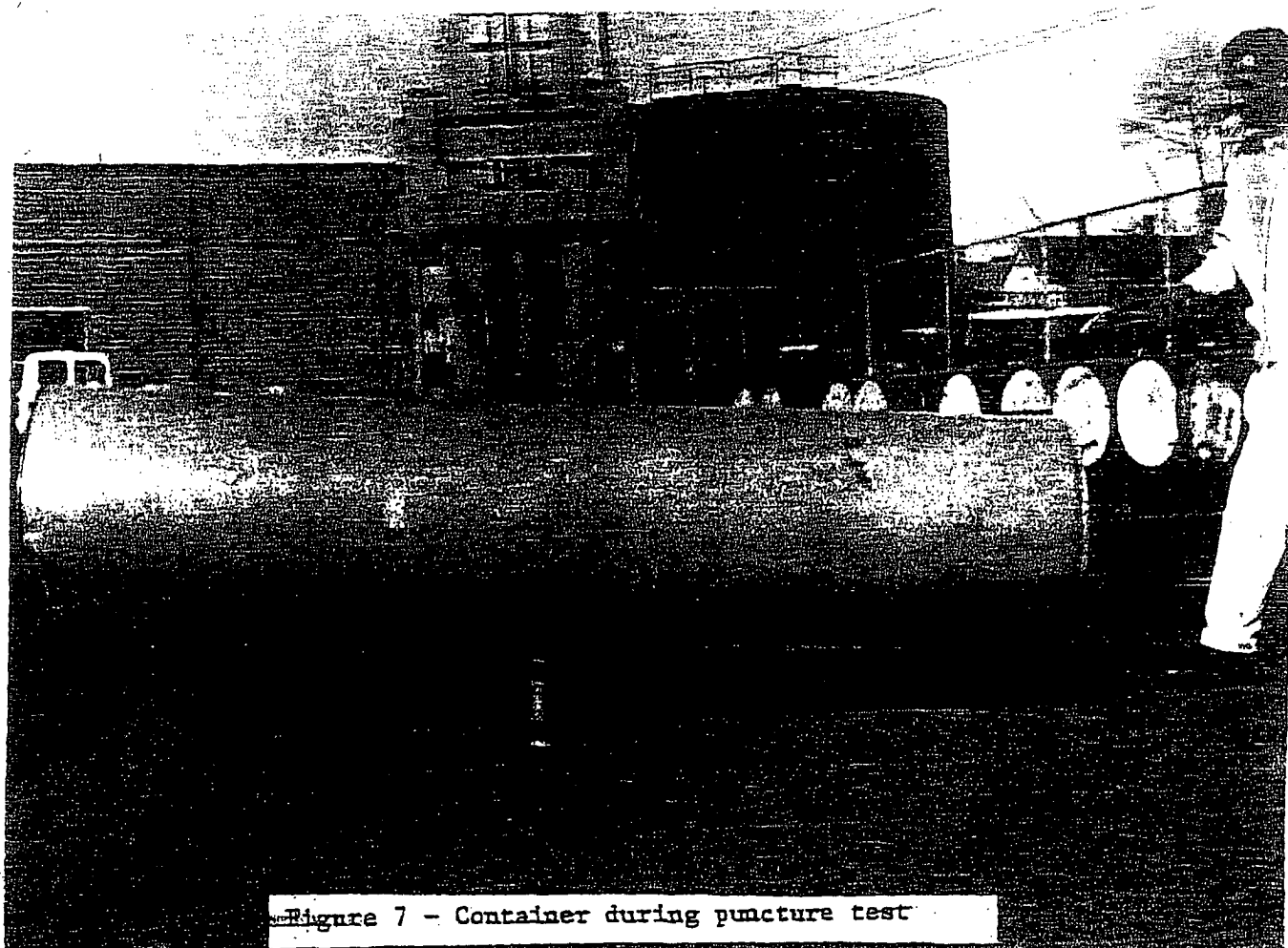


Figure 5 - Container with lid removed showing maximum damage after free fall test

Figure 6 - Deleted



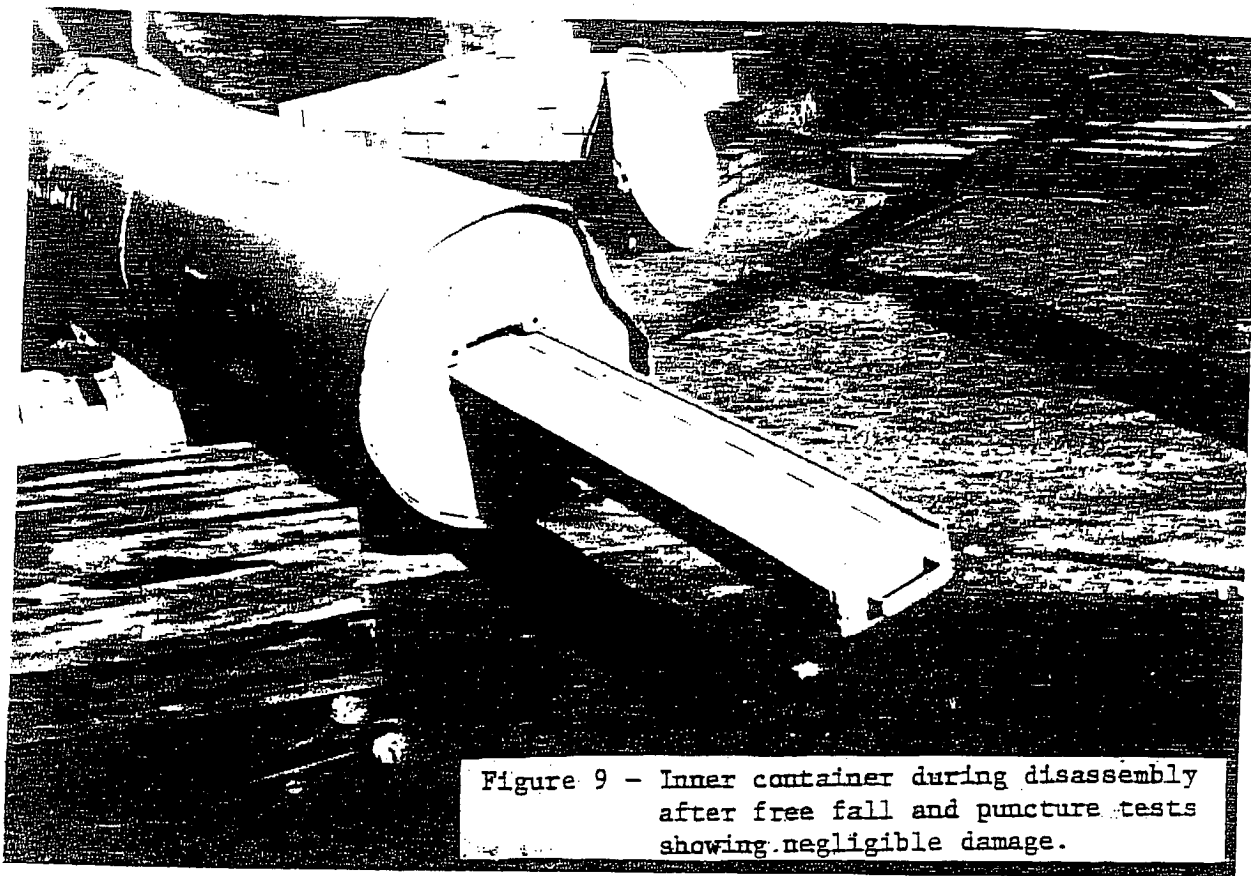
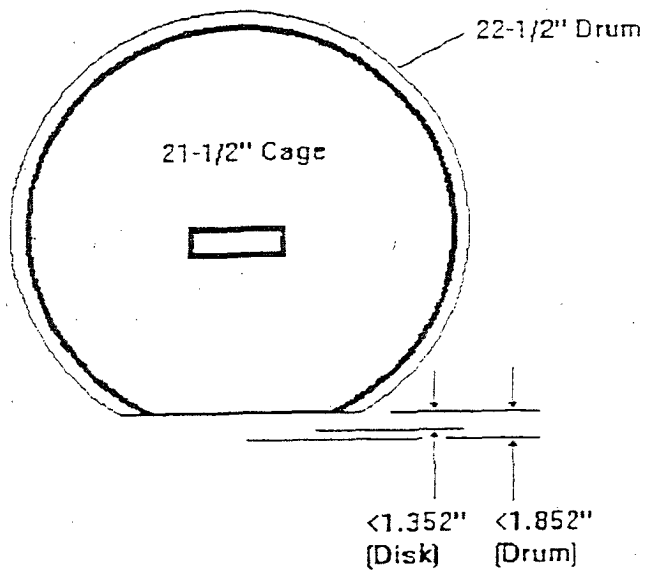


Figure 9 - Inner container during disassembly  
after free fall and puncture tests  
showing negligible damage.

Figure 10 of Appendix 2.10.3



Area of damaged drum in a triangular array is >421.1 sq. inches.  
Effective radius in sq. array is >10.26"  
FEA analysis shows less displacement.

Appendix 2.10.4

Finite Element Analysis of Current Design

# **Nonlinear Finite Element Drop Analysis of Nuclear Scrap Shipping Drum**

Dr. Kenneth W. Brown  
Computer-Aided Structural Analysis  
(203)-872-3020  
Nov. 5, 1993

## SUMMARY

Detailed, nonlinear transient finite element analyses of the end, side, and angle drops of a scrap shipping package onto a rigid floor from a height of 30 feet have been conducted. The analyses predict that for all drop orientations the fuel box will remain safely contained within the cage after conclusion of the event. While the outer drum and the shipping cage themselves are predicted to sustain significant permanent deformation and damage, the closure flange and the associated retention bolts are predicted to remain well within minimum strength and load limits.

## DISCUSSION

The goal of the current analysis is to show analytically that the scrap shipping drum design can survive a drop in any orientation from a height of 30 feet, onto a rigid floor. This verification has been performed by analytically simulating and studying the system response to the following drop events:

1. an end drop from a height of 30 feet, followed by a second drop onto a steel pin, from a height of 40 inches,
2. a side drop from a height of 30 feet,
3. an angle drop with the drum center of gravity located directly over the drum corner, and
4. drop at an angle of 45 degrees from a height of 30 feet.

The shipping package drop event is a highly nonlinear phenomenon, with energy being dissipated through plastic deformations of the outer drum and the cage, as well as through hyperelastic deformations of a rubber energy absorbing disk. The accurate analytical solution of such a problem, with its plasticity, possible material failures, and complex contact interactions would have been quite impractical just a few years ago. Today, however, due to advances in computer hardware and structural analysis software, such a detailed analysis is indeed feasible to perform, using today's high speed workstations and nonlinear finite element transient analysis programs.



## **Analytical Approach**

Due to the highly complex, nonlinear nature of the shipping drum drop event, an analysis of this event requires a robust, general analysis code, with detailed nonlinear geometric, material, and interaction capabilities. This technology is today most efficiently available through the application of explicit transient finite element analysis procedures.

The current analyses have been performed using the public domain version of the DYNA3D (Reference 1) code. DYNA3D is one of the leading codes for nonlinear, transient finite element analysis in use today, with very general material, failure, and contact capabilities. To facilitate DYNA3D analysis preprocessing and postprocessing, Computer-Aided Structural Analysis (CASA) has developed two data format translators, that enable the preprocessing and postprocessing of DYNA3D analyses to be conducted using the ANSYS program (Version 4.4A) (Reference 2).

Thus, for the current analyses, all finite element models were constructed using the powerful solid modelling capabilities of the ANSYS PREP7 preprocessor. The models were subsequently translated into DYNA3D input files using the CASA proprietary ANSDYN program. The translator automates the generation of not only the basic finite element mesh, but also automates creation of boundary conditions, contact surfaces, and initial velocities.

The DYNA3D analysis, when run, creates the D3PLOT series of binary time history results files. This series of files was subsequently translated to ANSYS FILE14.DAT text results files by the DYNANS program. This results file, after subsequent conversion to binary FILE12.DAT format via the AUX1 module of ANSYS, was then postprocessed in ANSYS, using both the POST1 general postprocessor, and the POST26 time history postprocessor.

## **Geometry Overview**

The shipping container redesign, drawing B-2600-2, shown on Figures 1 to 3, 3A and 3B, is an improved version of a currently successfully used configuration. The redesign upgrades the scrap box retention disc to a high strength steel, held in place by 8 retention bolts, as well as incorporating many other enhancements.

The shipping container consists of a scrap box, contained within a cage, inside a shipping drum. The lid of the drum is held on by a circular clamp. During a drop, it is acceptable for the lid to separate from the drum. It is not acceptable, however, for the scrap box to become free of the support of the cage.

## Finite Element Model Overview

In any finite element analysis, certain approximations are required regarding the representation of the structure and its geometry and boundary conditions. To create an accurate yet computationally efficient model for the complex drum drop analysis, symmetry considerations were used, where appropriate. The finite element model of the shipping drum employed a combination of beam, shell, and brick elements. Critical, crushable areas, including the first cage disk, the closure flange, and the rubber, were modelled using detailed brick element meshes. Beam elements were used to simulate the disk to closure flange bolts. The beams connected nodes on opposing faces of the first disk and the closure flange, and were placed at actual bolt locations, to properly simulate the bolted connection, and also to allow later extraction of detailed bolt loading histories. In areas away from the critical first disk/closure flange region, shell elements were employed. Thus, the mass and stiffness of all areas of the shipping drum were well represented. An overview of the quarter symmetry model used for the end drop analysis is shown on Figure 4, which illustrates plate elements in blue, and brick elements in purple.

The cage structure was modelled using a combination of shell and brick finite elements. Brick elements were used for the first disc, to provide detailed analysis of local stresses, including angle iron connections, closure beam stresses, and closure flange contacts. The remainder of the cage, including discs and angle iron and strap supports, was constructed using quadrilateral shell bending elements, shown on Figure 5. Thus, shell elements were used in the model of the second through ninth discs, the inner angle irons, and the outer straps. Further, shell elements were used to model the top closure flange. The cage model was constructed of separate component parts, oriented such that the merging of coincident nodes would connect the angle irons and the outer straps to the disc models, including the connection with the first disc.

The bottom cage disc, shown in red on Figure 6, was modelled using brick elements, to include analytically the proper contact definitions with both the closure flange and the rubber bumper, and also to provide the closure flange bolt contacting surface. Due to these requirements, the model of this first disc contains more detail than the models of the other cage discs, to provide for compatibility with the angle irons, the outer cage ribs, and also the closure flange bolt circle. Thus, in the disc finite element model, nodal points were included at the 0, 45, and 90 degree (measured counter-clockwise from horizontal on Figure 6) angular locations, at a 5" radius, so that beam elements could be employed to connect the closure flange to the disc, accurately simulating the bolted flange connection, as well as flange to disc interactions during a drop analysis. Contact surfaces were included for interactions between the first disc and the closure flange, as well as between the first disc and the rubber bumper. (A contact surface is here defined as an analytical barrier that allows two bodies to separate, but will not allow them to interpenetrate. These nonlinear contact interactions also include friction effects.)

The fuel box is held within the cage by a 1/2" thick, 12" diameter closure seal, bolted to the first cage disc using 8 bolts on a 10" diameter bolt circle. The seal was modelled using brick elements, and is the green component of Figure 6. The model included nodal points on a 5" radius, at the 0, 45, and 90 degree angular locations, compatible with the bolt locations on the first cage disc, for the bolt elements, to be included separately. Contact surfaces on the closure seal were included to allow the analysis to monitor contact interactions between the seal and the first cage disc, as well as seal to fuel box and seal to rubber bumper interactions. Notably, the contact surface between the end cap and the first disc will carry only compression. All tensile loads across this interface must be carried by the beam bolt elements.

The closure seal is connected to the first cage disc using eight 7/8" bolts evenly spaced angularly on a 5" radius bolt circle. For this DYNA3D finite element model, the bolts were included as beam elements, with axial stiffness (based on bolt shank area) only. Thus, only axial loads may be carried by the bolted connections. The bolt elements physically connect nodes on the bottom face of the closure seal to nodes on the top face of the first cage disc. Thus, the model incorporates a realistic bolt length and stiffness. Where appropriate, based on symmetry condition, the areas of bolts on symmetry planes were halved. In later extracting bolt loads from the beam post data, then, we must double the analysis bolt loads along symmetry planes. Full area bolt elements were assigned an area of .419 square inches, corresponding to the area at the bottom of the thread of a 7/8" American Standard Bolt (Reference 3).

In modelling the top closure seal, plate elements were employed. Coincident nodes were included in the model at the three bolt locations. Thus, the top seal became connected to the top cage disc by a merger of coincident nodes, giving a good approximation to the seal to disc connection, although we are not able to extract bolt loads at this upper connection.

Notably, the point to point approach to modelling the bolted attachments forces all of the load from a bolt into the single nodal points at the end of the bolt, rather than distributing the bolt load over a designated washer surface area. Thus, given the level of detail in the current model, the analysis results will be conservative regarding local contact stresses at the disc/bolt interfaces. In the limit of very fine meshes, the current approach would yield unacceptably high local stresses, requiring that the washer be included in the model. For the current level of modelling detail, which was in large part dictated by the computer requirements of the highly detailed, nonlinear, transient finite element analysis, the single point load distribution is appropriate, and somewhat conservative. The possibility of the bolt shearing a hole through the first cage disc under the nut footprint will be considered separately when we review analysis results.

Additionally, this analysis considers that the bolts are snug, without appreciable preload. A bolt preload would tend to delay closure seal to disc separation, with minimal increase in maximum bolt load, but has not been included in the current analytical model.

The rubber bumper energy absorber was modelled using brick elements, and is shown in blue on Figure 6. Its geometry consists of a 1.75" thick 10.5" radius disc, with a 1/2" thick, 6.1" radius cut-out to fit over the end cap. Contact surfaces were included between the front face of the rubber and either ground or the drum seal, depending on the analysis case. Additional contact considerations include the rear face of the rubber and the first cage disc, as well as the rear face of the cut-out and the closure seal. Additionally, for the end drop condition, the nodes of the rubber outer diameter are constrained against radial and tangential motion, to account for the lip of the outer drum barrel. This encapsulation of the rubber allows the generation of hydrostatic pressure, thus adding to its crush resistance.

The scrap box assembly, the long brick segment seen in Figure 4, was approximated as a homogeneous box, 2.625" x 7" x 96" long. The box was given the elastic modulus of steel, with a density of .218 lb/in\*\*3, to yield a proper total mass of 385 lb. Notably, this is a conservative approach to modelling the scrap box, for the wood blocks at the ends of the scrap box assembly will absorb some energy from the scrap material during the drop, which is neglected by the current level of analysis detail. Contact surfaces account for the interactions of the scrap box and the closure seal, as well as the interactions between the scrap box and the inner support angle irons. For the end drop analyses, the load box is assumed to be in initial axial contact with the closure seal. The load box is otherwise constrained only by symmetry and contact considerations.

For the analyses of the angle drop conditions, the effects of the barrel assembly were included. The barrel drum was modelled as a cylinder, 22" in diameter, .078" thick, and 100.5" long, using shell elements. The barrel lid was modeled (also using shells) as a .078" thick circular plate, 22" in diameter, with corner nodes to match the nodes of the barrel.

At assembly, the barrel lid is attached to the barrel via the ring seal. The drum construction is specified to withstand 20 psi of internal pressure. In the barrel/lid finite element model, then, it would not be appropriate to assume parent material at the barrel/lid interface. Instead, in the finite element model a series of breakable joints was employed around the circumference to model the junction of the barrel with the lid. In DYNA3D, this was accomplished by using the sliding interface type 8, node spotwelded to surface. Making the conservative assumption that the lid would separate from the barrel at 15 psi of barrel internal pressure, a joint was constructed at each lid/barrel drum node, with the appropriate failure load.

Barrel and lid contact surfaces consisted of the following:

1. Cage disks to barrel,
2. Cage outer straps to barrel, and
3. Rubber energy absorber to lid.

## Materials

The cage and drum are constructed of low carbon commercial grade steel. To ensure that the drop analysis utilized minimum yet realistic capabilities for this material, the following procedure was employed:

1. 1010 steel was assumed.
2. Using the ASM Handbook (Reference 4), p205, the following minimum properties were found:
  - E = 30.E6 psi
  - Density = .3 lb/in\*\*3
  - Yield Stress = 30,000 psi
  - Ultimate Stress = 49,000 psi
  - Ductility = 15%

Within DYNA3D, material type 24, Rate-Dependent Tabular Isotropic Elastic-Plastic, was employed, using bilinear hardening, with a plastic hardening modulus of .127E6 psi. This material model includes general strain hardening, as well as element failure based on a maximum for plastic strain. When any element integration point exceeds the plastic strain limit, the stresses in that element are effectively set to zero throughout the rest of the analysis. The analysis continues, although that section of the model carries no further load.

The closure flange is constructed of 4130 steel, of Rockwell Hardness 28 to 33. Tensile test of a specimen of the 4130 steel gave the following properties:

- Yield Stress = 106,700 psi
- Ultimate Stress = 126,400 psi
- Ductility = 18%

This material was modelled in DYNA3D similarly to the low carbon steel, but with adjusted properties, and a plastic hardening modulus of .109E6.

The cap retention bolts are constructed of SAE Grade 5 steel. Marks Mechanical Engineering handbook (Ref 3) lists the proof stress of this material as 85 ksi, along with a yield stress of 92 ksi. For the analysis, DYNA3D material type 1, elastic was used. As will be shown later, during the drop event, no bolts exceed the proof stress level, thus validating the linear elastic material characterization that was employed.

The energy absorbing rubber end bumper is fabricated of a 60 Durometer, greater than or equal to 2500 psi rubber, with a brittle point temperature of at least -70 degrees F., and an elongation of at least 6.0. Lacking an actual compressive stress-strain curve for this material, a detailed hyperelastic model, such as a Mooney-Rivlin representation, could not be employed. Instead, within DYNA3D, material type 7, Blatz-Ko Hyperelastic Rubber, was used. Besides the material density, this material model requires only the material shear modulus, G. The value used for G was determined by evaluating an average elastic modulus,  $E = \text{ultimate stress} / \text{elongation} = 416.67 \text{ psi}$ . Assuming that the material responds incompressibly (poisson's ratio,  $\nu = .5$ ), G was evaluated as:

$$G = E / (2 * (1 + \nu)) = E / 3 = 138.9 \text{ psi.}$$

## **ANALYSIS RESULTS**

### **End Drop Analysis**

In the end drop event, the lid end of the shipping drum strikes a rigid wall, perpendicular to the drum axis. For the analytical simulation of this event, a quarter symmetric model was employed. Due to the relatively small strength of the barrel lid retention, for this analysis the lid and the barrel were not included. The outer lip of the barrel was assumed present only to the extent that it provides radial support to the rubber end bumper. The barrel is assumed able to arrest its own motion. For the present analysis, then, the cage, the end bumper, and the scrap box were modelled using finite elements, to determine the time response to a 30 foot drop.

The shipping box was assigned an initial axial velocity of 527.4 inches per second, corresponding to the velocity in free fall from a height of 30 feet. The bottom end of the rubber strikes a rigid wall shortly after the analysis initiates. Figure 7 shows the analysis displacement history for points along the centerline of the load cell, at its top, middle, and bottom. The load cell comes to rest at a time of .0035 seconds, and begins to rebound from that point.

Figure 8 shows an overall effective (von Mises) stress snapshot of the drum end drop model (rubber energy absorber removed), taken at the .005 second time point. The initial velocity was down the drum axis, toward the ten o'clock position on figure 8. Displacements are true to scale, showing significant bending of the bottom cage disc, as well as significant buckling of the outer cage straps, between the first and second, and second and third discs.

#### **Closure Flange Stress:**

In the closure flange, the peak stress occurs at the .003 second time point, just as the load cell is coming to rest. Figure 9 shows the von Mises stress distribution in the closure flange at this highest stress point. As seen in the Figure, much of the flange is stressed above the 106.7 ksi yield stress of this high strength steel. However, if we examine the plastic strains in the closure flange, as shown on Figure 10, we find a maximum plastic strain of 6.6%, which is well below the measured material ductility of 18%. This peak plastic strain occurs at the outer corner of the load box.

#### **Bolt Loads, Bolt Head Displacements:**

Figure 11 shows a time history of the loads on the 0, 45, and 90 degree bolts connecting the end cap to the first disc. For the bolts on symmetry planes, the loads have been doubled to reflect the total load in the bolt. The maximum bolt load from the analysis is predicted to be 7744 pounds, at a time of .0015 seconds into the drop event. Given the minimum bolt cross sectional area of .419 square inches, this results in a maximum bolt axial stress of 18,500 psi. Notably, this result gives a factor of safety of 4.9 over the bolt

proof stress of 85 ksi. A fully stressed bolt would thus carry a maximum load of 35,600 pounds.

Figure 12 shows a time history of the bolt head displacements, at the 0, 45, and 90 degree bolt locations. Notably, the rubber energy absorber is initially 1.25" thick in the area between the closure flange and the drum lid. For a 7/8" bolt, Reference 5 gives a maximum bolt head height of .620", which thus leaves a bolt head clearance of .63". Thus, the bolt heads are predicted to fully penetrate the rubber, contacting the floor, at the .0015 second time point. While this contact was not included in the analysis (bolt heads were not modelled), it is not expected to significantly change the load box retention response.

**Additional possible failure modes at the bolts include:**

1. the nut head may shear through the first disc, and
2. the nut (or bolt) threads may strip.

To study the possibility of the nut head shearing through the bottom cage disc, consider the response of the disc section immediately under the nut head. Reference 5 gives the minimum width across the flats of the 7/8" nut as 1.269". If we take this dimension as the diameter of a circular plug to be sheared through the first disc thickness, the surface area of the shear plug is its circumference times its thickness, or  $A_{\text{plug}} = 1.495$  sq. in. At the maximum bolt load of 7744 pounds, this results in an average plug shear stress of 5200 psi, which is well below a pure shear yield stress of 15 ksi for this soft steel. At shear-through, the bolt load would thus have to be 22,425 lb.

To consider the possibility of bolt thread stripping, note equations 15.2, 15.7, and 15.8 of Reference 6. Assuming simultaneous failure of both the bolt and nut thread, the maximum bolt force allowed is:

$$F = 2 * S_u * A_s$$

where:  $S_u$  = ultimate shear strength of bolt material, and  
 $A_s$  = shear stress area of bolt threads.

Assuming that three threads are involved in the thread engagement, the shear stress area is:

$$A_s = 3 * \text{Pitch Circum} * \text{Pitch Length}$$

For a 7/8 x 9 bolt, Reference 5 gives  $R_s$  (pitch inner radius) as .3533", and the pitch as .111". Thus,  $A_s = .739$  sq. in. For a material shear allowable of 42 ksi, the thread stripping load is seen to be 31,000 pounds, which is quite significantly above the maximum analysis bolt load of 7744 pounds.

### First Cage Disc:

The bottom cage disc is predicted to exhibit some material failure under the drum end drop. As such, it is somewhat deceiving to study just von Mises stresses – failed elements will have a zero stress! We may keep track of failed elements by noting those elements with an accumulated plastic strain beyond the material ductility limit, however.

At the .003 second time point, when the load cell is coming to rest, 5 elements in the bottom disc model have strained beyond failure. Figure 13 shows the bottom disc von Mises stresses at this .003 second time point, with all failed elements removed. Notably, the failed elements all occur at the inner angle iron to disc junction. Figure 14 shows the disc plastic strains at this time point. While some angle iron junction elements have failed, the great majority of the disc remains intact.

By the .005 second time point, 12 elements from the bottom disc model have failed. All of the failed elements are in the vicinity of the inner angle iron, however. Thus, after the drop has completed, the edge straps and the second interior angle iron remain connected to the bottom disc, and the cage remains intact.

### Rubber:

Figure 15 shows a deformed to scale effective stress contour plot of the rubber, at the .003 second time point, which is the time of maximum rubber stress. Notably, there is significant thinning of the rubber at its central section, under the pressure of the closure flange. Flow to the thicker outer edges has occurred, due to the hydrostatic state, and the outer diameter boundary condition imposed by the outer drum. The maximum effective stress in the center of the rubber, is slightly above ultimate. Any failure in the rubber would be limited to this local central section, however. Also, by this time, the load cell has essentially been halted, and its energy has all been absorbed. The rubber, then, with the possible exception of a small region near its center, is predicted to remain intact after the end drop has been completed.

### End Drop Results Summary:

The shipping drum is predicted to survive the end drop event, with some local damage to the energy absorber, and loss of the weld between the first cage disc and the interior angle iron.

### 40 Inch Redrop

To be fully acceptable, the shipping drum, after having survived the 30 foot drop, must also survive a 40 inch drop onto an 8" high, 6" diameter steel pin. To consider the effects of this redrop, the following situation was analyzed in DYNA3D:

1. For the redrop, consider that the drum lid has popped off, and the rubber energy absorber has fallen out.



2. To account for damage due to the previous drop, the inner angle iron was disconnected from the first cage disc.
3. Initial shipping drum velocity is 175.8 in/sec (40 inch free fall).
4. The drum symmetrically strikes the steel pin at the closure flange.

To analyze the above conditions, the rubber was removed from the DYNA3D model. An elastic steel pin was added, and fully constrained at its bottom. Contact conditions were imposed between the bottom of the closure flange and the top of the steel pin. The redrop analysis finite element mesh is shown on Figure 16, color coded by material.

Due to the close proximity of the load cell, the closure flange, and the pin, the load cell is halted very quickly, and in fact bounces from the steel pin/closure flange. Figure 17 shows the displacement history for the top, middle, and bottom of the load cell during this redrop event. The cage comes to rest well after the load cell motion has been halted, however, finally halting at the .003 second time point. In part, the cage is halted by the damaged bottom disc. Most of the cage motion, however, is halted by the reaction of the top closure flange contacting the upper end of the load cell. Loads pass through this upper flange, to the top disc, and in turn to the entire cage, halting it by the .003 second time point. Figure 18 shows the axial deflections for the entire model at the .003 second time point. Note that most of the axial deflection gradient occurs through bending of the cage discs.

The peak closure flange stress during the redrop event occurs at the .0003 second time point. The peak effective stress of 60.2 ksi, shown in Figure 19, is well below the material yield stress.

The maximum bolt load is predicted to be 2726 lb, at the .0008 second time point. This is safely below the bolt damage level.

The maximum stress in the first cage disc occurs at the .0009 second time point. The disc stress distribution is shown on Figure 20. Some yielding has occurred at the remaining inner angle iron, but stresses are well below limit values.

In the steel cage shell model section, the stresses peak initially at the secondary interior angle iron, which was intact after the initial drop. After the .001 second time point, the upper closure flange contacts the top of the load cell, and stresses begin to develop in the upper flange, and upper angle iron sections. The cage stresses peak at the .0024 second time point, and are shown on Figure 21. While some of these cage stresses are above yield, none are at all close to the material limit stress.

#### Redrop Analysis Results Summary:

With the innermost angle iron weldment disconnected from the first cage disc, the cage structure is still strong enough to survive with no further material failure the drop from 40" onto a steel pin.

### **Shipping Drum Side Drop Analysis**

To determine the response of the shipping drum to a direct side landing of a drop from 30 feet, the finite element model was adjusted somewhat from that used for the end drop analysis. For this analysis, half symmetry was used by reflecting the previous quarter symmetry model about the X axis. The rubber energy absorber was deleted. Additionally, the first disc model was changed to a plate model. The DYNA3D finite element model used for the side drop analysis is shown in Figure 22.

The shipping box was assigned the initial drop velocity of 527.4 inches per second. The bottoms of the cage spacer discs strike a rigid floor shortly after the analysis initiates. The load box is assumed to be initially centrally located within the cage, and is restrained only by cage contact interactions and the analysis symmetry plane. As such, the load box has an initial clearance of .6875". To monitor vertical displacements correctly, then, we must either follow actual disc nodes, or deduct the .6875" clearance from the load cell deflections.

Figure 23 shows the analysis load cell relative vertical displacement history for points along the centerline of the load cell, at its end and middle. The maximum cell displacement, reflected in compressing of the spacer discs, is .516", occurring at the .003 second time point. Figure 24 shows the vertical deflections of the entire model, at the critical .003 second time point. The maximum deflection occurs at the central disc, although in general there is little bending of the load cell.

The maximum spacer disc effective stresses occur at the .003 second time point, and are shown in Figure 25 for the central (highest stressed) disk. The peak stress occurs at the inner angle iron junction, under the load cell bearing load. While stresses in the spacer disc are above yield, no material is predicted to fail. Figure 26 shows the vertical deflections of the central disc. The two sections that show appreciable deformation are:

1. At the bottom of the disc, which has flattened to create a broader footprint to the ground, and
2. Under the inner angle iron junction.

#### **Side drop results summary:**

A side hit after a 30 foot drop results in no material loss. The maximum cage disc vertical deflection during this drop event is .516".

### **Angle Drop Analysis, CG Over Corner**

A commonly analyzed, challenging drum impact orientation is an angular impact, with the drum center of gravity located directly over the corner where contact will first occur. For this analysis, a half symmetry model is again appropriate. The model, viewing the cut-away side, and turned so that the rigid floor is at the bottom of the page, is shown

color coded by material in Figure 27. During an angled drop impact, the effects of the barrel drum and lid closure may well prove important. As such, shell models of these components have been included. The lid to drum lock consists of breakable contact connections, as discussed earlier.

As with the previous drop analyses, the shipping box was given an initial total velocity of 527.4 in/sec, but now oriented 12 degrees off the barrel axis, to properly orient the CG over the barrel corner. Shortly after the analysis commences, the box nodes begin to encounter the rigid floor.

Figure 28 shows the vertical displacement time history of the node at the bottom of the load cell, along the barrel centerline. The maximum vertical displacement of 3.306" occurs at the .008 second time point. Figure 29 shows the deformed shape of the DYNA model, at the .009 second time point – when the load cell has begun to rebound from its drop. Notably, the barrel lid has broken its retention. The rubber has been squeezed, and slid to the left side of the drum, but has absorbed much of the energy of the drop. The right cage straps, as well as the right side of the barrel, have buckled under the impact loadings.

#### Closure Flange Stresses:

The peak stress in the closure flange occurs at the .008 second time point. Figure 30 shows the von Mises effective stresses at this most severe time point. The closure flange shows significant bending during this angled drop event, with stresses above yield. Figure 31 shows the plastic strains at this time point. The maximum plastic strain of 7.4% remains well below the material limit of 18%.

#### Bolt Loads:

Figure 32 shows the bolt load history (full loads) for the CG over corner drop. The maximum bolt load of 9278 lb occurs in the bottom bolt, at the .003 second time point, as the lower corner of the bottom disc is bending due to interactions with the rigid floor. This bolt load is safely below the bottom disc shear-thru load of 22,425 lb.

#### First Cage Disc:

The bottom cage disc is heavily worked by this angle drop event. By the .012 second time point, 48 of the disc finite elements have experienced failure. Figure 33 shows the disc stresses at this time point. The failed elements carry no stress, and are primarily located at the 10 o'clock position (upper 45 degree rib connector), with a few more failed elements located at the inner angle iron connection points. Thus, DYNA3D is predicting that the support bar welds at one of the outer ribs, and at the inner angle irons, will fail under this angled impact. However, four rib connections remain (although some of the ribs are buckled), along with the second (wider placed) set of interior angle irons.

### Cage Shells:

Figure 34 shows the stresses in the cage shells at the .009 second time point. The maximum stress of 35 ksi, at an inner angle iron, is above yield, but well below the material ultimate stress of 49 ksi. Thus, even though some of the angle irons show significant buckling, no material failure is expected.

### Rubber:

The peak stress in the rubber for this angular drop occurs at the .008 second time step, and is shown on Figure 35, as viewed looking from the cage towards the rubber, with the symmetry plane to the left. The peak value of 2590 psi is slightly above the material limit. Interestingly, the location of the peak rubber stress corresponds with the failed area of the bottom cage disc outer diameter. Under the hydrostatic pressure experienced by the rubber, a segment is being extruded through the hole created on the bottom cage disc. In the more critical crushing area under the closure flange, the rubber stresses are below 2 ksi.

### CG Over Corner Results Summary:

DYNA3D predicts the following responses to the CG over corner drum drop:

1. No bolt failures.
2. Loss of bottom cage disc connection to one edge strip.
3. Loss of bottom cage disc connection to two inner angle irons.
4. Local extrusion failure of some rubber local to the failed section of the bottom cage outer diameter.

### Angle Drop Analysis, 45 Degree Drop

To investigate the shipping drum response to an orientation that would result in significant disc rolling moment, the response to a 45 degree drop was studied. The shipping drum hits the ground on the bottom of the drum, which gets significantly bent. This side comes to a stop vertically, while a gross rotation of the drum occurs, until a side impact ultimately brings the drum to rest. To carry the DYNA3D analysis to this full conclusion would be prohibitively time consuming, however. The current analysis was carried past the maximum first disc and closure disc stresses, and we will study those results.

Figure 36 shows a to-scale deformed shape plot of the 45 degree drop at the .012 second time point. At this time, the cage left corner has essentially stopped vertically, and the drum is pivoting about this end, towards a side hit.

#### Closure flange:

The peak stress in the closure flange reaches 99200 psi at the .009 second time point. This peak stress occurs at the 7:30 bolt position, when the flange is viewed from below. Some plastic strain does occur in the flange - .029 in/in plastic strain is reached by the .012 second time point. This is well below the 18% material ductility limit, however.

#### Bolt loads:

The maximum bolt load occurs in the bottom bolt, and is 7734 lb., well below the bottom disc shear-thru limit of 22,425 lb.

#### Cage:

The first cage is predicted to lose significant amounts of material in the vicinity of the lower inner angle irons. By the .012 second time point, 90 disc finite elements are predicted to have failed. By the .010 second time point, 86 had already failed, so the significant damage was sustained between .008 and .010 seconds into the event. Figure 37 shows the first disc stress distribution at the .012 time point, with the failed elements removed. Notably, the elements near the innermost lower angle iron have completely failed. This failure has propagated to the 7:30 bolt connection point, severing the disc at this bolted connection location.

The cage shell elements peak in stress at the .009 second time point. Figure 38 shows a local view of the cage end stresses at this critical time. The end of the innermost lower interior angle iron has failed, causing the blue triangle of zero stress heading towards the floor. Recall that a failed element has no strength. The nodal points retain their mass, however, and are now free to deform their associated element definitions, making the results look artificially severe.

Note also the inward buckling of the lowest outer cage support under the impact with the rigid floor.

#### Rubber:

The peak stress in the rubber is 923 psi, and occurs at the .003 second time point. This stress level is well below the 2500 psi material strength.

#### Lid and Outer Drum:

On impact with the floor, the bottom of the outer drum is severely bent, causing the lid to pop off, and freeing the rubber. A close up view of this cage/drum/lid/rubber interaction at the .012 second time point is shown on Figure 39. Notably, the outer drum barrel has bent around the lowest cage disc, effectively locking the cage into the drum, even though the lid has popped open. The maximum drum stress is 38,800 psi, at the .006 second time point. This stress value is above yield, but well below the material ultimate strength

of 49,000 psi. Thus, while the drum barrel will undergo significant permanent deformation, the only failure predicted by DYNA3D is the popping off of the lid.

#### 45 Degree Drop Results Summary:

DYNA3D predicts that the cage will remain intact, although significantly damaged, after the 45 degree drop. The lower inner angle iron to first cage disc connections are predicted to fail, along with the connection of the lower 45 degree angle bolts. The remaining angle iron to first cage disc connections stay intact, however.

The lid is predicted to pop off the barrel, freeing the rubber. The drum barrel will bend around the bottom cage disc, entrapping the cage within the drum.

## SUMMARY OF ANALYSIS CONSERVATISMS

For the analysis of these complex drop events, every effort has been made to ensure the accuracy of the analysis model, including proper load paths, contact relationships, and geometries. Any finite element analysis model has some approximations, however. Where approximations were made, every effort has been made to ensure the conservatism of the model. These conservatisms (and their possible ramifications) include:

1. Bolts, modelled as tension/compression only beams, are connected from solid element node to node. This results in a higher than actual local head stress distribution.
2. Should the elements under the bolt head fail, the bolted joint will become immediately disconnected, although in reality the bolt must be pulled completely through the plate before the connection can be fully severed.
3. The load cell is modelled as homogeneous. In reality, it is a box, containing waste, with hardwood at its ends. The wood, not included in the analysis, is capable of absorbing some of the energy of the system on impact.
4. The barrel to lid connection is designed for 20 psi barrel internal pressure. The lid connection of the analytical model assumes the lid will pop off at a load equivalent to 15 psi.
5. Minimum properties were used for all materials.
6. In DYNA3D, when an element fails, it is set to a condition of zero stress – DYNA3D's element failure algorithm fails an entire element by zeroing its stiffness at the instant that the element exceeds the plastic strain (ductility) limit. Thus, the analysis essentially "vaporizes" sizable chunks of material. In an actual drop event, cracks would form, and connections would be severed over time, but the material would remain present, capable of absorbing energy in certain deformation modes.

## SUMMARY OF ANALYSIS RESULTS

Four impact orientations have been studied, with varying amounts of damage predicted to the shipping drum system, with damage occurring most often at the junction of the first cage disc and the inner-most angle iron support. In all cases, however, DYNA3D predicts that the cage will retain sufficient integrity after the drop event.

Of the orientations studied, the most severe load observed in the closure flange retention bolts was 9278 lb, during the CG over corner drop orientation. The vertical hit and the 45 degree hit both gave bolt loads of 7800 lb. While there is no guarantee that the CG over corner drop is indeed the most severe orientation for the closure bolts, the bolt load is such a weak function of the hit orientation angle that it is extremely difficult to expect another orientation to suddenly more than double the observed bolt loads to the limit value of 22425 lb for cage disc bolt head shear-through. As such, we can safely conclude that the closure flange retention is a good design, and will remain intact for a 30 foot drop of any orientation.



## DYNA3D VERIFICATION

DYNA3D [1] is widely recognized as one of the leading explicit transient nonlinear finite element analyses available today. It is utilized by the military, academia, and industry for a wide range of applications, including ballistic impacts, automobile crashes, rotor blade containment, and pipe whip. The code has an extensive library of finite elements and material characterizations. As such, it is neither feasible nor appropriate to fully validate the analytical capabilities of DYNA3D for this report. Instead, let us verify the accuracy of the current installation of the public domain version of the DYNA3D code, and the combination of DYNA and ANSYS, using the proprietary ANSDYN and DYNANS translators.

For the solution of the shipping drum drop problem, both brick and shell element technologies were employed, along with extensive use of nonlinear contact and plasticity capabilities. By showing that the current DYNA3D installation can accurately utilize these capabilities for two of the example cases of Reference 7, we will validate the current code installation.

DYNA3D example problem 1 consists of a cylindrical bar impacting a rigid wall at a right angle. This example problem utilizes brick elements and material plasticity, and is in many regards similar to the current analyses. Initially, difficulties were encountered in matching the results of Reference 7 for this geometry. Later study of the data set for this sample problem as provided by Lawrence Livermore Labs revealed a typographical error in Reference 7. The bar actually has a .32 cm RADIUS, not the .32 cm diameter listed on page 10 of Reference 7. After this adjustment was made, nearly perfect correlations with the Reference 7 results were noted. Figure 40 shows the displacement time history for the projectile top surface central node. This corresponds very closely with Figure 2.3 of Reference 7. Reference 7 reports a displacement of -1.087 cm at a time of 75. The current analysis did not have a history snapshot at this time. At a time of 80, however, the current analysis reports a displacement of -1.086. Figure 41 shows the plastic strain distribution in the projectile at the 80 time point. This correlates extremely well with Figure 2.4 of the Reference. Indeed, the maximum plastic strains of 2.805 are identical. Thus, for brick elements, plasticity, and contact, the current ANSYS and DYNA3D combination works very well, duplicating the results of Reference 7 for example problem 1.

DYNA3D example problem 8 simulates an impact on a section of a cylindrical shell, and is useful for validating the shell element technology employed in the cage model of the current analyses. Figure 42 shows the y displacement history of analysis node 8, corresponding to Figure 9.3 of Reference 7. Again, nearly perfect correlation is noted with the reference. Figure 43 contours the von Mises equivalent stresses at the .001 time point. This figure compares extremely well with Figure 9.7 of Reference 7, after noting that, accounting for symmetry, another half of the shell has been added to the figure in the Reference.

## REFERENCES

1. DYNA3D, a Nonlinear, Explicit, Three-Dimensional Finite Element Code for Solid and Structural Mechanics – User Manual. R. G. Whirley. UCRL-MA-107254, May, 1991.
2. ANSYS Engineering Analysis System User's Manual. G. J. DeSalvo. Swanson Analysis Systems, May, 1989.
3. Standard Handbook for Mechanical Engineers. Baumeister and Marks, eds. Seventh Edition, McGraw-Hill, 1967.
4. Metals Handbook, Vol. 1 ASM International, Mar. 1990.
5. Machinery's Handbook. Industrial Press, 21<sup>st</sup> Edition.
6. An introduction to the Design and Behavior of Bolted Joints. John H. Bickford, Marcel Dekker, Inc., 1981.
7. DYNA3D Example Problem Manual. S. C. Lovejoy and R. G. Whirley, UCRL-MA-105259, Oct. 1990.

## RESUME

Dr. Kenneth W. Brown  
13 Valley View Dr.  
Tolland, Ct. 06084  
203-872-3020

### Employment History:

Pratt & Whitney, Division United Technologies, East Hartford, Ct.:

1970 to 1975;

Analytical Engineer in Structures Technology group. Involved in the development of shell finite element codes.

1975 to 1980;

Senior Analytical Engineer in Structures Technology group. Involved in the development of finite element transient computer codes for the analysis of foreign object ingestion damage. Developed a full nonlinear transient Kevlar containment analysis capability.

1980 to 1990;

Research Engineer in Structures Technology group. Responsible for development of automated blade design packages, with application to compressor, fan, and propfan stages. Responsible for maintenance, development, and user education for P&W's NASTRAN installation, including associated pre and post processing capabilities. Responsible for design and analysis of hollow fan blades involved in a blade-out event.

Computer-Aided Structural Analysis, Tolland, Ct. :

1990 to Present;

Consulting in field of finite element analysis and technology development. Support and education for usage of the ANSYS general purpose finite element program. User education for the NASTRAN and PATRAN programs. Software development, including development of a fluid load model for MARC dynamic analysis. Application of the ANSYS program to difficult, nonlinear design problems. Application of the DYNA3D nonlinear transient analysis to containment, contact, and impact dynamics applications.

Hartford Graduate Center, Hartford, Ct.:

1984 to 1987;

Adjunct Lecturer in Mechanical Engineering department, teaching graduate courses in basic and advanced finite element analysis.

1987 to Present;

Adjunct Associate Professor in Mechanical Engineering department, teaching graduate courses in basic and advanced finite element analysis.

Education:

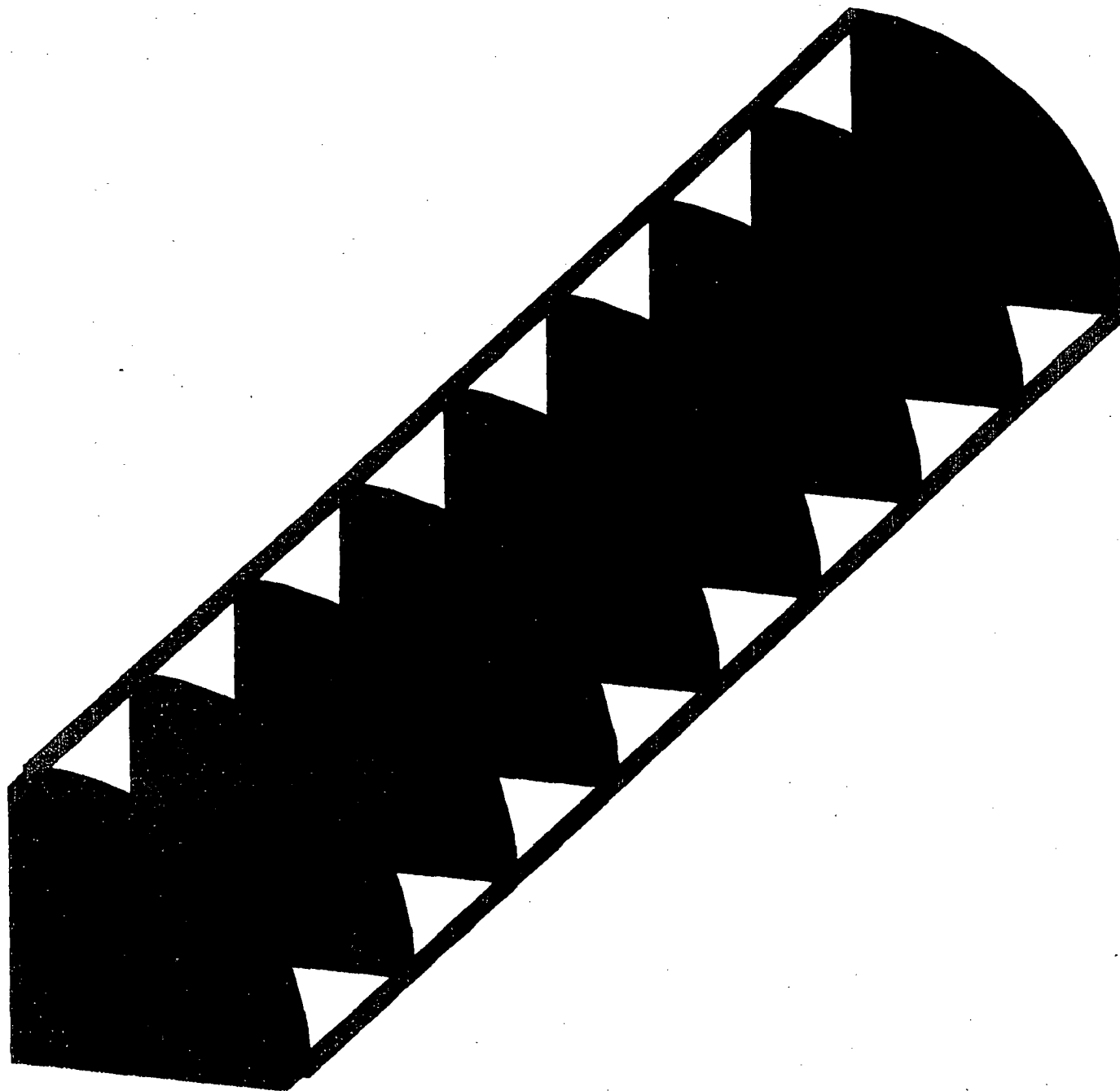
BSME: Worcester Polytechnic Institute, 1970.

MS: Rensselaer Polytechnic Institute, 1973.

Dr. Eng: Rensselaer Polytechnic Institute, 1980.

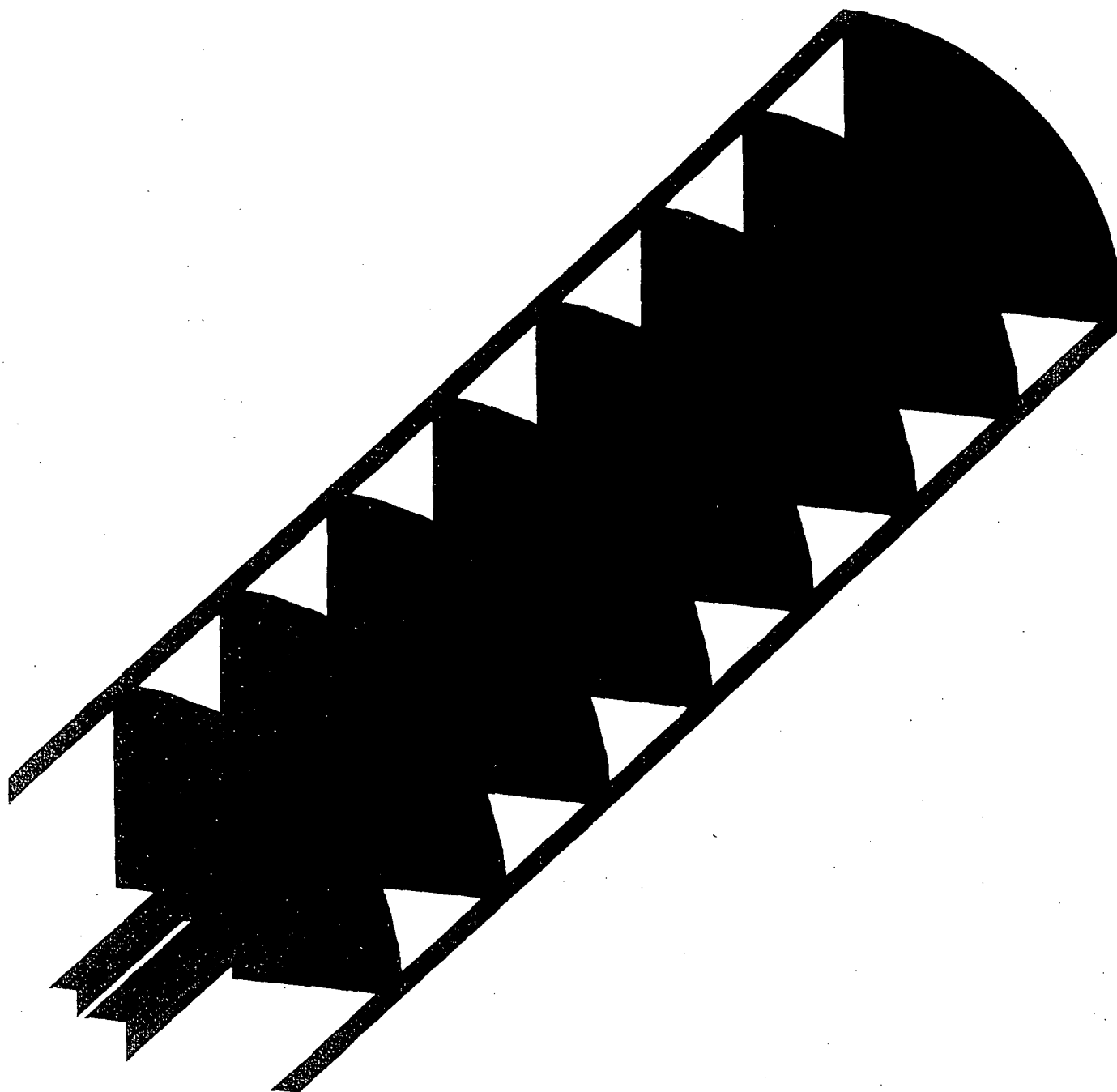
Publications:

Available on Request



ANSYS 4.  
OCT 19 1993  
13:17:25  
PLOT NO. 1  
PREP7 ELEMENTS  
TYPE NUM

XV =-1  
YV =-1  
ZV =3  
DIST=22.676  
XF =5.375  
YF =5.375  
ZF =46.938  
PRECISE HIDDEN



ANSYS 4.  
OCT 19 1993  
13:18:39  
PLOT NO. 1  
PREP7 ELEMENTS  
TYPE NUM

XV =-1  
YV =-1  
ZV =3  
DIST=22.306  
XF =5.375  
YF =5.375  
ZF =48  
PRECISE HIDDEN

# Load Cell End Drop, Cell Displacements

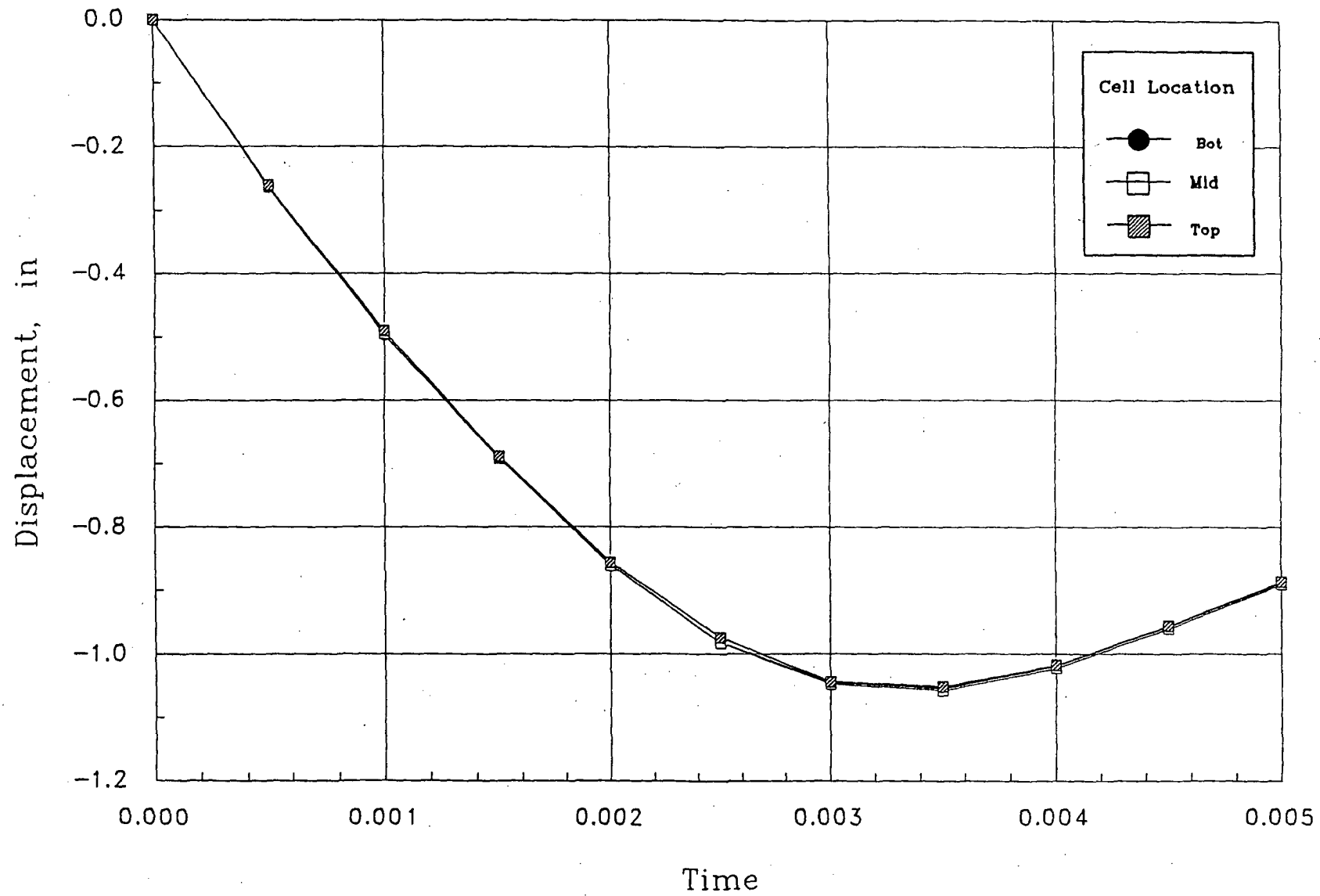
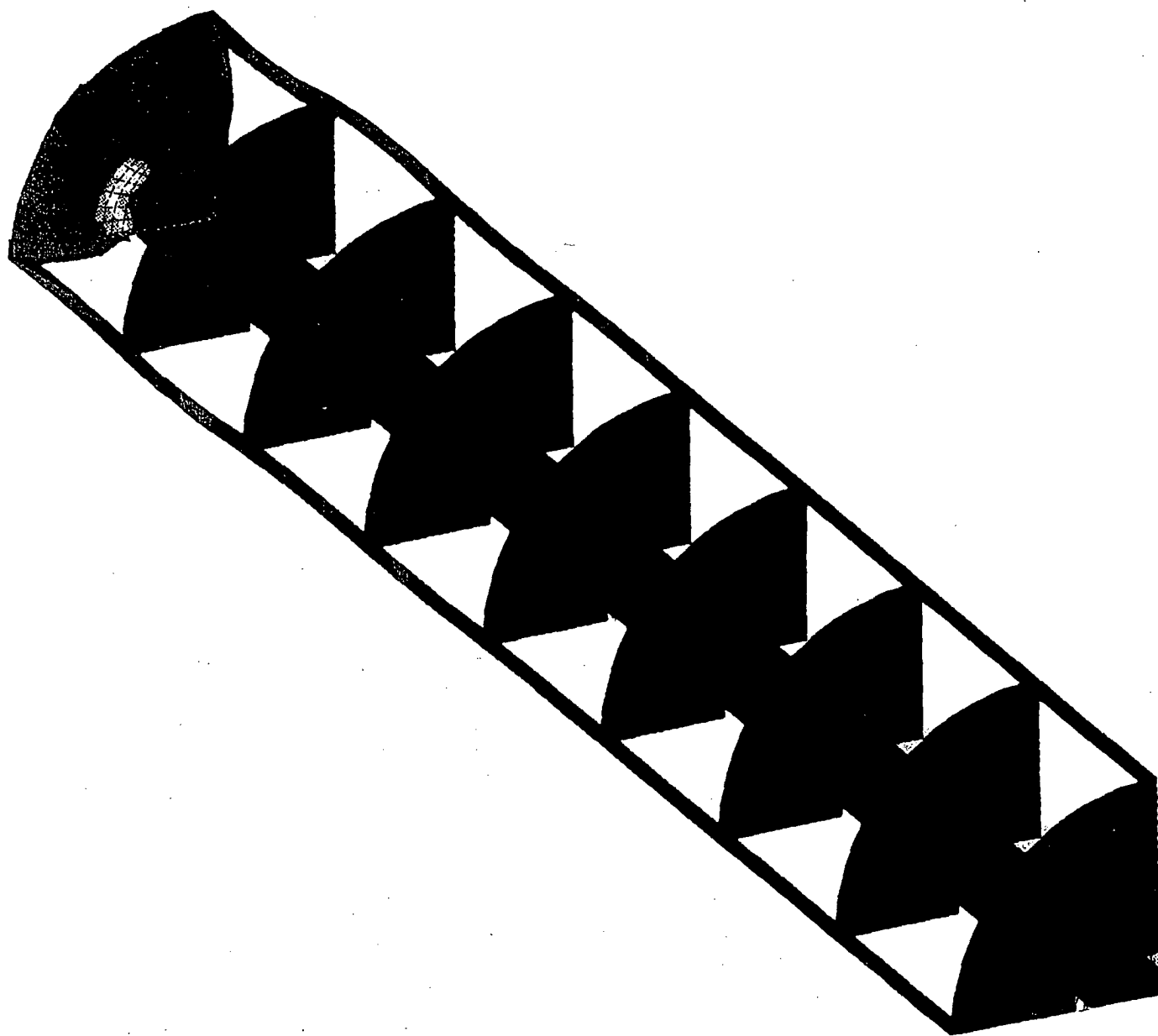


Figure 7

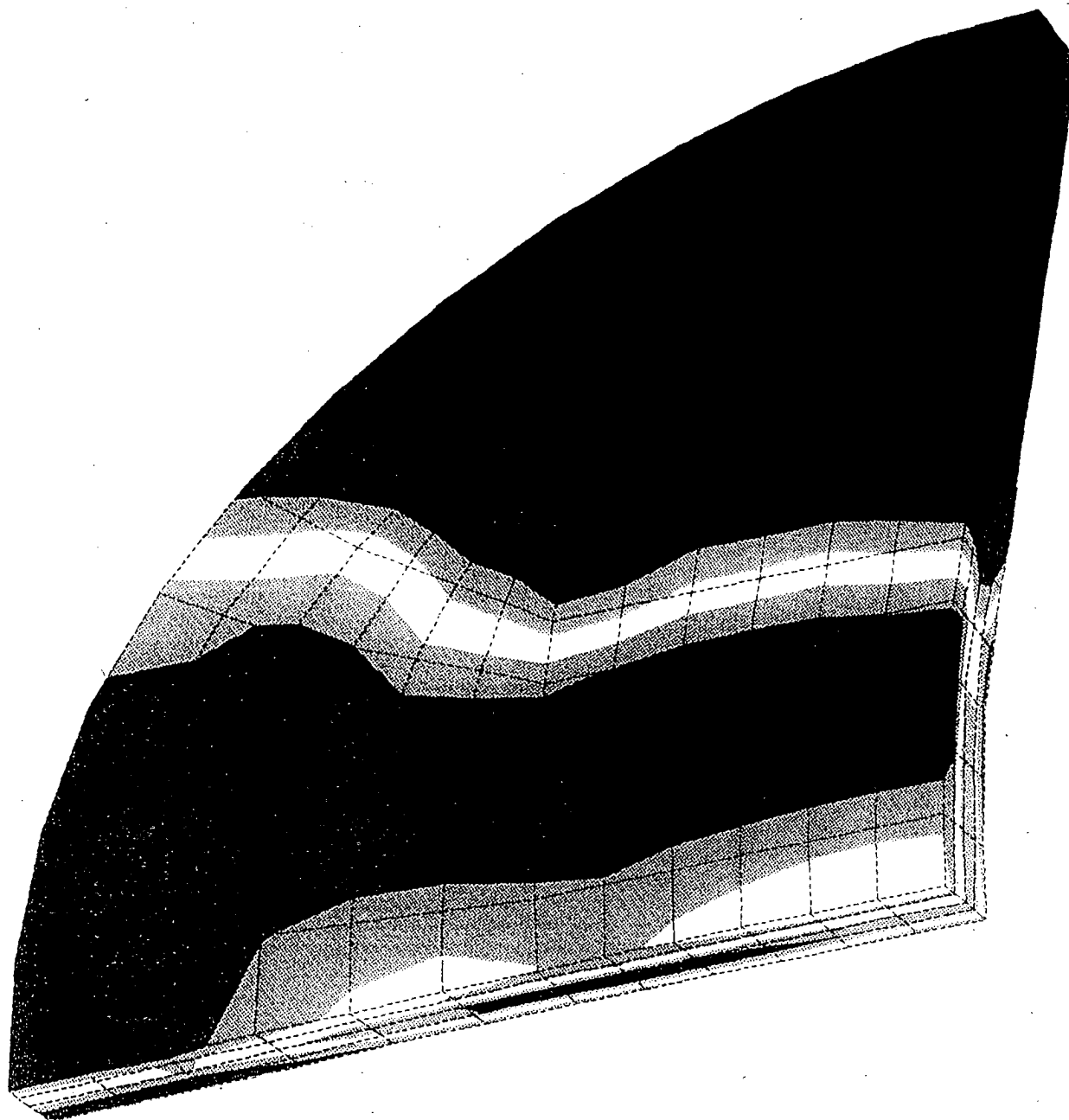


ANSYS 4.  
 OCT 19 1993  
 13:32:29  
 PLOT NO. 1  
 POST1 STRESS  
 STEP=1  
 ITER=10  
 TIME=0.005  
 SIGE (AVG)  
 TOP  
 SMN =1425  
 SMX =98102

XV =-1  
 YV =-1  
 ZV =-2  
 DIST=29.116  
 XF =5.375  
 YF =5.375  
 ZF =47.563  
 PRECISE HIDDEN

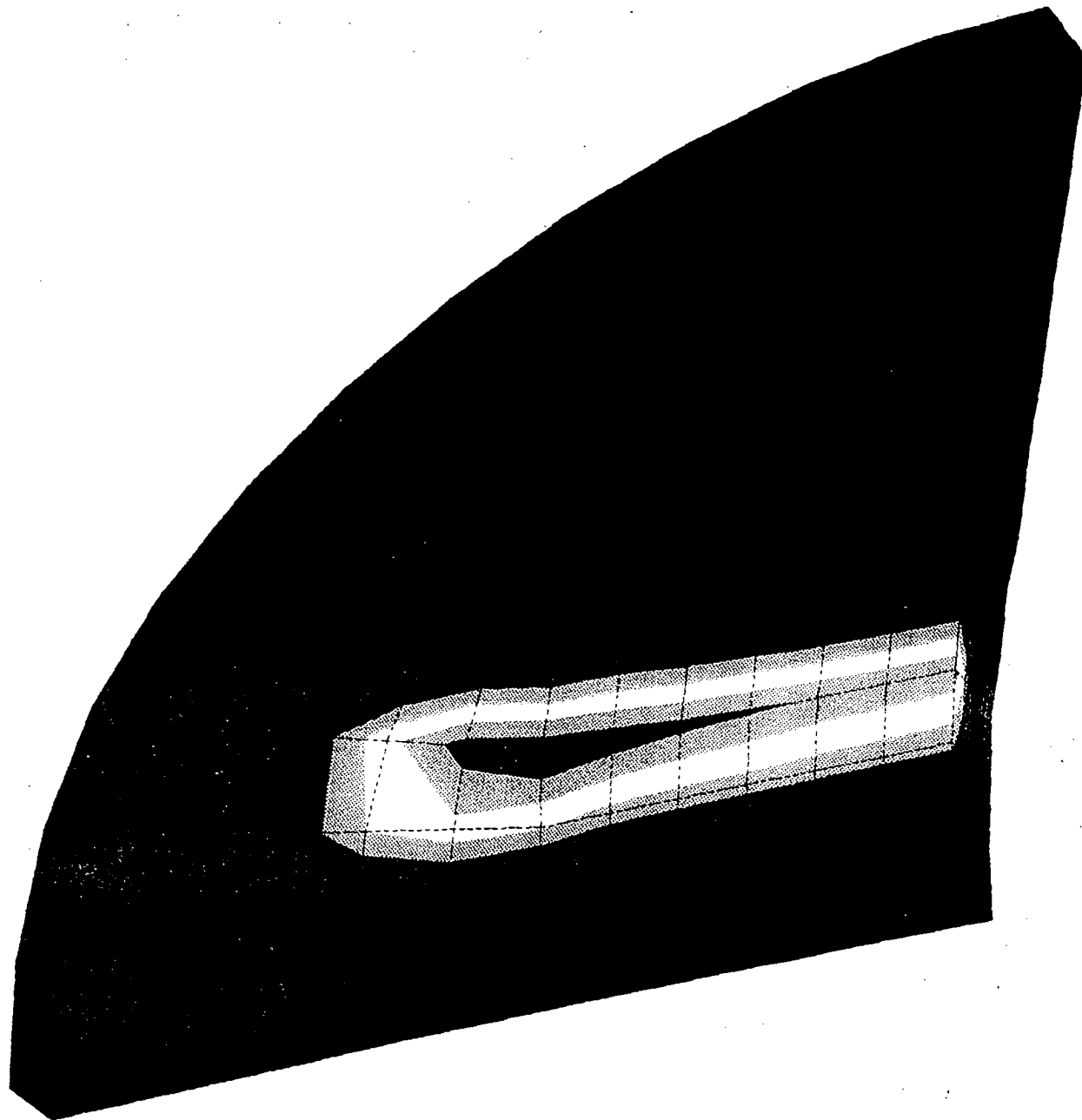
1425
12167
22909
33650
44392
55134
65876
76618
87360
98102





ANSYS 4.  
OCT 19 1993  
13:38:55  
PLOT NO. 1  
POST1 STRESS  
STEP=1  
ITER=6  
TIME=0.003  
SIGE (AVG)  
TOP  
SMN =11262  
SMX =113701

XV =-1  
YV =-1  
ZV =-2  
DIST=3.715  
XF =3  
YF =3  
ZF =-0.625  
PRECISE HIDDEN  
11262  
22644  
34026  
45408  
56790  
68172  
79554  
90936  
102318  
113701



ANSYS 4.  
 OCT 19 1993  
 13:40:18  
 PLOT NO. 1  
 POST1 STRESS  
 STEP=1  
 ITER=6  
 TIME=0.003  
 EPL (AVG)  
 SMX =0.065778

XV =-1  
 YV =-1  
 ZV =-2  
 DIST=3.715  
 XF =3  
 YF =3  
 ZF =-0.625  
 PRECISE HIDDEN  
 0  
 0.007309  
 0.014617  
 0.021926  
 0.029235  
 0.036543  
 0.043852  
 0.051161  
 0.05847  
 0.065778

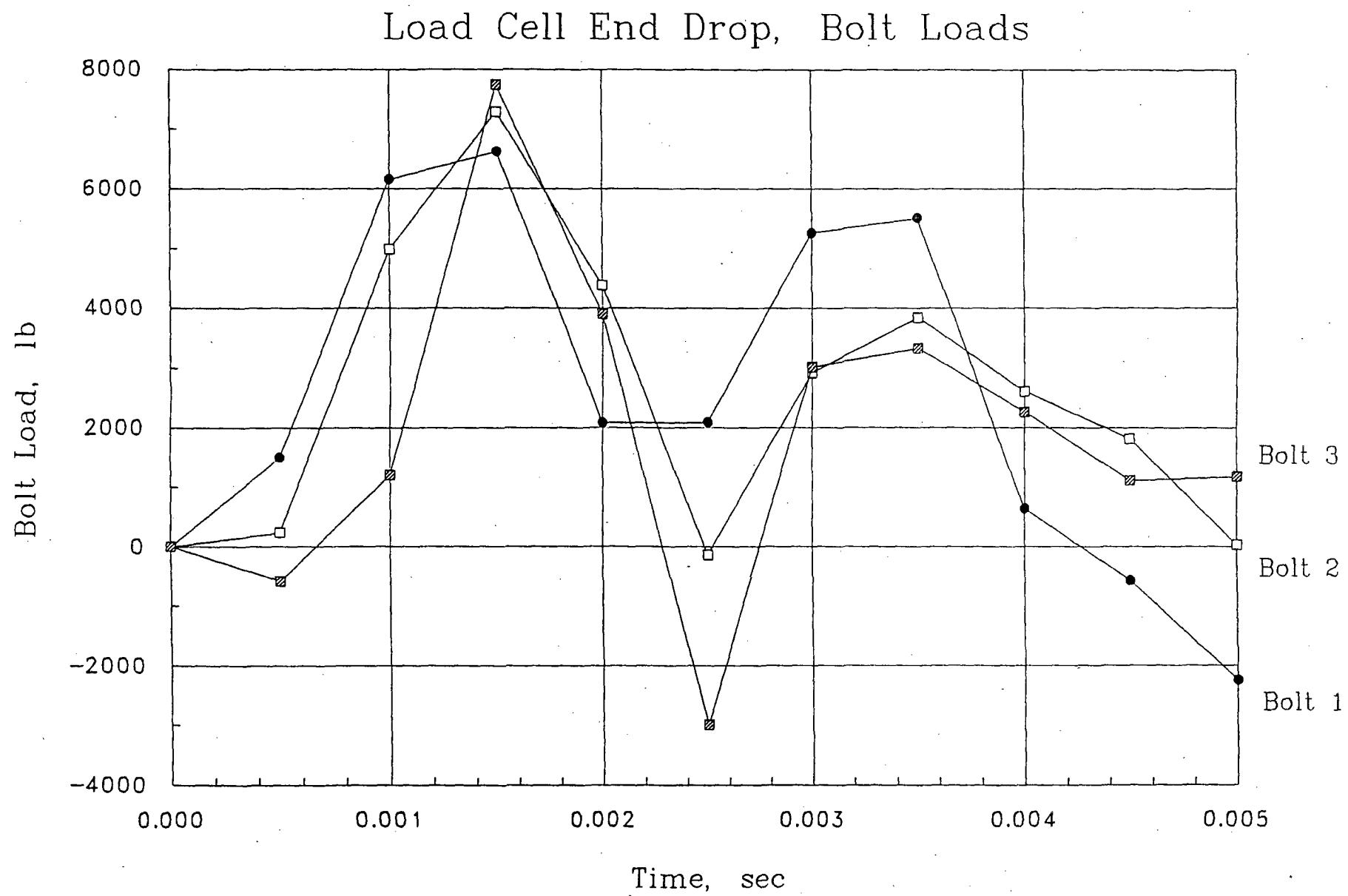


Figure 11

# Load Cell End Drop, Bolt Head Axial Displacements

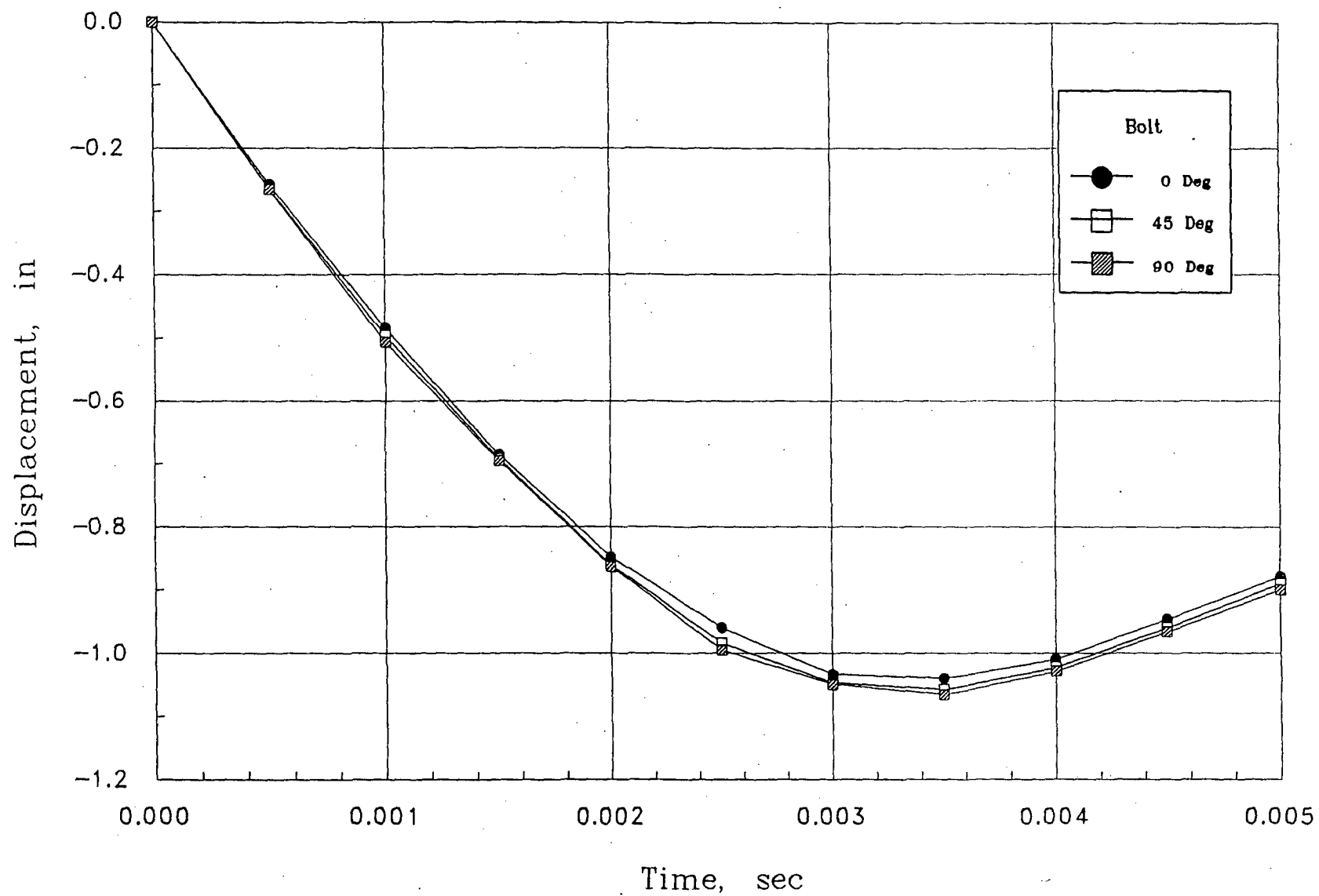
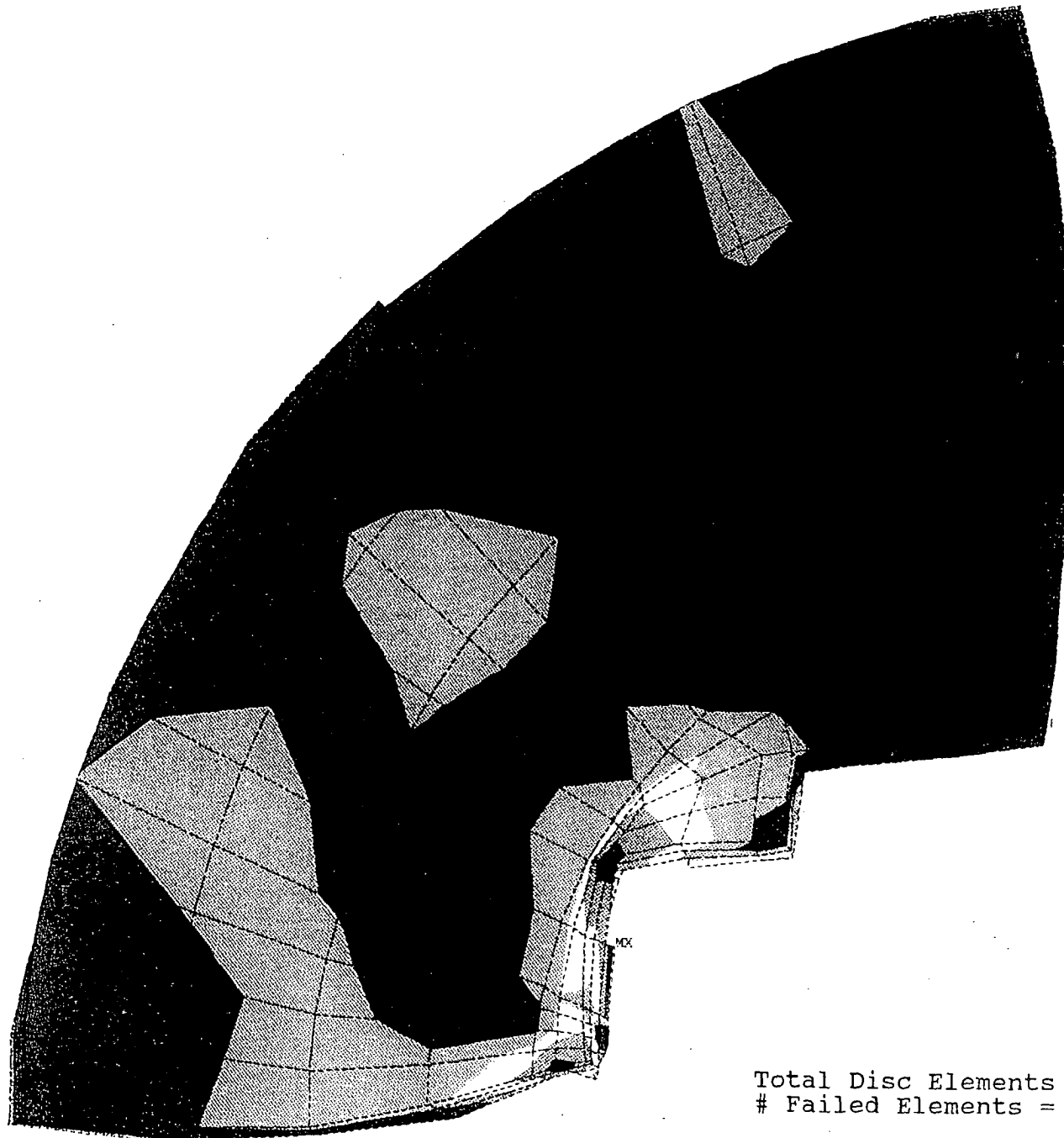


Figure 12



Total Disc Elements = 648  
# Failed Elements = 5

ANSYS 4\  
OCT 19 1993  
13:45:00  
PLOT NO. 1  
POST1 STRESS  
STEP=1  
ITER=6  
TIME=0.003  
SIGE (AVG)  
TOP  
SMN =17430  
SMX =47496

XV =-1  
YV =-1  
ZV =-3  
DIST=6.26  
XF =5.375  
YF =5.375  
ZF =-0.1875  
PRECISE HIDDEN

17430
20771
24111
27452
30793
34133
37474
40815
44155
47496

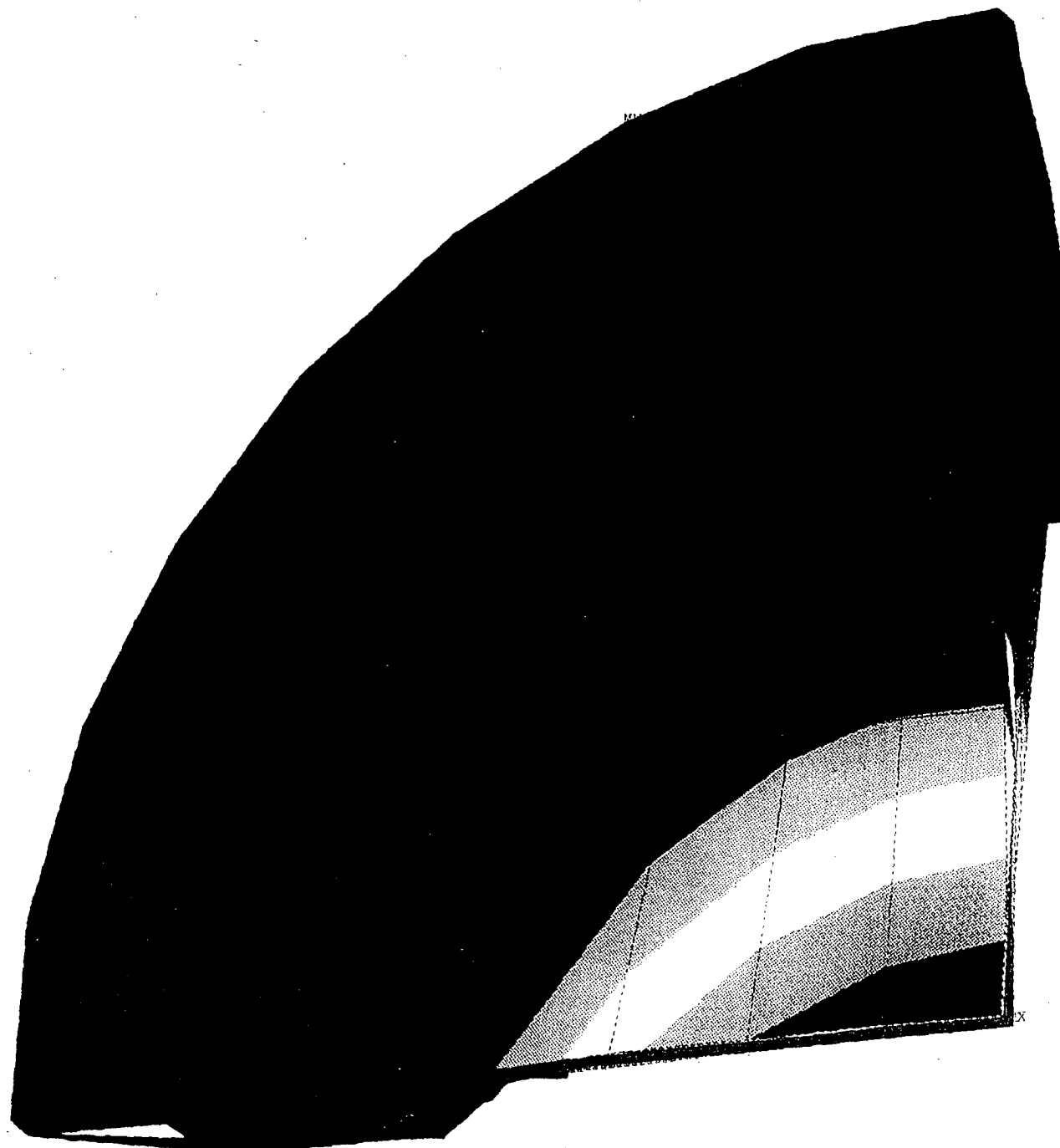
ANSYS 4.4(  
OCT 19 1993  
13:46:10  
PLOT NO. 1  
POST1 STRESS  
STEP=1  
ITER=6  
TIME=0.003  
EPL (AVG)  
SMN =0.002241  
SMX =0.13718

XV =-1  
YV =-1  
ZV =-3  
DIST=6.26  
XF =5.375  
YF =5.375  
ZF =-0.1875  
PRECISE HIDDEN  
0.002241  
0.017234  
0.032227  
0.047221  
0.062214  
0.077207  
0.0922  
0.107194  
0.122187  
0.13718



Shipping Drum End Drop Analysis - Bottom Disc

Figure 14

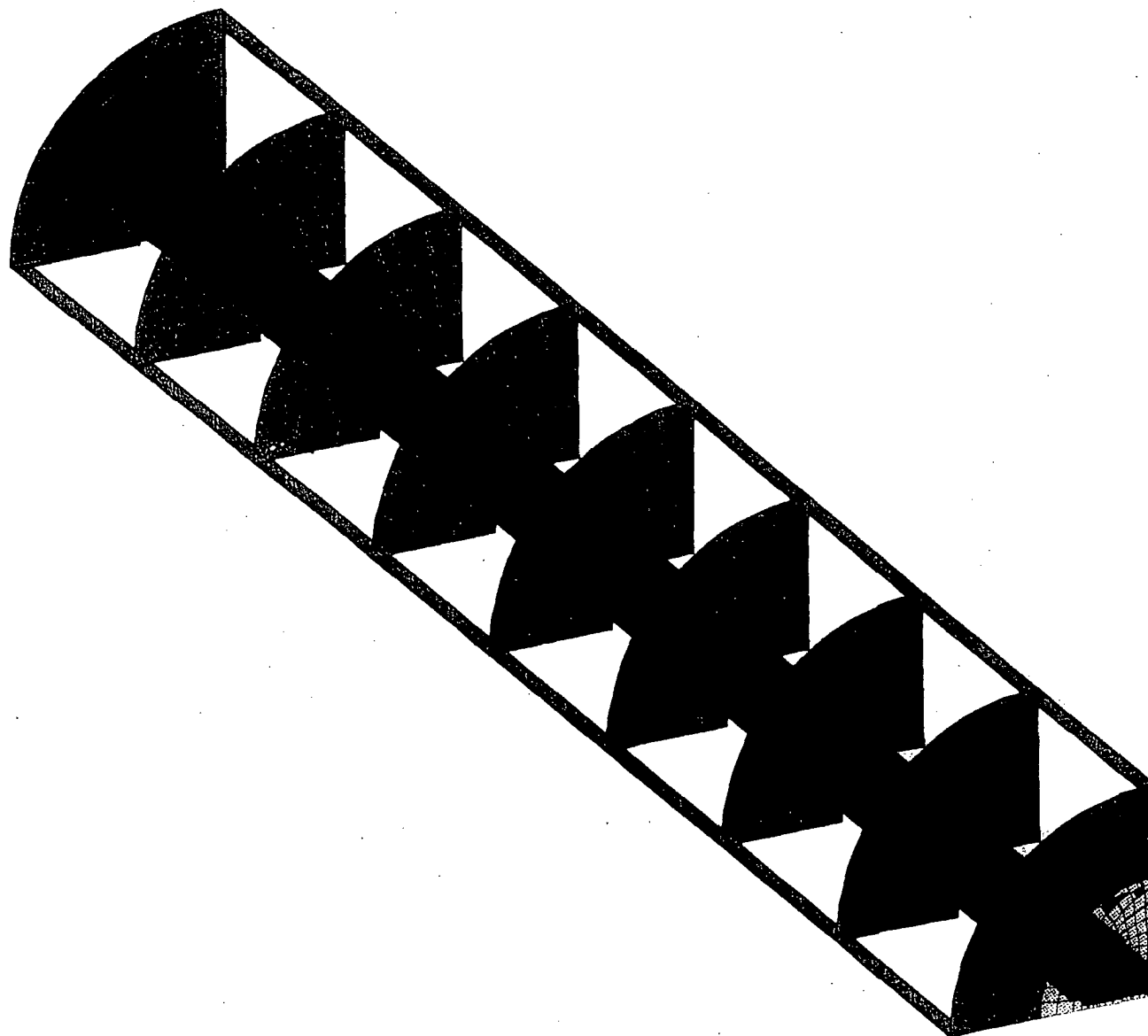


ANSYS 4.  
OCT 19 1993  
13:48:29  
PLOT NO. 1  
POST1 STRESS  
STEP=1  
ITER=6  
TIME=0.003  
SIGE (AVG)  
TOP  
SMN =24.867  
SMX =2738

XV =-1  
YV =-1  
ZV =-3  
DIST=6.332  
XF =5.25  
YF =5.25  
ZF =-1.25  
PRECISE HIDDEN  
24.867  
326.317  
627.767  
929.217  
1231  
1532  
1834  
2135  
2436  
2738

Shipping Drum End Drop Analysis - Rubber

Figure .15



Redrop, Element Plot

ANSYS 4.  
OCT 30 1993  
17:41:49  
PLOT NO. 1  
POST1 ELEMENTS  
MAT NUM  
  
XV =-1  
YV =-1  
ZV =-2  
DIST=31.084  
XF =5.375  
YF =5.375  
ZF =43.562  
PRECISE HIDDEN

Figure 16



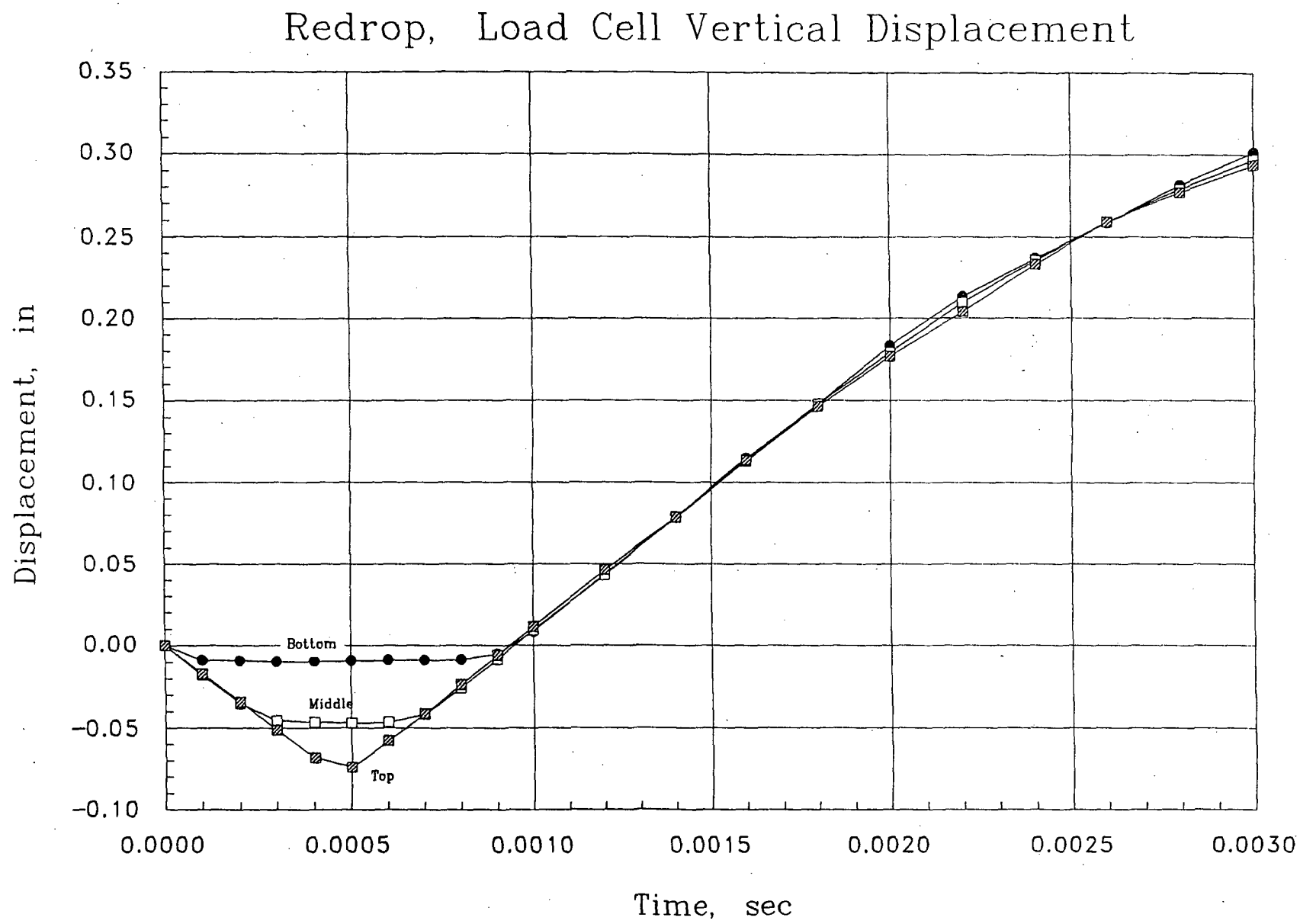
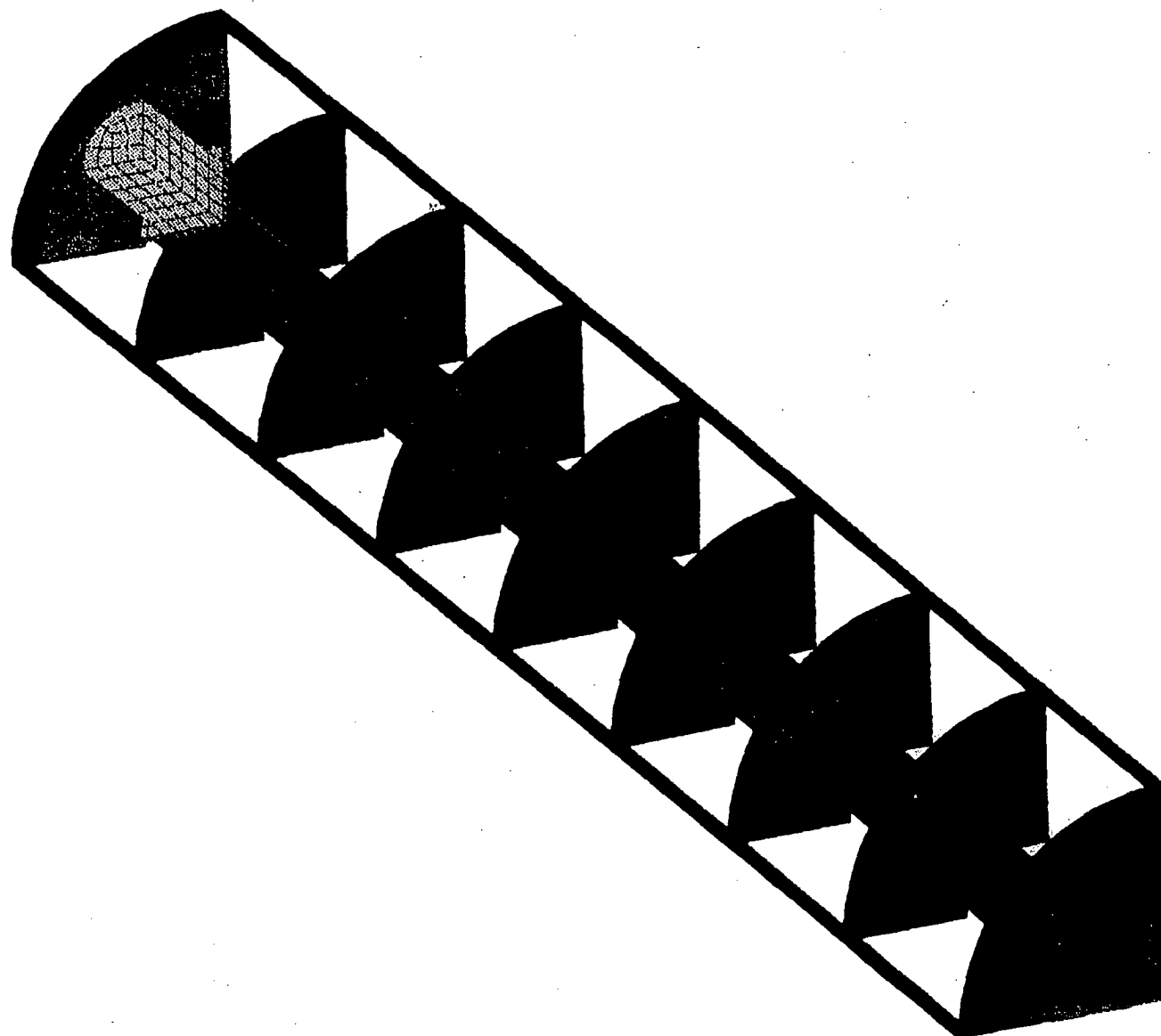


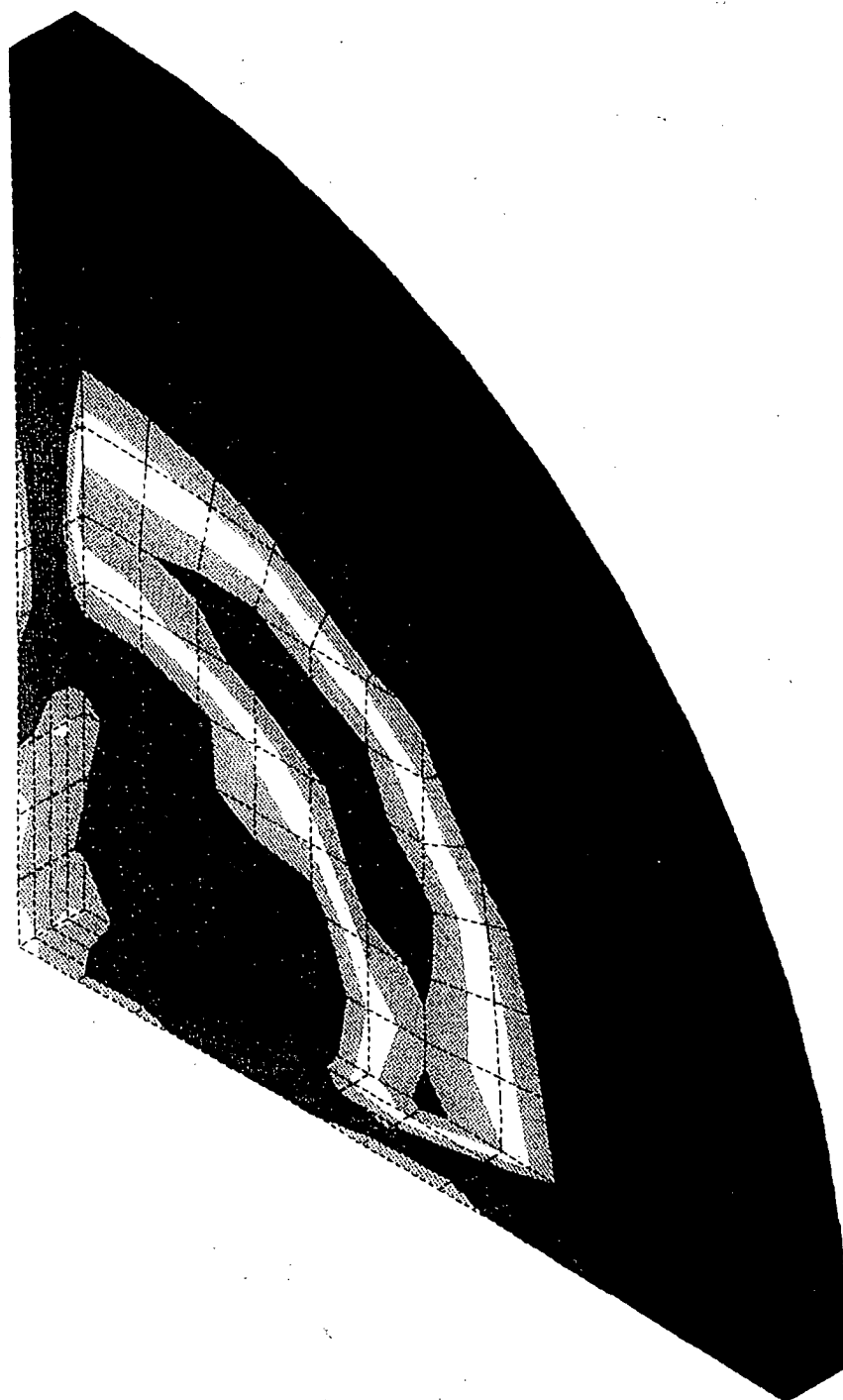
Figure 17



ANSYS 4.4  
 OCT 30 1993  
 17:39:44  
 PLOT NO. 1  
 POST1 STRESS  
 STEP=1  
 ITER=15  
 TIME=0.003  
 UZ  
 D GLOBAL  
 DMX =0.419975  
 SMN =-0.43978  
 SMX =0.30187

XV =-1  
 YV =-1  
 ZV =-2  
 DIST=31.084  
 XF =5.375  
 YF =5.375  
 ZF =43.562  
 PRECISE HIDDEN

■	-0.43978
■	-0.357374
■	-0.274969
■	-0.192563
■	-0.110158
■	-0.027752
■	0.054653
■	0.137059
■	0.219464
■	0.30187



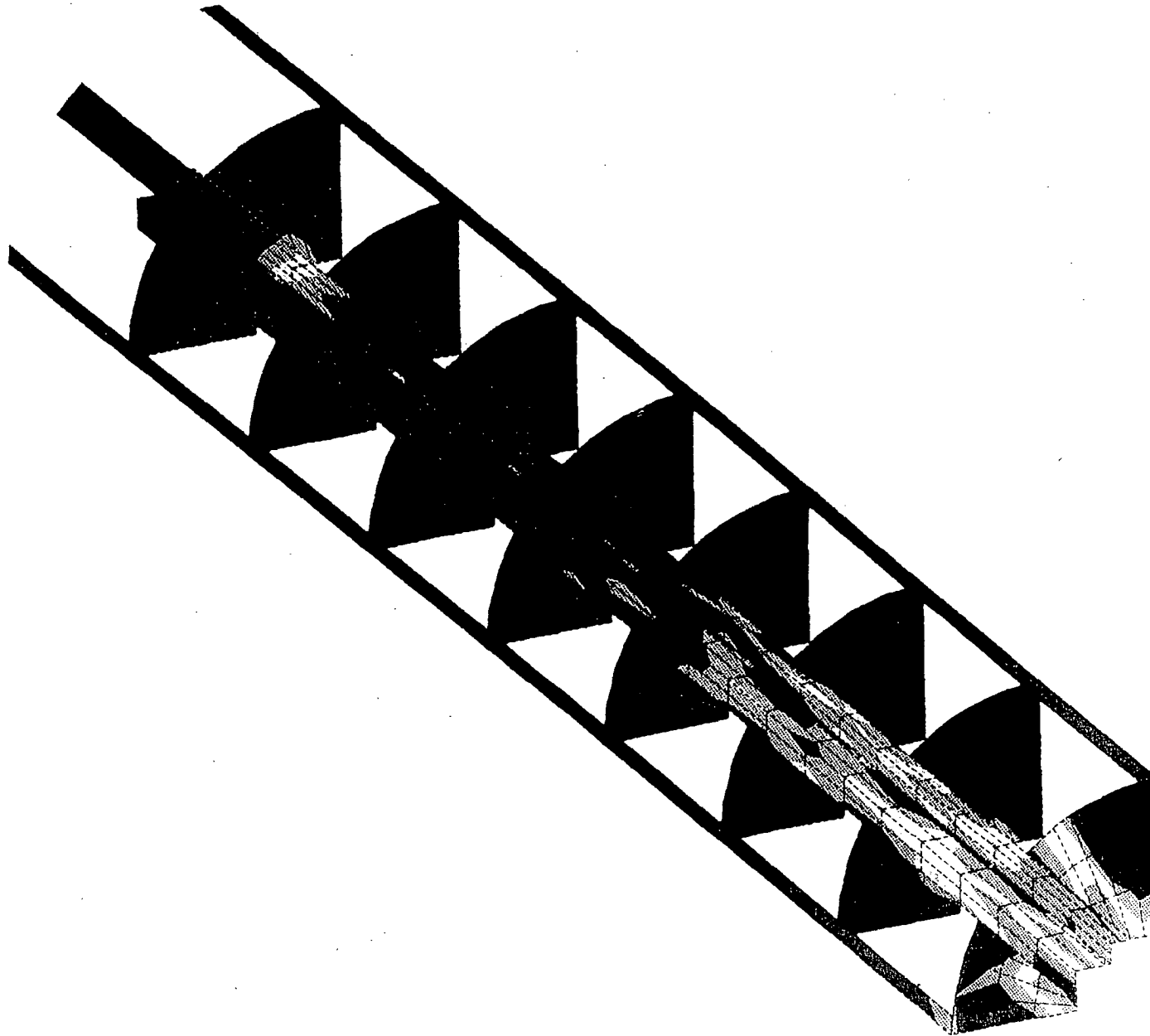
ANSYS 4.  
 OCT 29 1993  
 14:28:26  
 PLOT NO. 1  
 POST1 STRESS  
 STEP=1  
 ITER=3  
 TIME=0.300E-03  
 SIGE (AVG)  
 MIDDLE  
 DMX =0.043483  
 SMN =3477  
 SMX =60178

XV =-1  
 YV =-1  
 ZV =1  
 DIST=4.154  
 XF =3  
 YF =3  
 ZF =-0.625  
 PRECISE HIDDEN

3477
9777
16077
22377
28677
34977
41277
47578
53878
60178

Redrop, Closure Flange Max Stress

Figure 19

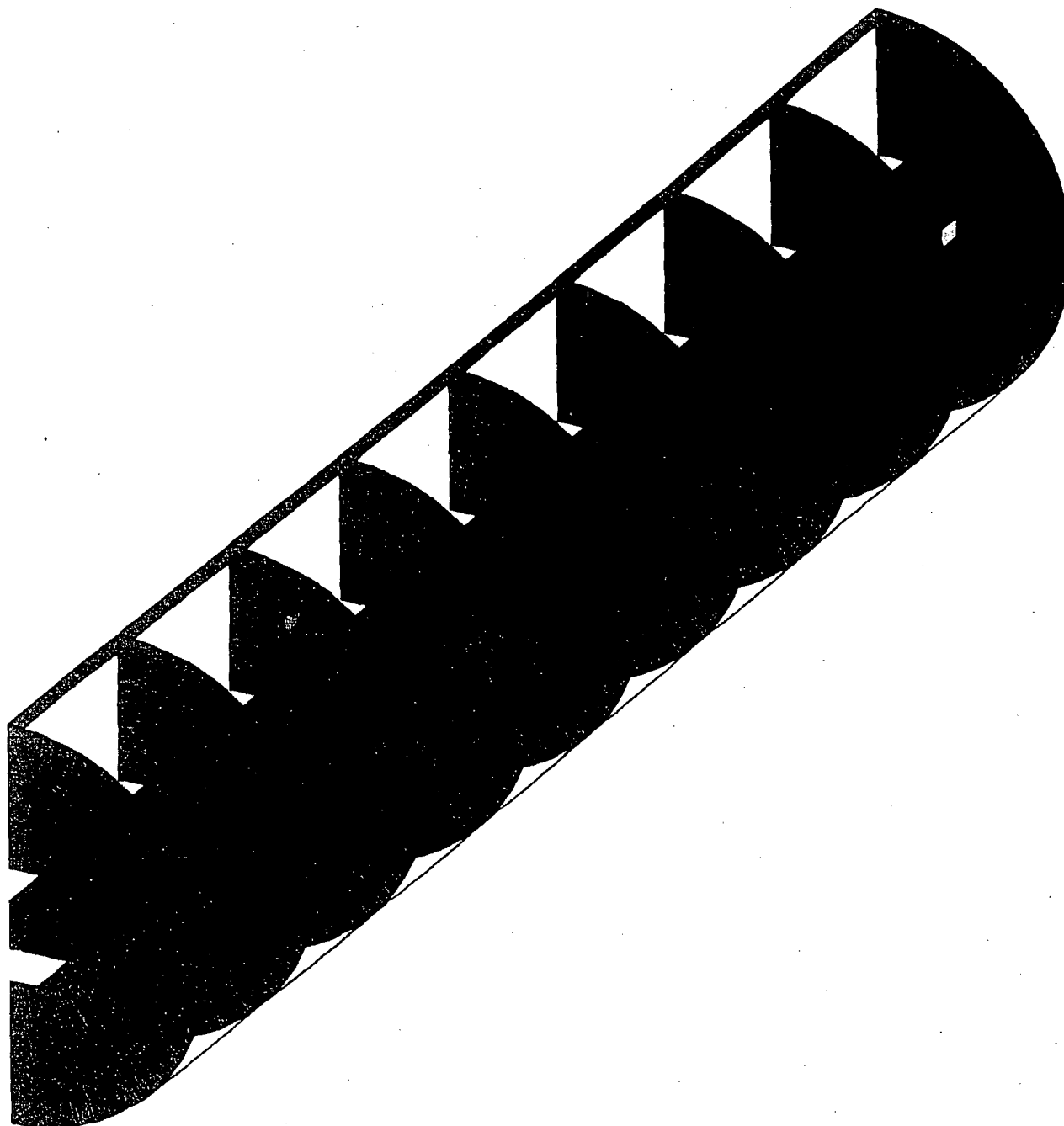


ANSYS 4.  
OCT 30 1993  
17:48:01  
PLOT NO. 1  
POST1 STRESS  
STEP=1  
ITER=12  
TIME=0.0024  
SIGE (AVG)  
TOP  
SMN =1329  
SMX =33256  
SMXB=54438

XV =-1  
YV =-1  
ZV =-2  
DIST=28.901  
XF =5.375  
YF =5.375  
ZF =48  
PRECISE HIDDEN  
1329  
4876  
8424  
11971  
15518  
19066  
22613  
26161  
29708  
33256

Redrop, Cage Shell Max Stresses

Figure 21



Shipping Box Side Drop FE Mesh

ANSYS 4.4  
SEP 1 1993  
14:33:48  
PLOT NO. 1  
PREP7 ELEMENTS  
TYPE NUM

XV = -1  
YV = -1  
ZV = 2  
DIST = 31.154  
XF = 5.375  
ZF = 48  
PRECISE HIDDEN

Figure 22

# Load Cell Side Drop, Cell Relative Displacement

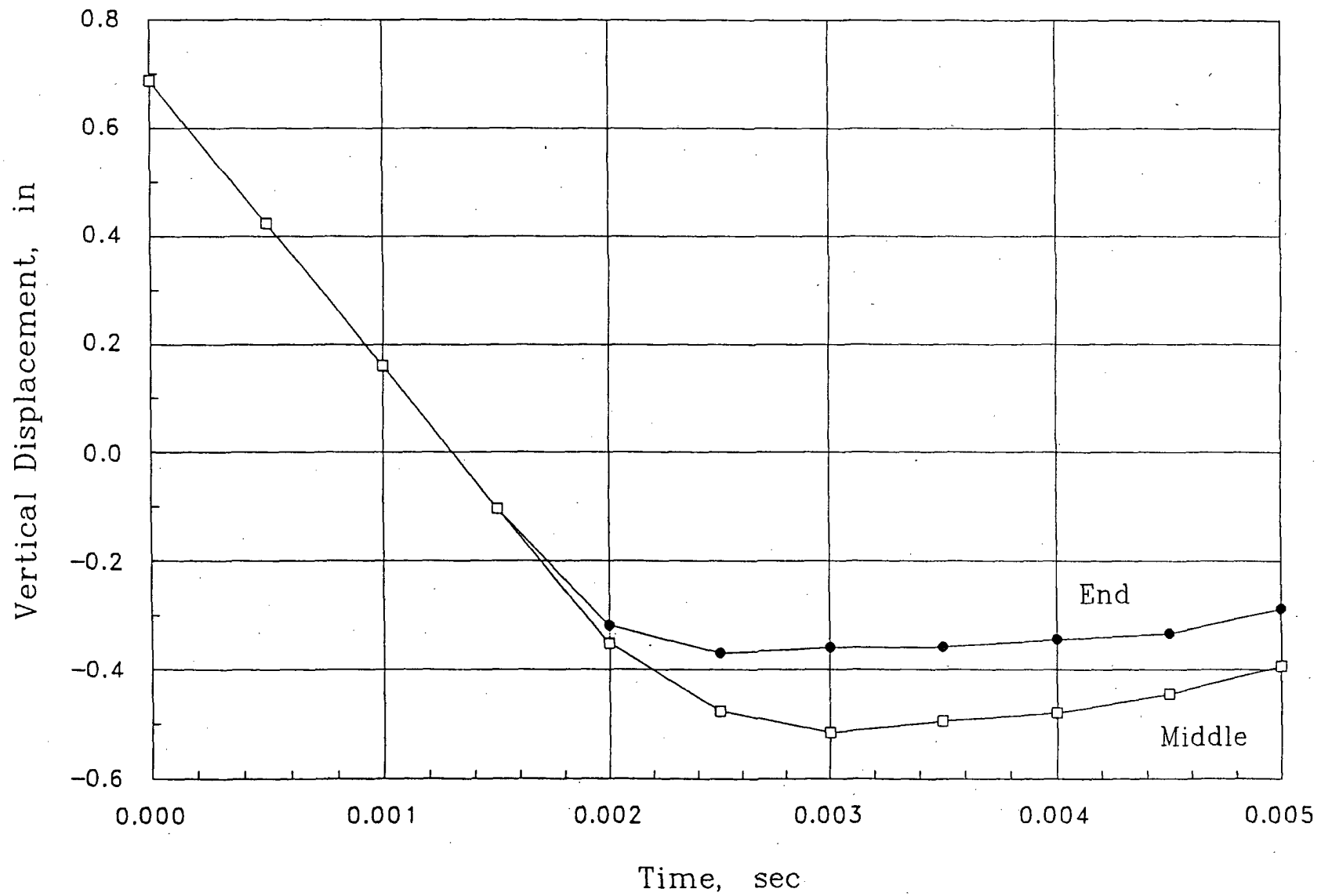
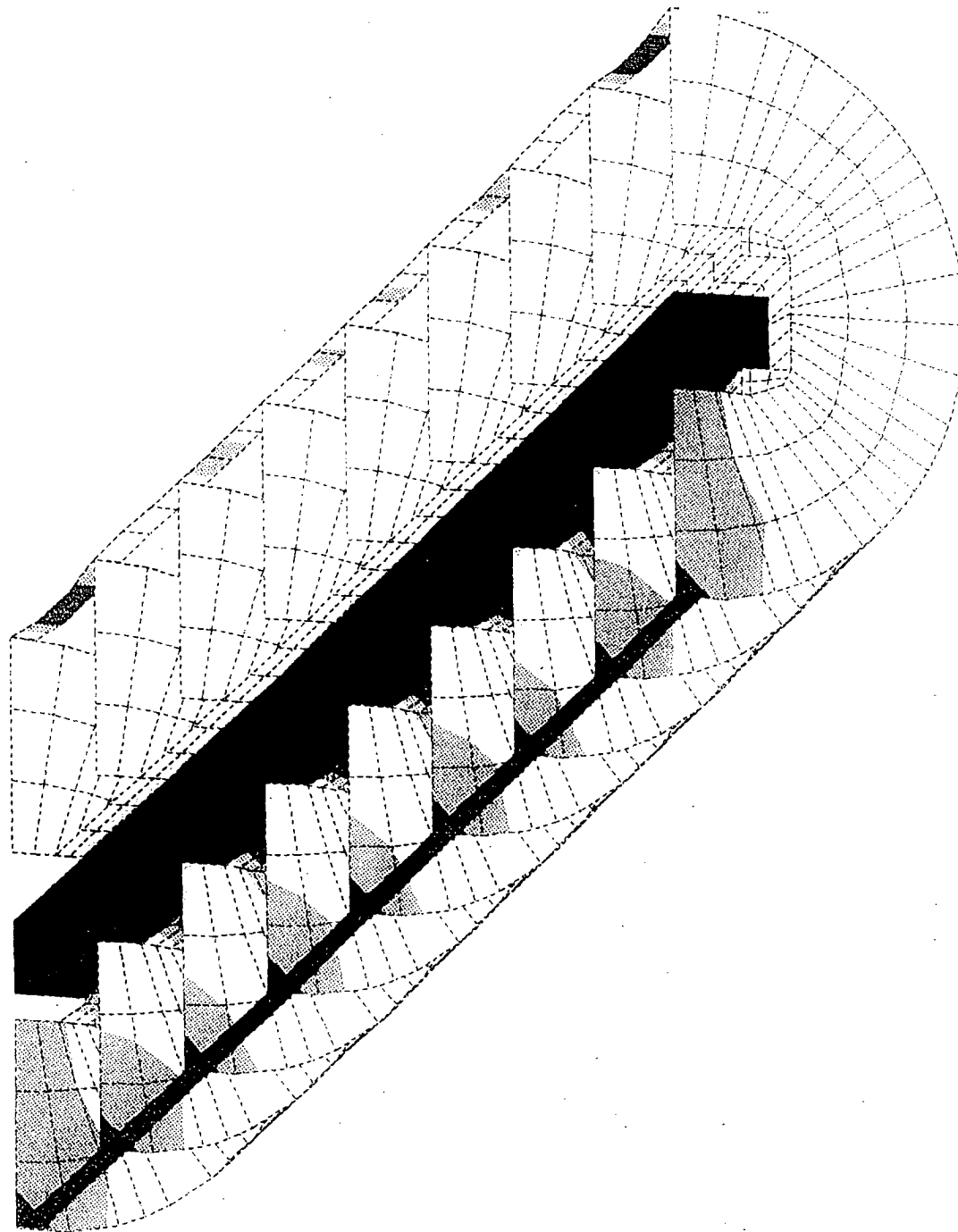


Figure 23



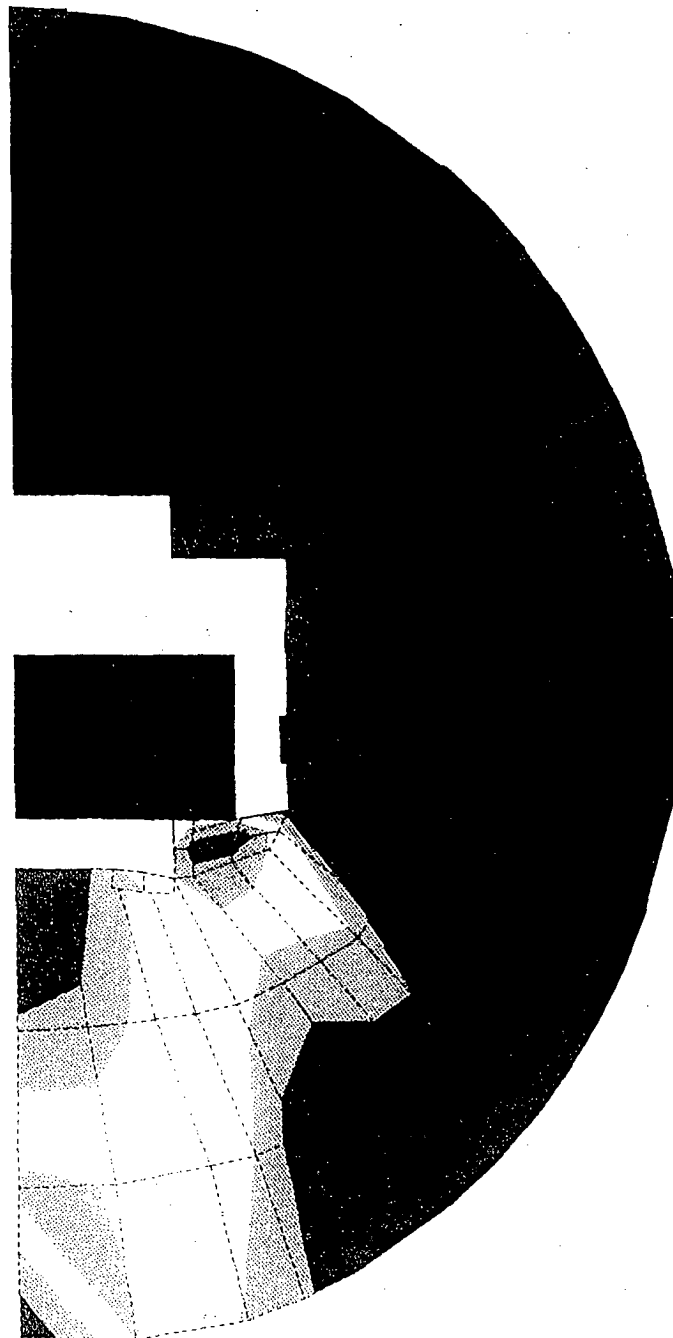
ANSYS 4.4  
 OCT 19 1993  
 15:51:01  
 PLOT NO. 1  
 POST1 STRESS  
 STEP=1  
 ITER=6  
 TIME=0.002999  
 UY  
 D GLOBAL  
 SMN =-1.214  
 SMX =0.020192

XV =-1  
 YV =-1  
 ZV =4  
 DIST=23.904  
 XF =5.375  
 ZF =48  
 PRECISE HIDDEN  
 -1.214  
 -1.077  
 -0.940046  
 -0.802869  
 -0.665692  
 -0.528516  
 -0.391339  
 -0.254162  
 -0.116985  
 0.020192

Load Cell Side Drop, Max Displacement

Figure 24

1



ANSYS 4.4A  
OCT 19 1993  
15:54:46  
PLOT NO. 1  
POST1 STRESS  
STEP=1  
ITER=6  
TIME=0.002999  
SIGE (AVG)  
TOP  
SMN =1556  
SMX =44364  
SMXB=76057

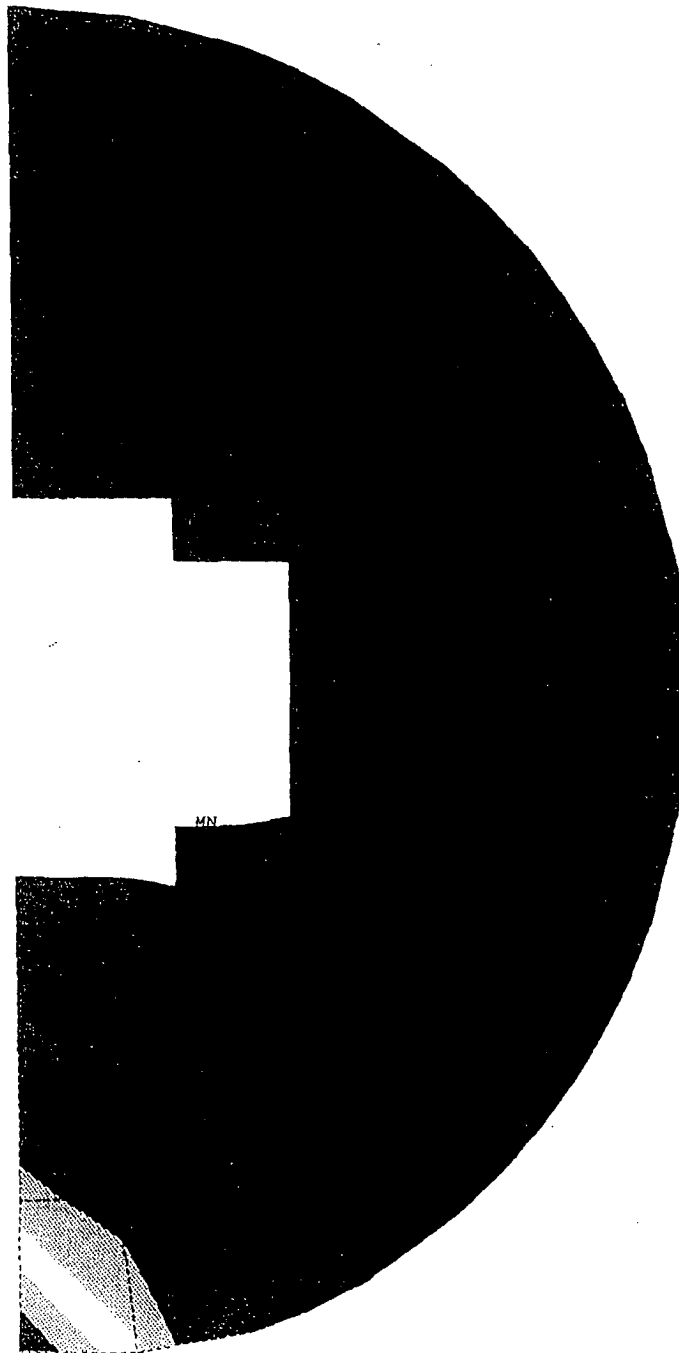
ZV =1  
DIST=11.825  
XF =5.375  
ZF =48  
PRECISE HIDDEN

	1556
	6312
	11069
	15825
	20582
	25338
	30095
	34851
	39608
	44364

Load Cell Side Drop, Max Displacement

Figure 25





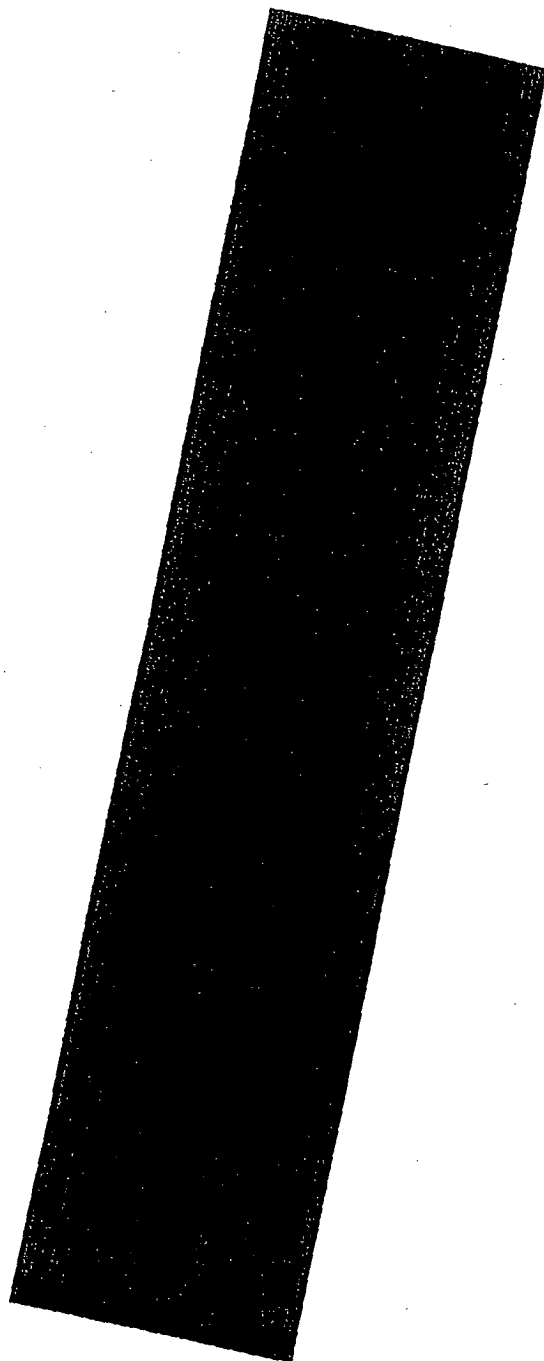
Load Cell Side Drop, Max Displacement

ANSYS 4.4/   
 OCT 19 1993   
 15:53:01   
 PLOT NO. 1   
 POST1 STRESS   
 STEP=1   
 ITER=6   
 TIME=0.002999   
 UY   
 D GLOBAL   
 SMN =-0.51327   
 SMX =-0.984E-03

ZV =1   
 DIST=11.825   
 XF =5.375   
 ZF =48   
 PRECISE HIDDEN   
 -0.51327   
 -0.456349   
 -0.399429   
 -0.342508   
 -0.285587   
 -0.228667   
 -0.171746   
 -0.114825   
 -0.057905   
 -0.984E-03

Figure 26

1



ANSYS 4.4A1  
OCT 27 1993  
13:45:24  
PLOT NO. 1  
POST1 ELEMENTS  
MAT NUM

XV =-1  
DIST=56.586  
XF =5.5  
ZF =47.998  
ANGZ=78.  
PRECISE HIDDEN

Shipping Drum, CG Over Corner Drop Analysis

Figure 27

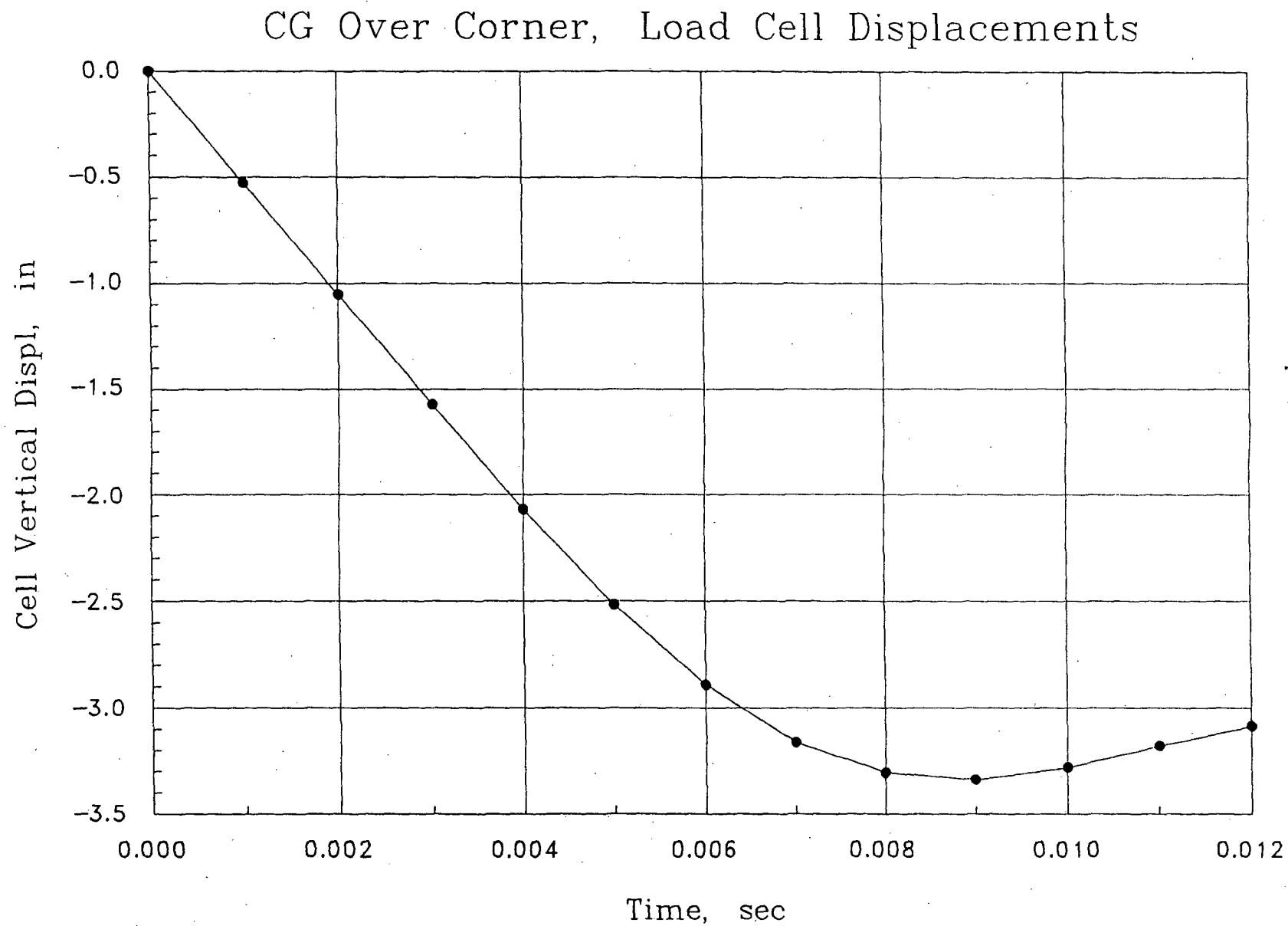
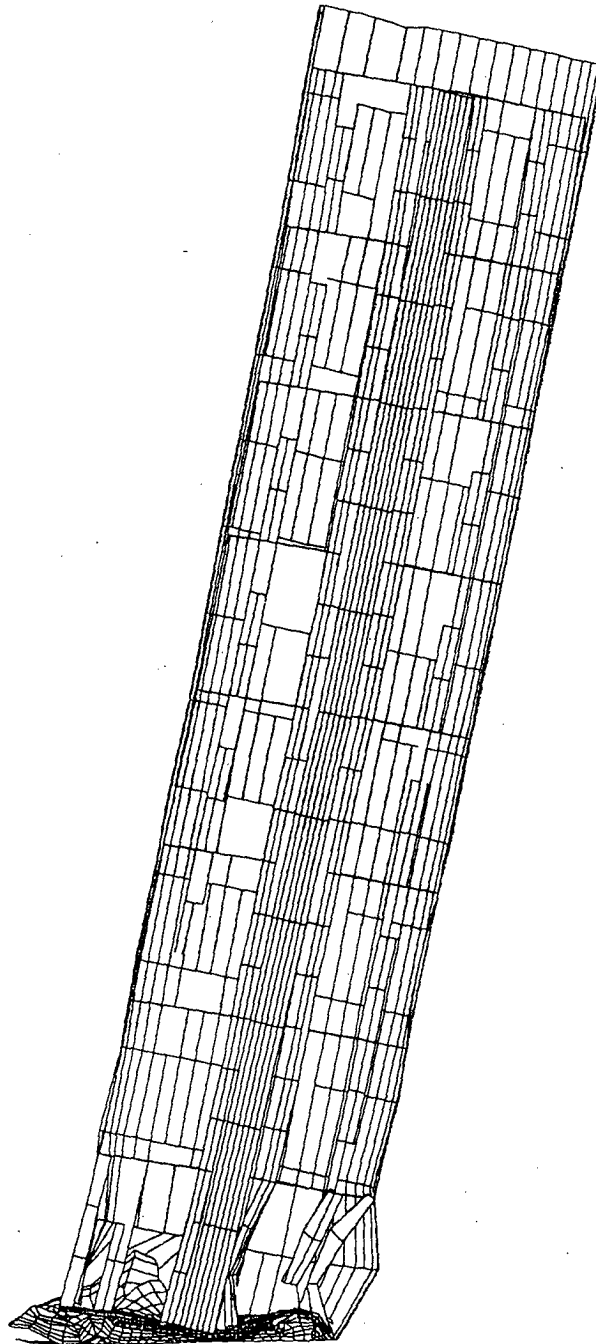


Figure 28

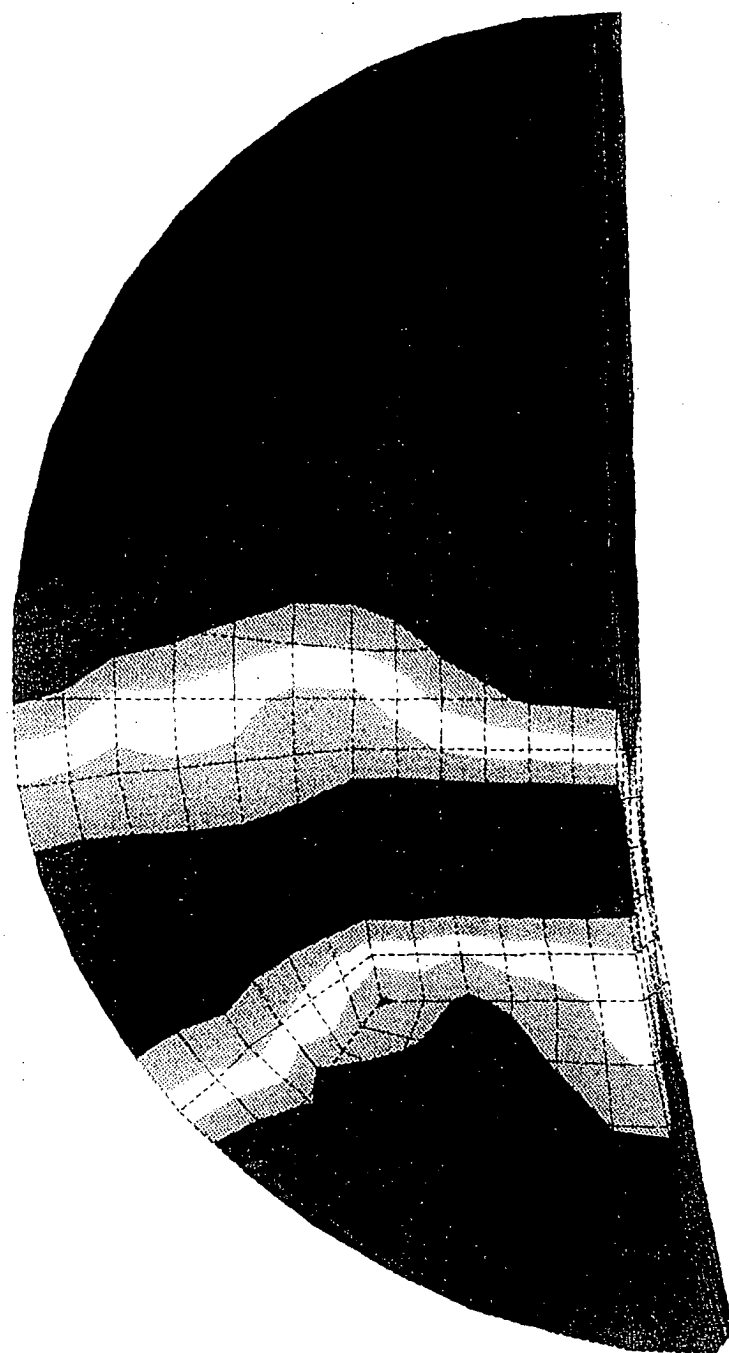


CG Over Corner, Deformed Shape

ANSYS 4.4  
NOV 5 1993  
10:11:22  
PLOT NO. 1  
POST1 DISPL.  
STEP=1  
ITER=9  
TIME=0.009  
DMX =6.781  
ERPC=0

\*DSCA=1  
XV =-1  
DIST=56.586  
XF =5.5  
ZF =47.998  
ANGZ=78  
PRECISE HIDDEN

Figure 29

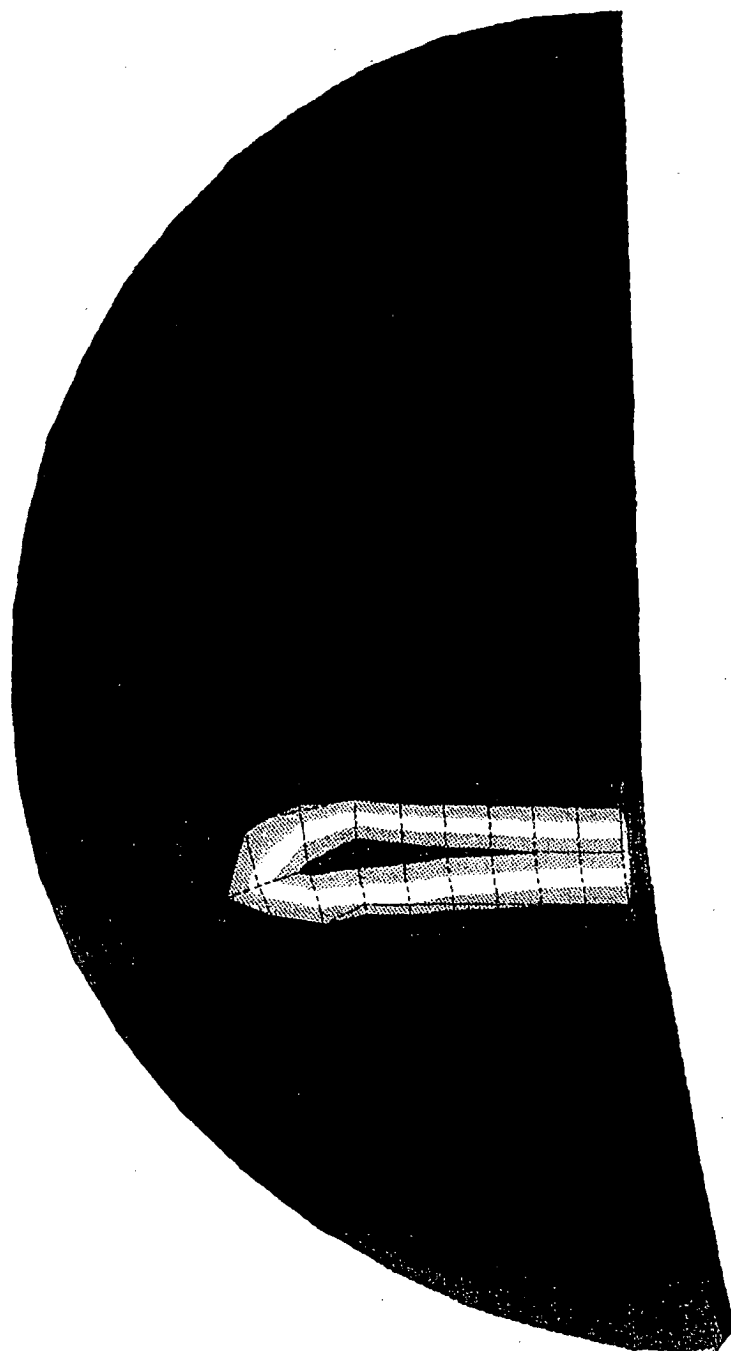


CG Over Corner, Closure Flange Max. Stress

ANSYS 4.4  
OCT 27 1993  
11:00:02  
PLOT NO. 1  
POST1 STRESS  
STEP=1  
ITER=8  
TIME=0.008  
SIGE (AVG)  
MIDDLE  
DMX =8.626  
SMN =9240  
SMX =114068

XV =-1  
ZV =-2  
DIST=6.6  
XF =3  
ZF =-0.625  
PRECISE HIDDEN  
9240  
20888  
32535  
44183  
55830  
67478  
79126  
90773  
102421  
114068

Figure 30



CG Over Corner, Closure Flange Plastic Strains

ANSYS 4.4  
 OCT 27 1993  
 11:00:19  
 PLOT NO. 1  
 POST1 STRESS  
 STEP=1  
 ITER=8  
 TIME=0.008  
 EPL (AVG)  
 DMX =8.626  
 SMX =0.073837

XV =-1  
 ZV =-2  
 DIST=6.6  
 XF =3  
 ZF =-0.625  
 PRECISE HIDDEN  
 0  
 0.008204  
 0.016408  
 0.024612  
 0.032816  
 0.04102  
 0.049224  
 0.057428  
 0.065632  
 0.073837

Figure 31

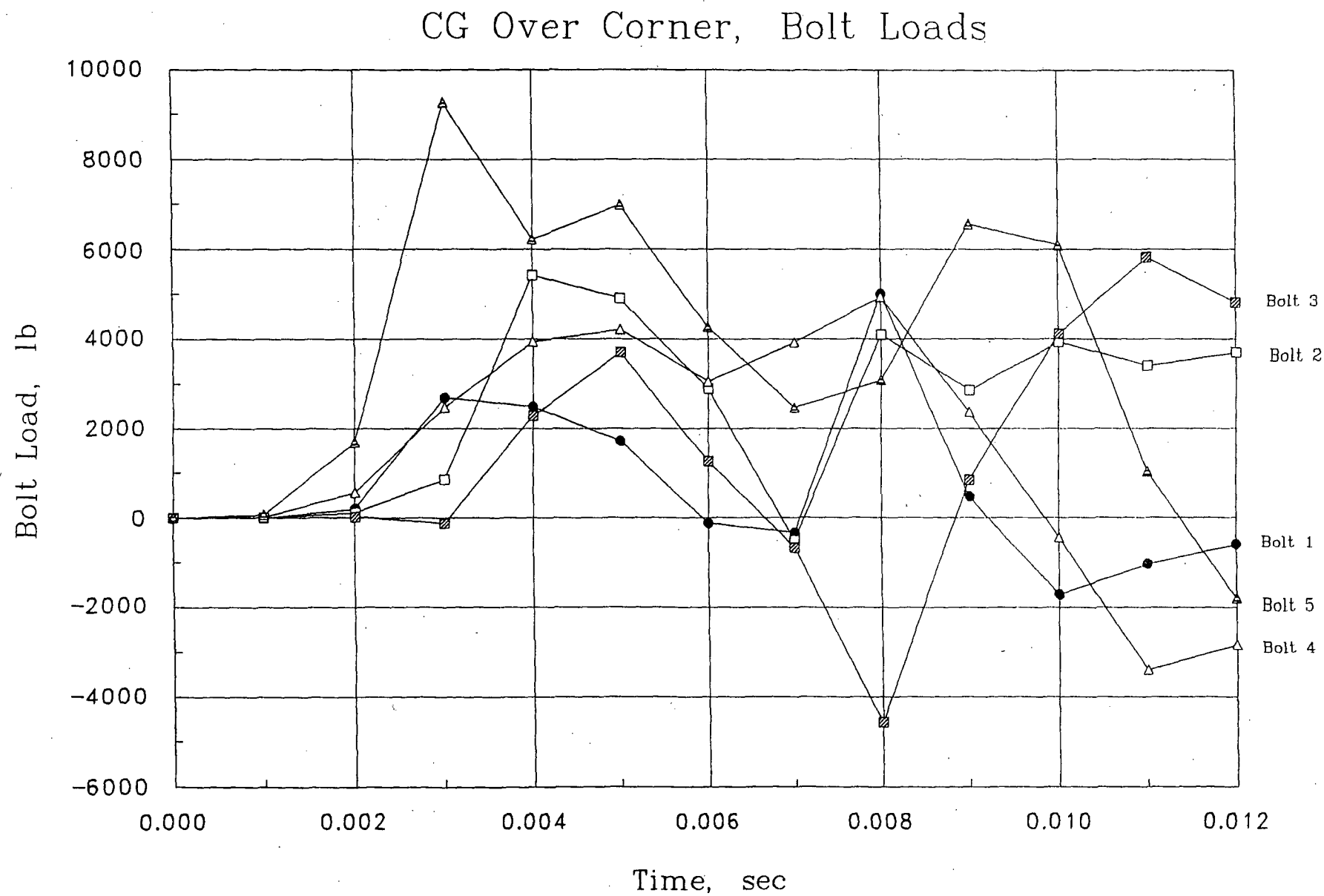
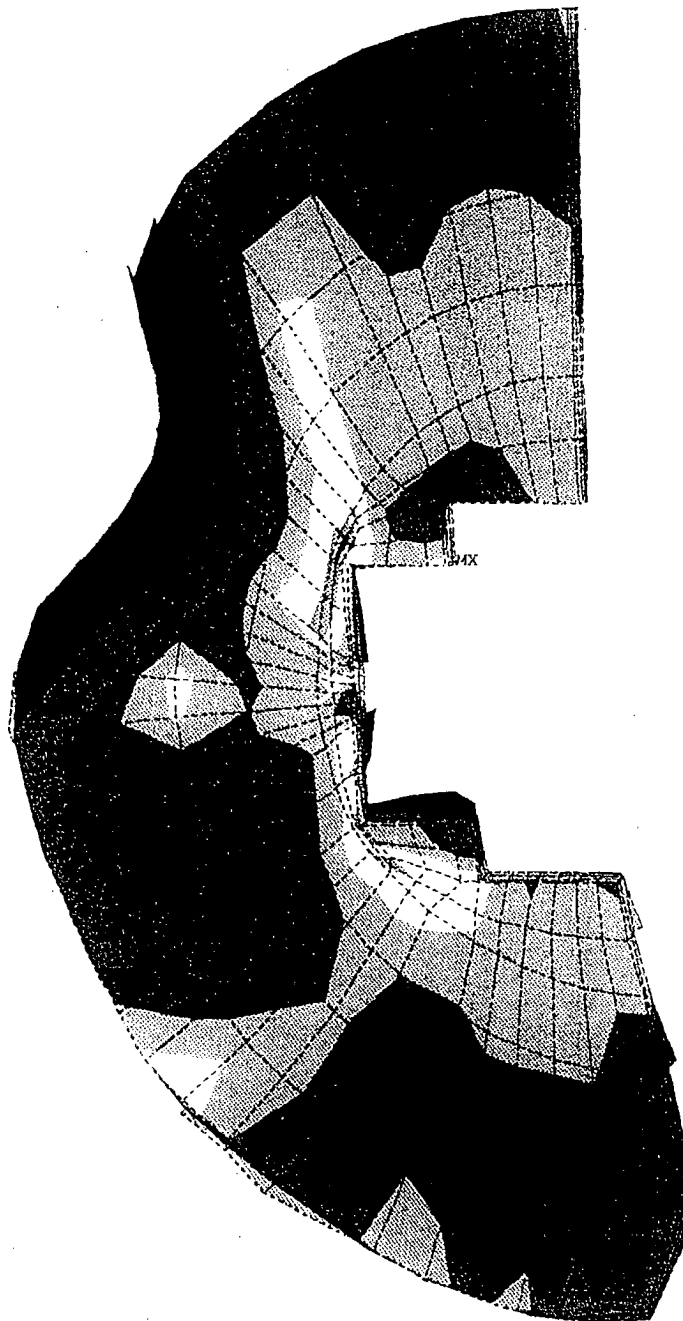


Figure 32



ANSYS 4.4A  
 OCT 27 1993  
 10:56:41  
 PLOT NO. 1  
 POST1 STRESS  
 STEP=1  
 ITER=12  
 TIME=0.012  
 SIGE (AVG)  
 MIDDLE  
 DMX =8.626  
 SMN =70.192  
 SMX =48761

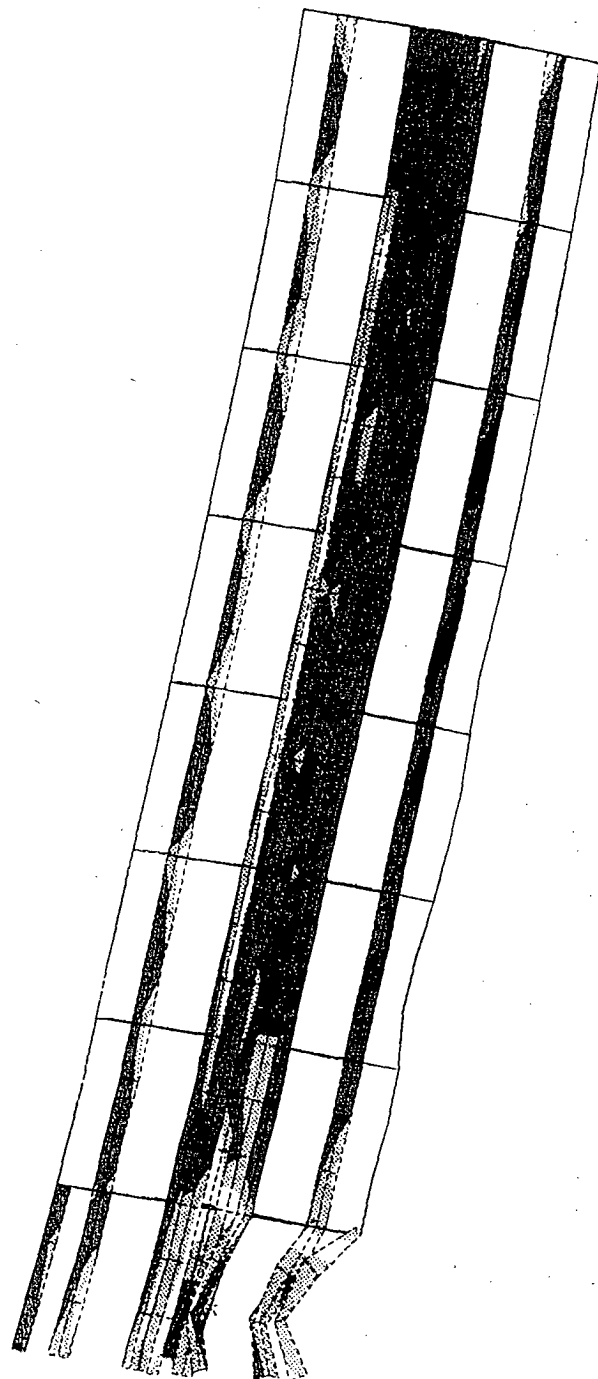
XV =-1  
 ZV =-2  
 DIST=11.825  
 XF =5.375  
 ZF =-0.1875  
 PRECISE HIDDEN  
 70.192  
 5480  
 10890  
 16300  
 21710  
 27120  
 32530  
 37941  
 43351  
 48761

CG Over Corner, Bottom Cage Disc Stresses

Total Disc Elements = 648  
 # Failed Elements = 48

Figure 33



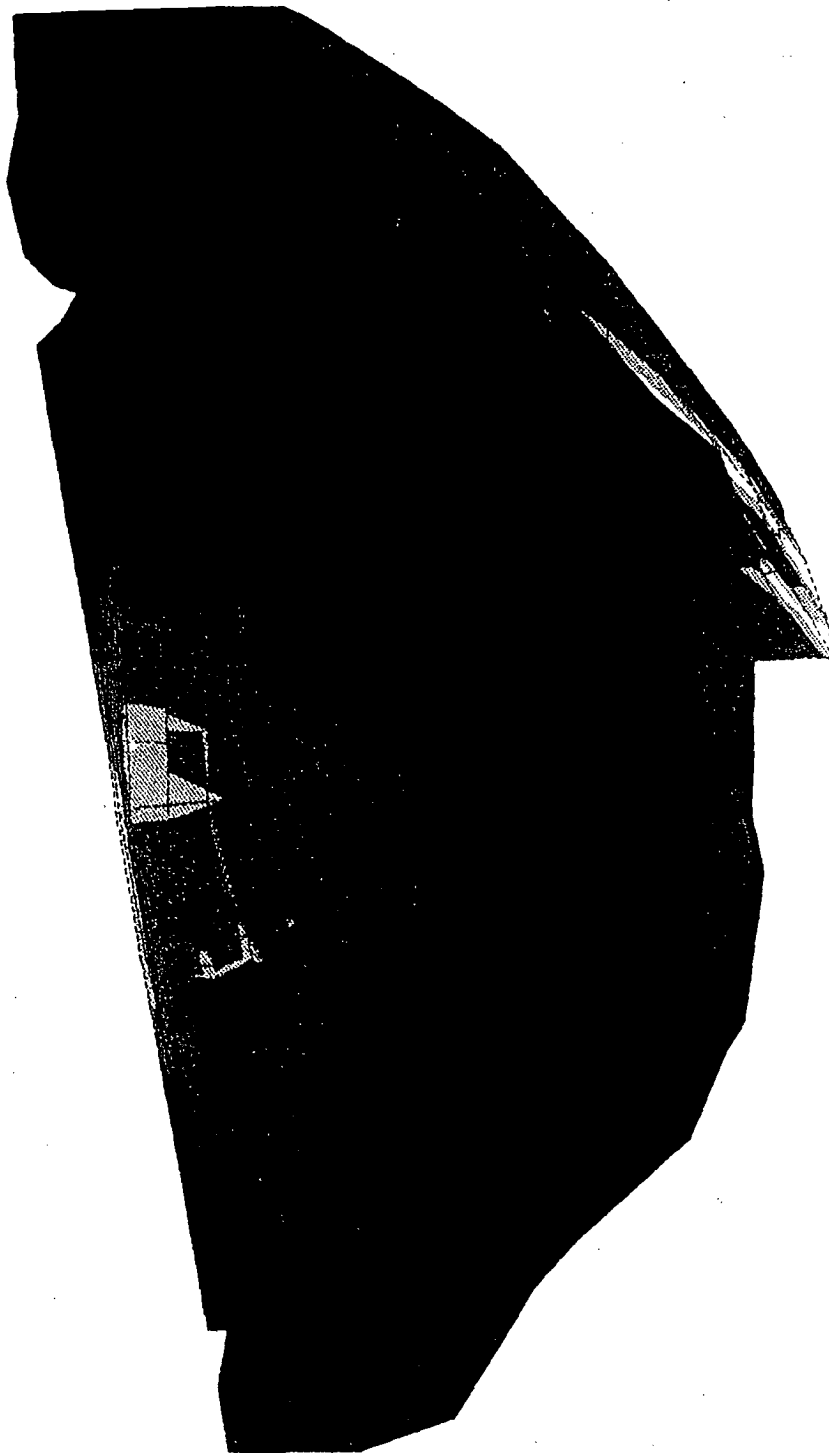


ANSYS 4.4  
 OCT 27 1993  
 11:20:20  
 PLOT NO. 1  
 POST1 STRESS  
 STEP=1  
 ITER=9  
 TIME=0.009  
 SIGE (AVG)  
 TOP  
 DMX =4.256  
 SMN =1917  
 SMX =35042  
 SMXB=77239

XV =-1  
 DIST=54.105  
 XF =5.375  
 ZF =48  
 ANGZ=78  
 PRECISE HIDDEN  
 1917  
 5597  
 9278  
 12958  
 16639  
 20319  
 24000  
 27680  
 31361  
 35042

CG Over Corner, Cage Shell Surface Stresses

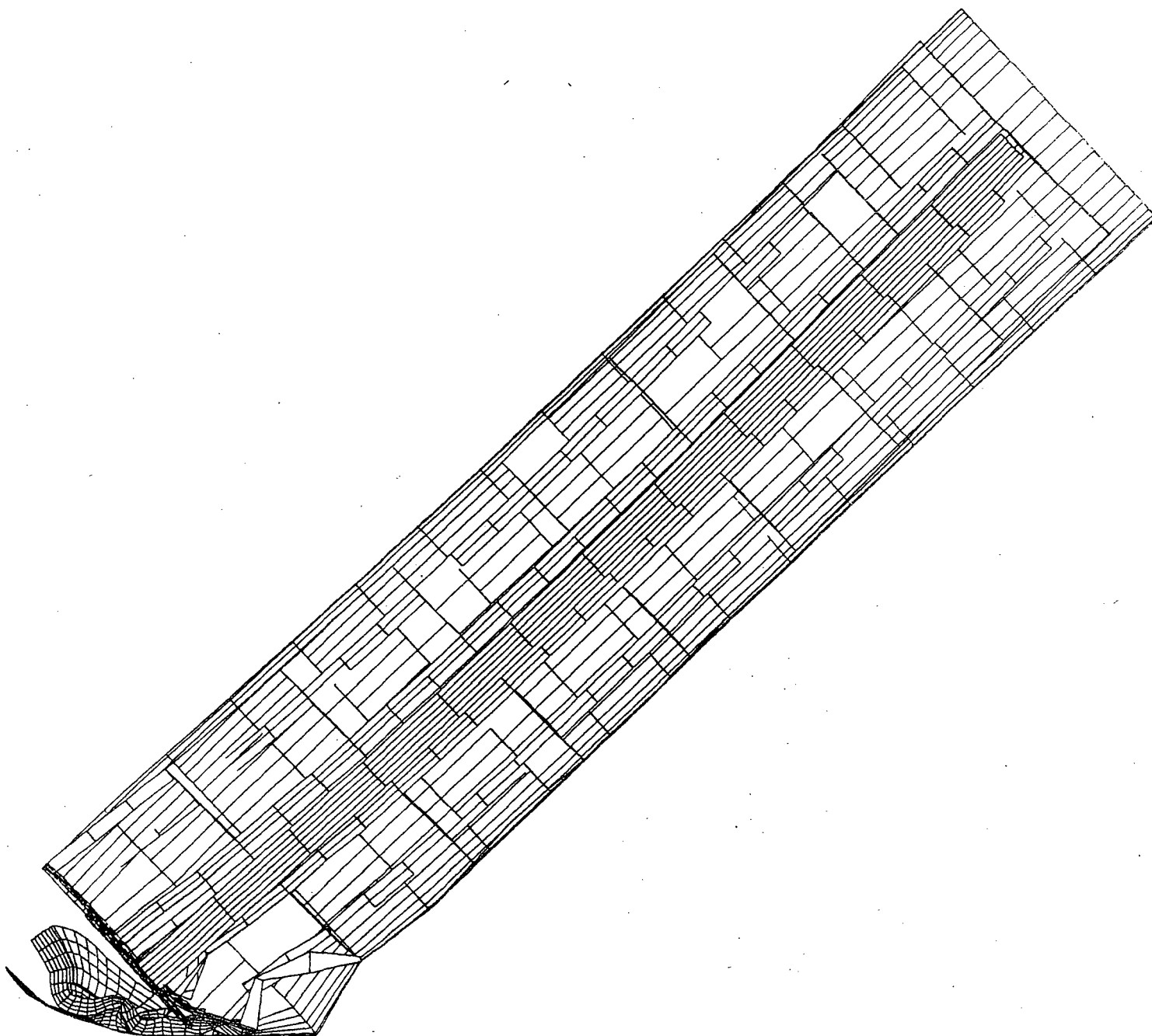
Figure 34



CG Over Corner Drop, Peak Rubber Stress

OCT 27 19  
 16:21:17  
 PLOT NO. 1  
 POST1 STRESS  
 STEP=1  
 ITER=8  
 TIME=0.008  
 SIGE (AVG)  
 MIDDLE  
 DMX =6.434  
 SMN =42.609  
 SMX =2590  
  
 XV =-1  
 ZV =1  
 DIST=11.55  
 XF =5.25  
 ZF =-1.25  
 CENTROID HIDDEN  
 42.609  
 325.644  
 608.679  
 891.714  
 1175  
 1458  
 1741  
 2024  
 2307  
 2590

Figure 35

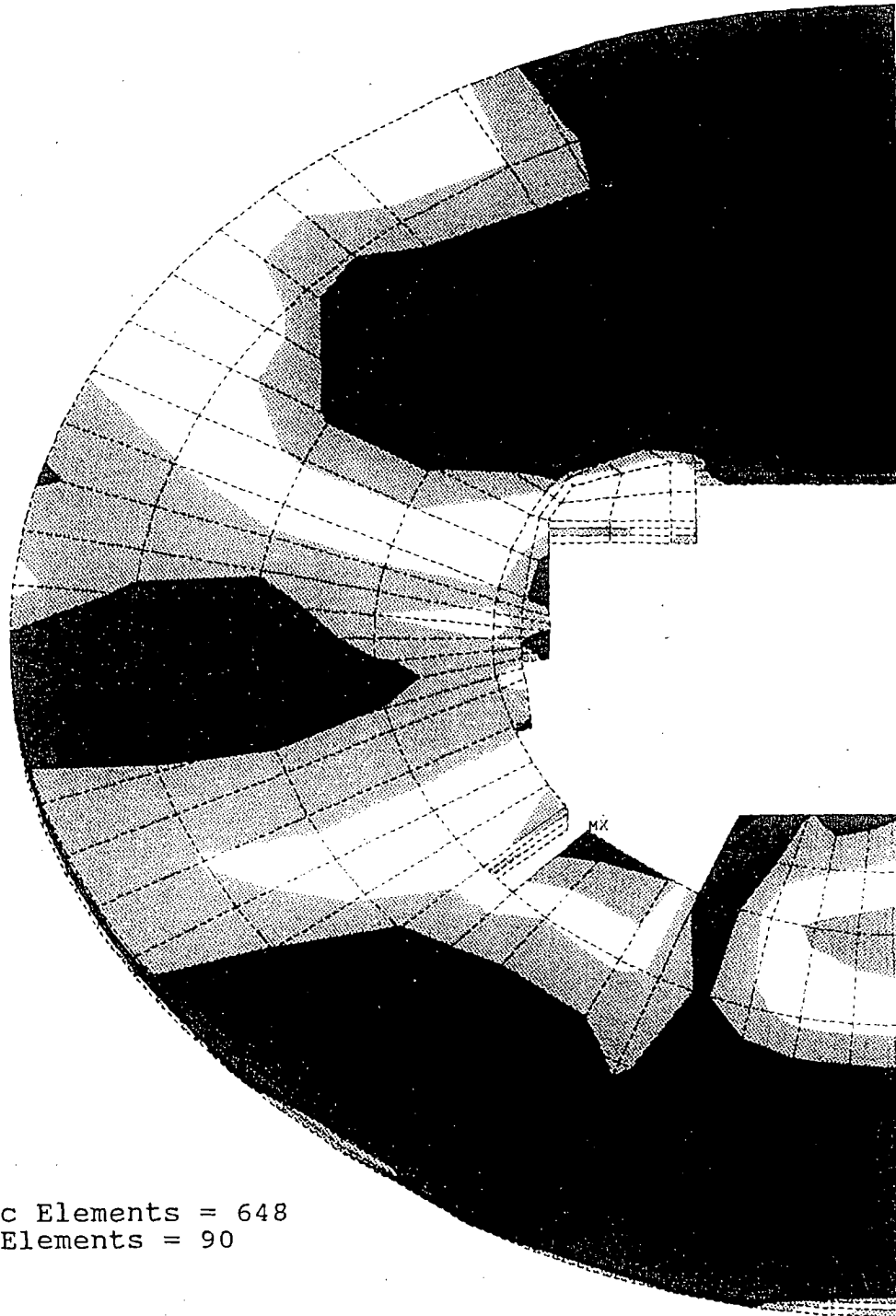


OCT 20 1996  
11:32:02  
PLOT NO. 1  
POST1 DISPL.  
STEP=1  
ITER=12  
TIME=0.012  
DMX =10.299  
ERPC=0

\*DSCA=1  
XV =-1  
DIST=47.643  
XF =5.5  
ZF =47.998  
ANGZ=45  
PRECISE HIDDEN

Shipping Drum Angle Drop, Deformed

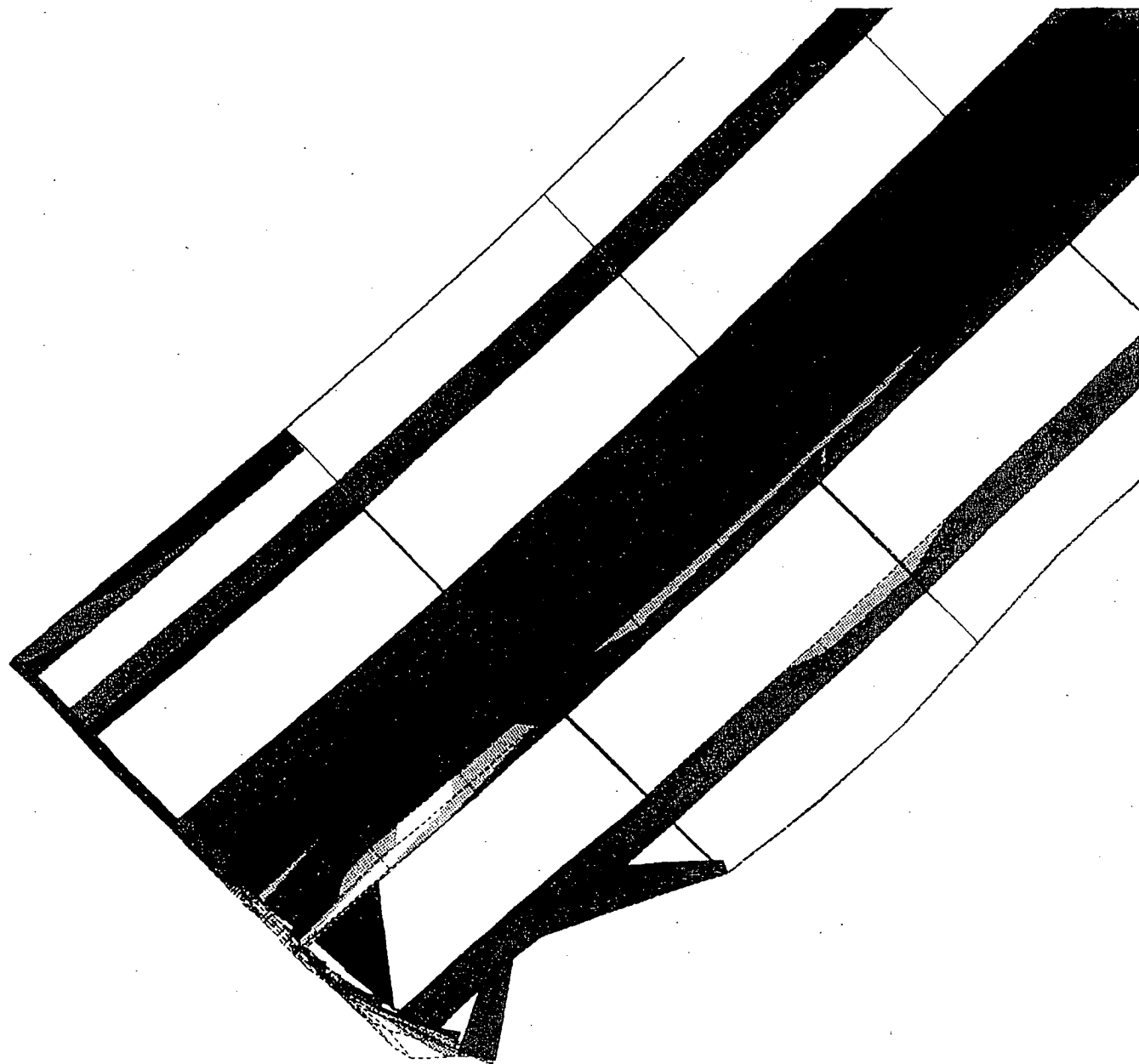
Figure 36



Total Disc Elements = 648  
# Failed Elements = 90

ANSYS 4.  
NOV 5 1993  
9:34:57  
PLOT NO. 1  
POST1 STRESS  
STEP=1  
ITER=12  
TIME=0.012  
SIGE (AVG)  
MIDDLE  
DMX =4.508  
SMN =4310  
SMX =40027

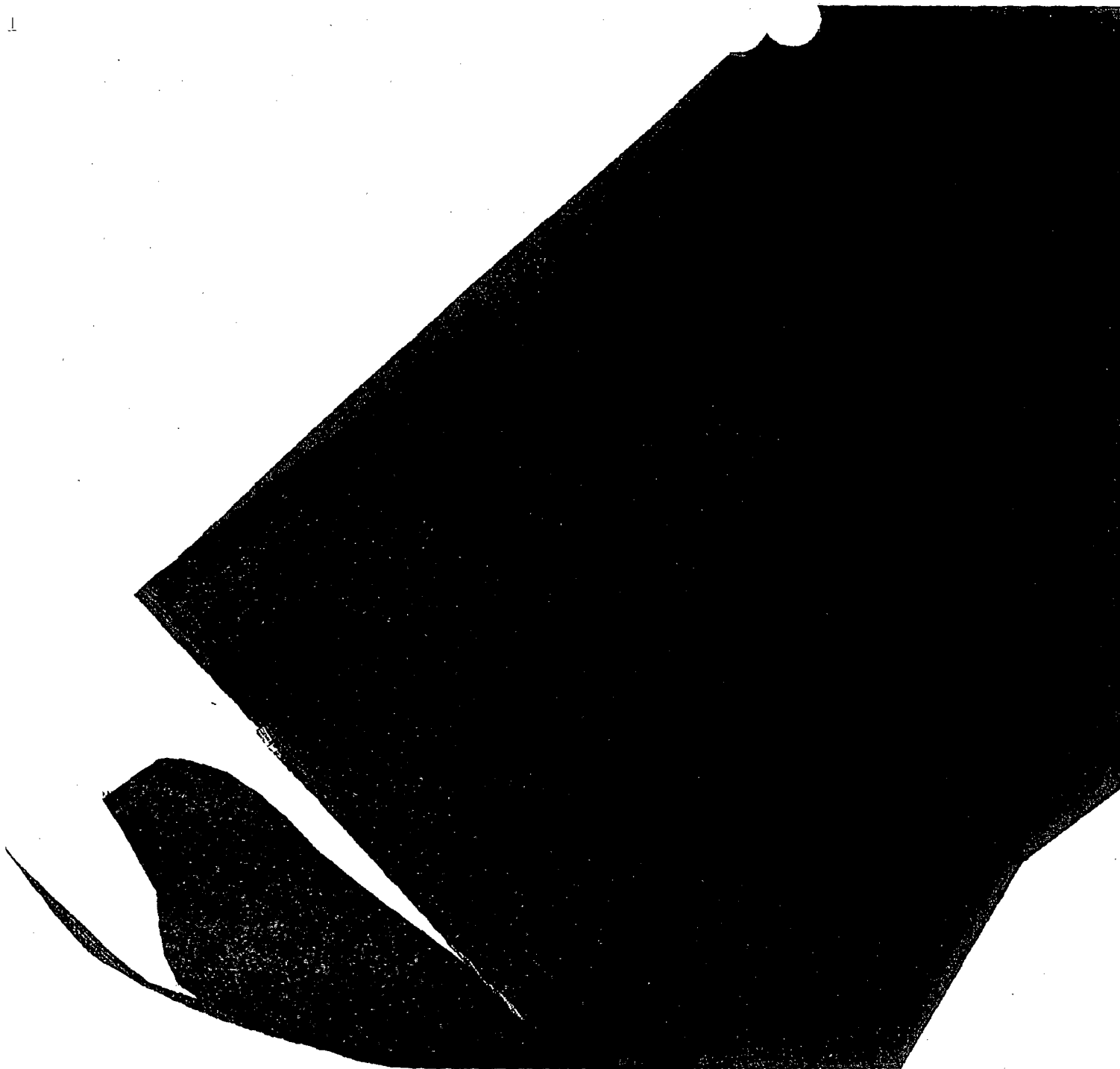
YV =-1  
ZV =-1  
DIST=8.508  
XF =5.375  
ZF =-0.1875  
PRECISE HIDDEN  
4310  
8278  
12247  
16216  
20184  
24153  
28121  
32090  
36059  
40027



ANSYS 4.  
 NOV 2 1993  
 14:00:11  
 PLOT NO. 1  
 POST1 STRESS  
 STEP=1  
 ITER=9  
 TIME=0.009  
 SIGE (AVG)  
 TOP  
 DMX =6.464  
 SMX =48541  
 SMXB=87856  
  
 XV =-1  
 \*DIST=22.261  
 \*XF =5.375  
 \*YF =-2.356  
 \*ZF =9.022  
 ANGZ=45  
 PRECISE HIDDEN  
 0  
 5393  
 10787  
 16180  
 21574  
 26967  
 32360  
 37754  
 43147  
 48541

Shipping Drum 45 Deg Drop, Max Cage Stress

Figure 38



ANSYS 4.  
OCT 20 1993  
10:20:39  
PLOT NO. 1  
POST1 STRESS  
STEP=1  
ITER=12  
TIME=0.012  
SIGE (AVG)  
TOP  
DMX =6.33  
SMN =15.902  
SMX =70596  
SMXB=71724

XV =-1  
\*DIST=15.917  
\*XF =5.375  
\*YF =1.47  
\*ZF =4.775  
ANGZ=45  
PRECISE HIDDEN  
15.902  
7858  
15700  
23543  
31385  
39227  
47069  
54912  
62754  
70596

Shipping Drum Angle Drop, Deformed

Figure 39

# DYNA3D Verification Problem 1

Projectile Top Displacement

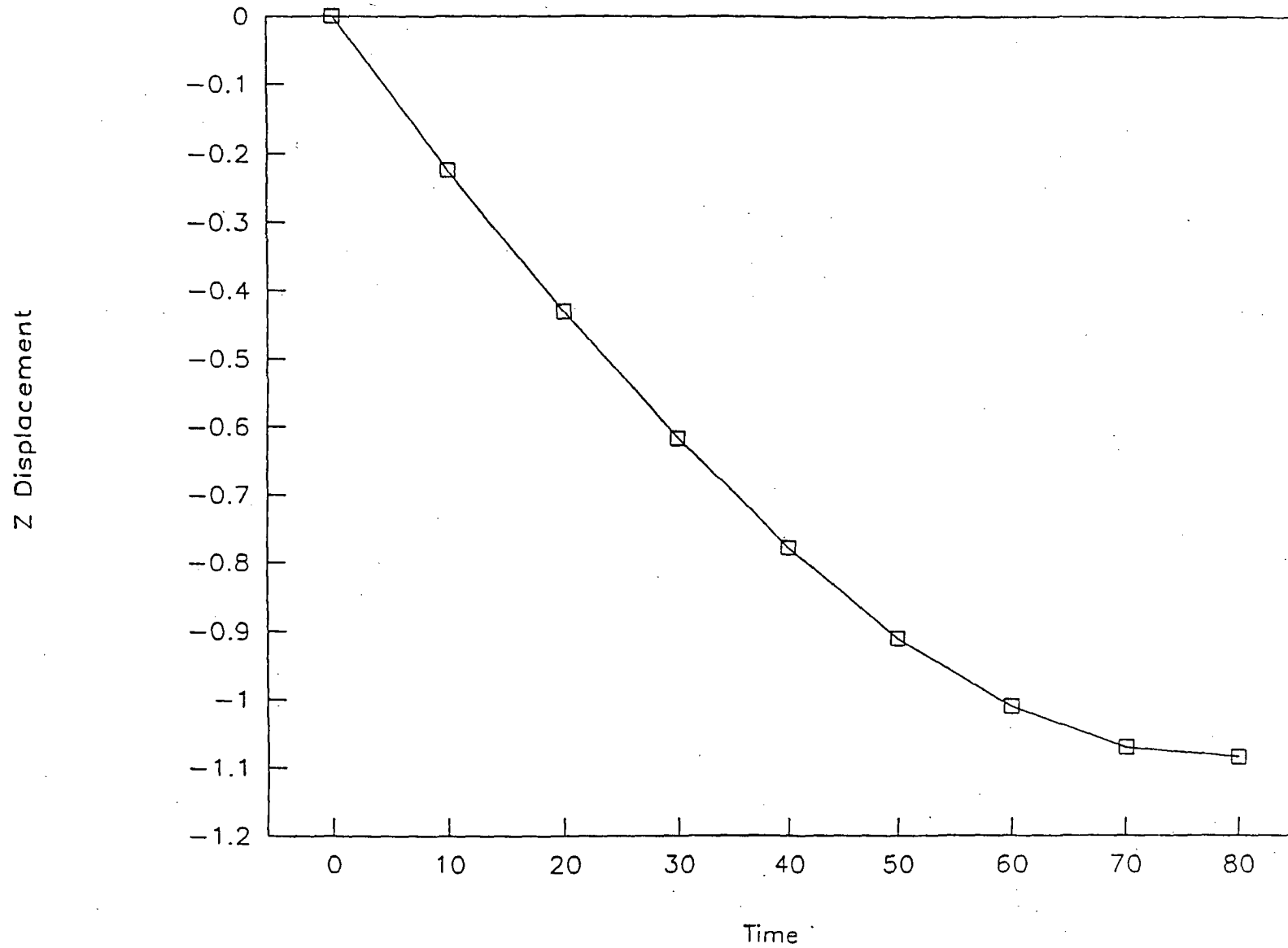
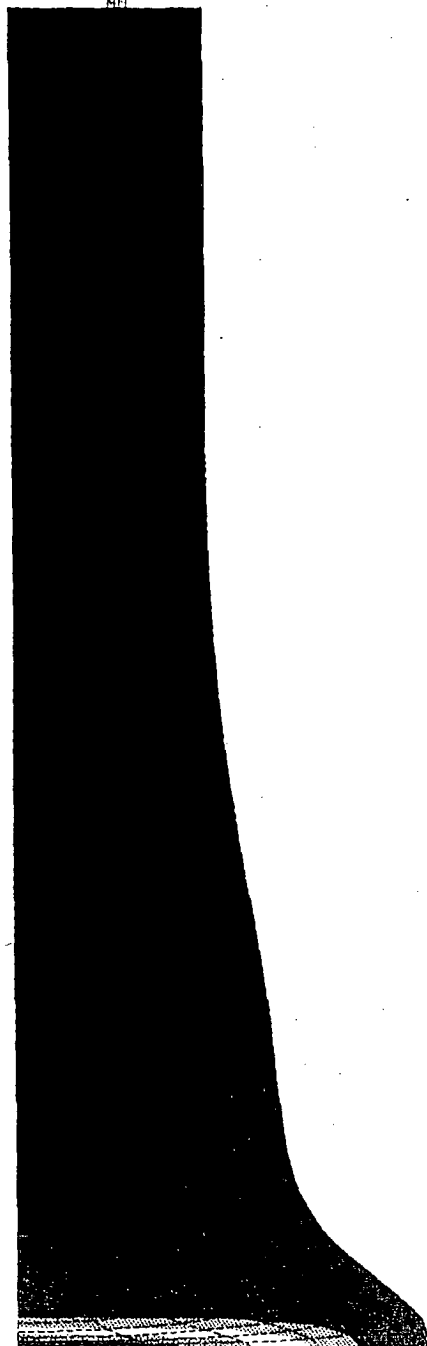


Figure 40

ANSYS 4.  
JAN 31 1993  
16:15:07  
PLOT NO. 1  
POST1 STRESS  
STEP=1  
ITER=8  
TIME=79.992  
EPL (AVG)  
DMX =1.086  
SMX =2.805

YV =-1  
\*DIST=1.238  
\*XF =0.035469  
\*YF =0.16  
\*ZF =1.077  
PRECISE HIDDEN  
0  
0.311711  
0.623422  
0.935133  
1.247  
1.559  
1.87  
2.182  
2.494  
2.805





# DYNA3D Verification Problem 8

Shell Node 8 Displacement

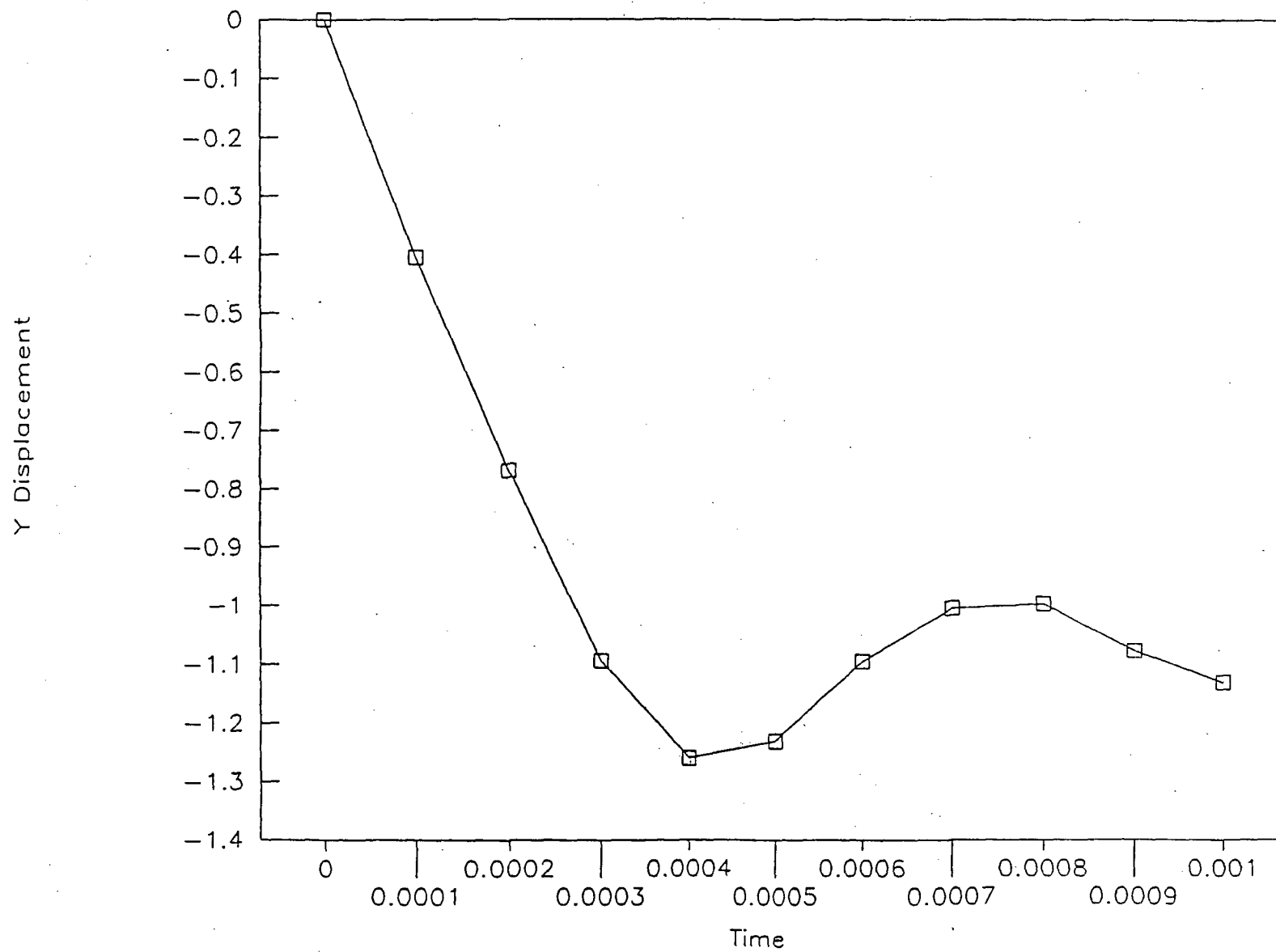
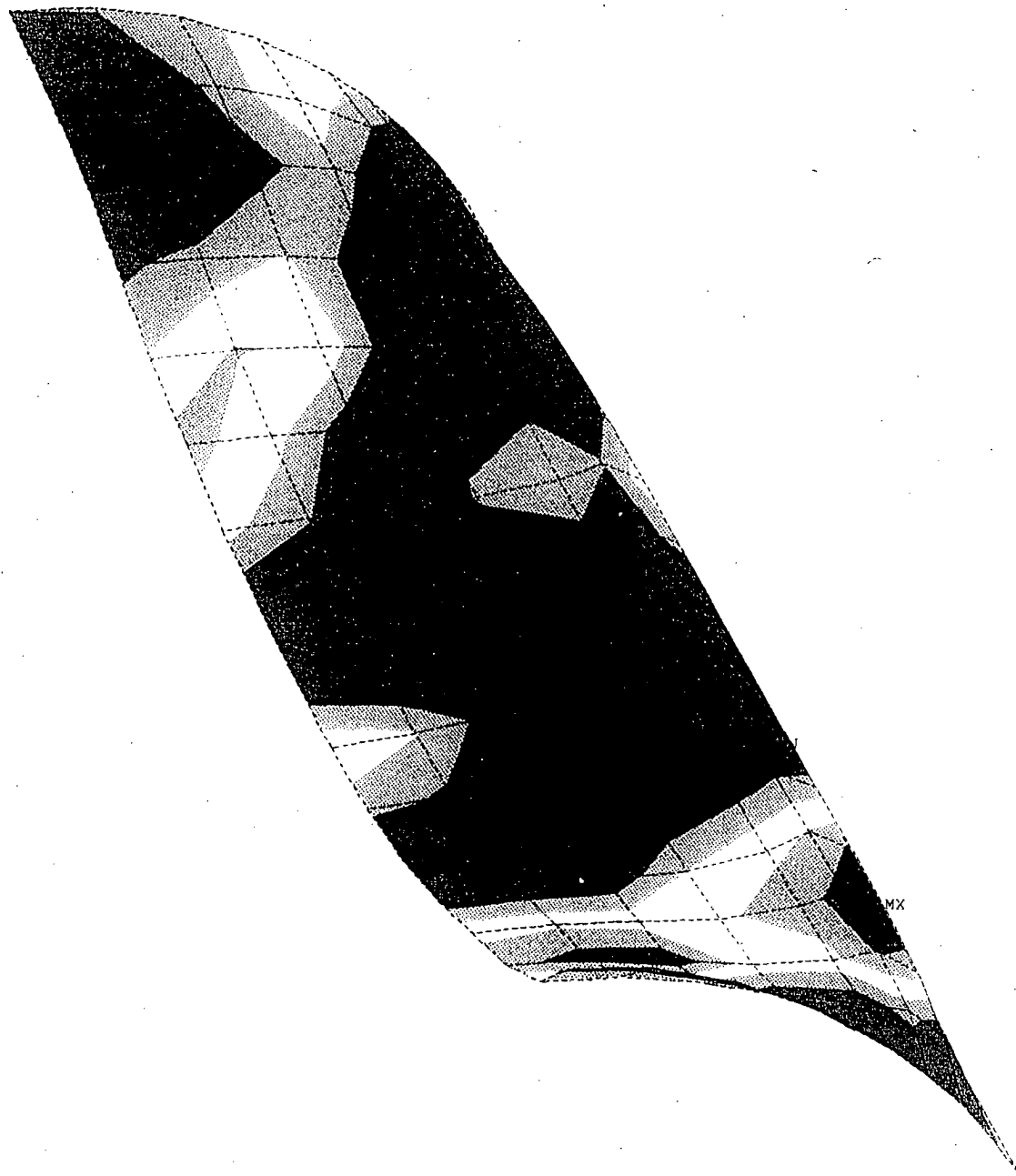


Figure 42



ANSYS 4.  
 FEB 2 1993  
 14:59:07  
 PLOT NO. 1  
 POST1 STRESS  
 STEP=1  
 ITER=10  
 TIME=0.100E-02  
 SIGE (AVG)  
 TOP  
 DMX =1.164  
 SMN =4127  
 SMX =42259  
 SMXB=65906

XV =-1  
 YV =2  
 ZV =4  
 DIST=3.8  
 XF =1.272  
 YF =2.204  
 ZF =-6.28  
 PRECISE HIDDEN

4127
8364
12601
16838
21074
25311
29548
33785
38022
42259

Figure 43

**Appendix 6.1.1**

**Square and Triangular arrays**

KENO modeling uses a square pitch to represent drum type containers which could configure into a triangular pattern. Accordingly, the effective radius for the drum in a triangular pattern is 93.06% of the actual radius. This is the square root of the area of a drum in a triangular pattern/square root of the area of that drum in a square pattern.

The use of an area adjusted square pattern is demonstrated by comparing triangular and square pattern single tier arrays of 2.76 liter bottles reported on pages 135 and 136 of LA-10860-MS. For this consideration:

$t_s$  = Solution Surface Density

H = Solution height in bottles

A = Array area, equal to the area associated with each array  
unit times the number of units in the array

and

The array shape factor is described as  $H/(A)^{1/2}$ .

Analysis of these symmetric arrays is provided in the Table and Figure of this appendix, and shows that the critical surface density as a function of the array shape factor is not sensitive to the array pattern (square or triangular). Accordingly, it is appropriate to evaluate these symmetric triangular pattern arrays in a square pattern model provided that the unit area of the triangular pattern is preserved.

Appendix 6.1.1

Consideration of square and triangular array patterns

Critical Array of U(92.6)02 (NO3)2 Solution at H/U-235 =59 in A Bottles  
Pages 135 & 136, LA-10860-MS

Number Of Units In Array	Pattern	Surface Sepr. (cm)	Pitch cm	Sq. Array Area, sq.cm. $A^2 \cdot N$	Triangular Array Area, sq. cm $N \cdot ((P/2)^2) \cdot 3.464$	Height cm	$H/(A^{0.5})$	Slab Thick 2760 cm * N/A
9	3 x 3 Square	4.45	18.15	2964.80		25.6	0.470	8.378
16	4 x 4 Square	8.40	22.10	7814.56		25.6	0.290	5.651
25	5 x 5 Square	11.60	25.30	16002.25		25.6	0.202	4.312
36	6 x 6 Square	14.30	28.00	28224		25.6	0.152	3.520
7	Triangular	3.89	17.59		1875.63	25.6	0.591	10.301
19	Triangular	11.60	25.30		10532.04	25.6	0.249	4.979

